

Supercritical Carbon Dioxide Circulated EGS Combined with IGCC in New Mexico

Optimizing geothermal energy production in arid
regions

National Geothermal Student Competition

June 2011

Penn State University

Divya Chandra

Caleb Conrad

Derek Hall

Andrew Weiner

Nicholas Montebello

Anukalp Narasimharaju

Vaibhav Rajput

Emilia Phelan

Ghazal Izadi

Executive Summary

Introduction: We explore the pairing of an integrated gasification combined cycle (IGCC) plant with an engineered geothermal system using supercritical CO₂ as the circulating fluid (scCO₂-EGS) and located near Albuquerque, NM. The IGCC plant generates electricity from the gasification of coal and the burning of the resulting hydrogen. Terminal effluents are water from the combustion of hydrogen and a pure stream of CO₂ that is consumed as make-up heat transfer fluid for the scCO₂-EGS. This pairing of IGCC-scCO₂-EGS reduces water use, utilizes and partially sequesters byproduct scCO₂ and overall has reduced emissions and environmental impact in the closed-cycle system.

Overview of Region: The proposed scCO₂-EGS site is located in the Rio Grande Rift Basin that stretches from south central Colorado into Mexico. The basin traverses a semi-arid region of scarce water resources with a broadly distributed rural population that also concentrates into a few large population centers – most notably Albuquerque. The rift represents a region of higher than average heat flow with geothermal gradients reaching 39°C/km. Fractured crystalline basement rocks exist at depths of 2 to 7 kilometers beneath the rift-filling sediments and older Mesozoic and Paleozoic formations.

We explore the design of a coupled scCO₂-EGS and IGCC system close to the power utilization center of Albuquerque, NM, pairing these energy conversion methods through the CO₂ effluent of the IGCC as the heat-transfer fluid of the scCO₂-EGS.

Technical Considerations - EGS: The EGS reservoir will be developed in basement rocks at a depth of 3.5 km approximately 8 km to the southeast of Albuquerque. This location provides shallow access to the crystalline basement rocks as confirmed by the adjacent hydrocarbon exploration well, TransOcean Isleta 1, with an anticipated reservoir temperature of 200 °C. The EGS reservoir will be developed using a 5-spot pattern with an injector-producer separation of 500 m and with scCO₂ as the heat transfer fluid. For an assumed fracture spacing of the order of 10m and with single-well injection rates of 100 kg/s the time to 50% thermal drawdown in the reservoir is of the order of 30 years, and triple-that for more widely spaced fractures. For an injection-recovery temperature differential of 60C-200C then a circulation rate of 100 kg/s results in a thermal power output of 19 MW-thermal (per injector-withdrawal doublet of 100 kg/s). The scCO₂ production from the IGCC supplies the make-up fluid to compensate from leak-off losses in the EGS. For anticipated fluid losses of 5-10% the 80 kg/s output from the IGCC translates to 800-1600 kg/s overall flow rate distributed in 8-16 injectors each of ~100 kg/s. This translates to projected outputs from the EGS of the order of 150-300 MW-thermal that may decline to half of these values after 30 years.

Technical Considerations – IGCC: The generation of electrical power by integrated gasification combined cycle (IGCC) presents an environmentally closed system with high energy conversion efficiency. Specifically, fugitive gases of high purity, particularly CO₂ can be used for sequestration, or in this case scCO₂-EGS. We design a plant with pre-combustion carbon capture as this allows the larger proportion of CO₂ to be captured as well as the capture of other pollutants. The principal components of a pre-combustion carbon-capture IGCC plant comprise processes of (i) oxygen production (ii) oxy-gasification (iii) the cleaning of the resulting synthesis-gas (iii) prior to burning and power generation and (iv) with the resulting pure stream of CO₂ used for scCO₂-EGS. These functions are as follows:

Oxygen production: The air separation unit splits the influent air stream into its principal components of oxygen and nitrogen. The separated oxygen is sent to the gasifier for the oxy-gasification of coal while nitrogen is sent to the gas turbine for reducing NO_x production and lowering the combustion temperature in the turbine. We use cryogenic separation as the most mature of the available technologies to provide 4000 metric tons/day of oxygen to the gasifier and Claus plant.

Oxy-gasification: Sub-bituminous powdered coal from the San Juan Basin is then gasified in a pure-oxygen environment to produce CO and H₂. The gasifier significantly reduces water use over traditional air-combustion thermal methods. We optimize reactor conditions and reactant concentrations to maximize synthesis gas output. For a nominal power output of 550 MW-electricity we require two entrained flow reactors consuming 7000 metric tons/day of coal water slurry and 3500 metric tons/day of oxygen. Both reactors operating with an average cold gas efficiency ranging from 70–75% supply synthesis gas capable of 1000 MW-electricity.

Synthesis gas cleaning: The output synthesis gas stream from the gasifier is of CO and H₂ and is passed through a water-gas shift (WGS) reaction. The WGS reactors convert the majority of the CO to CO₂ (97% conversion efficiency) in an effort to produce more hydrogen by freeing it from H₂O (an added reactant in the form of steam). This is accomplished by using a series of two reactors at different temperatures to increase the conversion efficiency and the concurrent use of a sulfur resistant catalyst which also serves to hydrolyze COS to H₂S. Sulfur-impregnated activated carbon removes 95% of the fugitive mercury.

Hydrogen combustion: CO₂ and H₂S are then stripped from the synthesis gas in the two stage acid-gas removal (AGR) reactor using Selexol as a solvent for high pressure absorption followed by flash depressurization to recover acid gases. The two stage AGR separately recovers CO₂, H₂ and H₂S. The H₂ stream is 91.4% pure and is co-combusted with O₂ and N₂ in a GE H-Class turbine to reduce the burn-temperature and to generate electricity. For a net output of 550 MWe from the burning of H₂, the IGCC produces a

separate stream of CO₂ at a rate of 80 kg/s. The CO₂ stream is 99.5% pure and is sent to the EGS for use as a heat transfer working fluid.

Environmental Considerations: The proposed project will minimize its impact on the local environment and residents through careful planning. The IGCC plant contains and processes the emissions that are commonly associated with coal-based power plants (CO₂, NO_x, SO_x and water) will be much reduced and turned into a resource. Potential impacts related to the EGS are subsidence, ground water contamination and induced seismicity. At the planned 3.5 to 5 km depth of the EGS reservoir ground water contamination is minimized if proper well construction procedures are followed. Due to the injection rates and close proximity of the proposed site to the city of Albuquerque induced seismicity may become an issue. This issue may only be addressed as the injection scheme is tuned, potentially involving reduced flow rates and alternating injectors and withdrawal wells as the response of the reservoir rocks is observed. This plant will save emissions of 8,200 tons of NO_x, 20,000 tons of SO₂ and 4.35 million tons of CO₂ emissions over one year compared to a conventional fossil fuel power plant.

Economic Considerations: An economic analysis for the combined scCO₂-EGS-IGCC system determines the Net Present Value (NPV) of the overall system and established probable payback periods based on the cost of electricity, possible electricity inflation rates, and the possibility of governmental funding for carbon capture and storage (CCS). The total capital cost and operational costs for the combined systems are \$1.7 billion (IGCC) and \$190 million (EGS), respectively. The assessment estimates that in the worst-case scenario (no increase in electricity prices and absent government funds to subsidize CCS) the system will pay for itself in its 8th year of operation. In this case the final present worth of the project over the 30 year lifetime would be \$3 billion and have an Return on Investment (ROI) of 91%. The best-case scenario results in a Payback Time (PBT) of 6 years, a \$5.5 billion total present worth over 30 years, and an ROI of 223%. These results of the economic assessment show that the project is a worthwhile investment. Further investigation of costs and benefits associated with both portions of the project would serve to reinforce the findings and provide a more accurate estimation of the outcome of the project.

Social and Cultural Considerations: For this proposed plant to become a good neighbor to the city of Albuquerque it must fit into the city's long term goals. Specifically, Albuquerque is molding itself into a growing city and tourist destination that supports industries with minimal visual impacts and with an ethos for the conservation of water and the environment. The minimized and symbiotic outputs of the scCO₂-IGCC plant also fit these environmental ethics. It is feasible for the aesthetic and environmental impact of the proposed plant to also satisfy this goal of minimal visual and environmental impact but it must be designed this way from the start. To address water use, the power plant will operate solely on gray water and produced water from the geothermal field.

Additionally, scheduled plant maintenance activities will take place during known drought conditions to relieve pressure on the water resources. Jobs will be created directly from this power plant. Jobs from the building and operation of the site will enhance employment for the next decade. Jobs will also arise from the lower electricity transmission costs and governmental incentives for green energy by attracting additional businesses.

Ownership and Land Use Considerations: The site is located on private land and should therefore avoid issues related to development on Native American territories or U.S military property. The proposed plant will utilize an otherwise barren section of the New Mexico desert. Of the 56 km² available, the combined power plants will occupy an area of 1.5 km². The entire 125 MWe EGS system will use 0.15 km² while a 550 MWe IGCC system will occupy an estimated 1.35 km². The remainder of the land is available for prior uses including use as range land.

Infrastructure: Temporary infrastructure will include temporary power, maintenance shop, labor camp, water and wastewater management facilities, staging areas, material sources and road access to the site. The permanent infrastructure includes both plant and support facilities. Plant infrastructure will comprise power generation, geothermal wells, plant equipment and machinery, piping and waste fluid disposal. Support facilities will include transmissions lines, road and rail links, living quarters, water supply and storage, wastewater treatment, maintenance shop, drilling equipment/ core shop and emergency shelters.

Overall, this pairing of scCO₂-EGS with IGCC has been shown both technically feasible and economically viable as a method for the generation of electricity where it is desired to both conserve scarce water resources and reduce overall environmental impact of fugitive emissions - in particular where the carbon footprint is to be minimized

Acknowledgement

This project is result of National Student Geothermal Competition (NGSC)-2011 managed by National Renewable Energy Laboratory (NREL). Their support is greatly acknowledged.

We would like to thank Dr. Derek Elsworth and Dr. Larry Grayson for their guidance and continuous encouragement. Dr. Elsworth's insightful questions and valuable suggestions led us to a better understanding of the project. We would also like to acknowledge Dr. Sarma Pisupati and Dr. Uday Turaga for their support.

Table of Contents

Executive Summary	i
Acknowledgement	v
Table of Contents	vi
Table of Figures	x
List of Tables	xii
List of Abbreviations	xiii
List of Symbols	xv
Problem Statement	1
1.0 Introduction.....	1
2.0 Overview of Region.....	3
2.1 Introduction:.....	3
2.2 Geology and Stratigraphy:	3
2.3 Structure:.....	8
2.4 Geologic concerns associated with the EGS system.....	8
2.5 Geothermal Resources:	13
2.5.1 Thermal Gradient and Temperature of the Reservoir:	13
2.5.2 Depth and Volume of the Reservoir:.....	14
2.5.3 Permeability of the Reservoir:	14
2.5.4 Presence or Absence of Water:	16
2.6 Evolution of Energy Release and Moment Magnitude in EGS Reservoirs	16
2.6.1 Moment Magnitude	17
2.6.2 Global Energy Balance for Fracture Networks	18
2.7 Conclusions and Recommendations:	20
3.0 Enhanced Geothermal System (EGS).....	21
3.1 Introduction.....	21
3.1.1 What is Enhanced Geothermal System (EGS)?	21
3.1.2 Advantages of using CO ₂ as a working fluid	22
3.2 Reservoir Simulation	24
3.2.1 Geothermal reservoir engineering concepts.....	24
3.2.2 CMG STARS™ Simulator	25

3.3 Model Preparation and Results	27
3.3.1 Model Parameters.....	27
3.3.2 Model results	29
3.4 Thermal Drawdown	33
3.5 Simplified Thermal Drawdown Calculations	34
3.5.1 Reservoir configurations	34
3.5.2 Thermal drawdown analysis.....	35
3.5.3. Thermal output	37
3.5.4 Thermal drawdown in prototypical reservoir.....	37
3.6 CO ₂ Corrosion.....	38
3.7 Geothermal Energy Conversion Systems	39
3.7.1 Introduction:.....	39
3.7.2 Binary Conversion Systems	40
3.7.3 Flash Conversion Systems	44
3.7.4 Gravity Separation- scCO ₂ -Double Flash Conversion System	45
3.7.4.1 Gravity Separation.....	45
3.7.4.2 Brayton Open Cycle Super-Critical CO ₂ Turbine	51
4.0 IGCC.....	53
4.1 Introduction.....	53
4.2 Air Separation Unit.....	54
4.2.1 Introduction	54
4.2.2 Types of ASU.....	54
4.2.2.1 Adsorption Process	55
4.2.2.2 Polymeric Membranes	56
4.2.2.3 Ion Transport Membrane	57
4.2.2.4 Cryogenic Separation	58
4.2.3 Conclusion:.....	59
4.3 Gasifier.....	60
4.3.1 Introduction	60
4.3.2 Methods.....	60
4.3.3 Results	62

4.3.4 Coal Water Slurry Preparation	65
4.3.5 GE Reactor	66
4.3.6 Oxygen and Water Supply	66
4.4 Gas Cleaning Unit.....	67
4.4.1 Introduction	67
4.4.2 Water Gas Shift	68
4.4.3 Mercury Removal.....	69
4.4.4 Acid Gas Removal	69
4.4.5 Claus Plant.....	70
4.4.6 Methods	71
4.4.7 Results:	72
4.4.8 Conclusion.....	73
4.5 Power Generation.....	74
4.5.1 Introduction	74
4.5.2 Methods.....	74
4.5.3 Results	76
4.5.4 Conclusion.....	79
4.6 Plant Performance.....	80
4.6.1 Assumptions	80
4.6.2 Power Summary	81
5.0 Policies and Environmental Issues.....	82
5.1 Introduction.....	82
5.2 Gaseous Emissions and the Clean Air Act:	83
5.2.1 Air Emissions:	83
5.2.2 Nitrogen Oxides:	83
5.2.3 Hydrogen Sulfide (H ₂ S):	84
5.2.4 Sulfur Dioxide (SO ₂):.....	84
5.2.5 Particulate Matter (PM):	85
5.2.6 Carbon Dioxide (CO ₂):	86
5.2.7 Mercury:	86
5.2.8 Permits and Enforcement:	88

5.3 Emissions Trading:	88
5.3.1 CO ₂ and cap-and-trade:	88
5.3.2 Allocation of credits:	89
5.3.3 Economics of cap-and-trade and Emission tax:	89
5.3.4 Acid Rain Program:.....	90
5.4 Water usage, Water Pollution and the Safe Drinking Water Act:	93
5.5 Coal Production and Reserves:	96
5.6 Conclusion	99
6.0 Social and Cultural Consideration	100
7.0 Infrastructure.....	102
7.1 EGS Infrastructure:	102
7.2 IGCC Infrastructure:	102
7.3 Support Facilities:	102
8.0 Land Usage and Ownership:.....	103
9.0 Economics.....	104
9.1 Introduction:.....	104
9.2 Governmental Derived Incentives:	104
9.3 Enhanced Geothermal System Economics	105
9.3.1 Exploration, drilling, and completion of wells.....	105
9.3.2 Construction of power conversion facilities.....	105
9.3.3 Discounted future re-drilling and well stimulation	108
9.4 Gravity Separation- scCO ₂ -Double Flash Conversion System.....	108
9.5 IGCC- Economics:.....	113
9.6 Economics of Water.....	117
9.7 Transportation and Costs	117
9.8 Overall Economic Analysis	119
9.8.1 Assumptions for Economic Analysis	119
9.8.2 NPV Analysis of Project	119
10.0 Conclusions:.....	121
11.0 References.....	123
Appendix.....	130

Table of Figures

Figure 1: scCO ₂ -circulated EGS combined with IGCC system.....	2
Figure 2: Tectonic Map of the Rio Grande Rift Basin in New Mexico (Kelly 1977)	5
Figure 3: Generalized Structural Framework	6
Figure 4: Stratigraphic Column (Molenaar, 1988)	7
Figure 5: Generalized geologic map of Albuquerque basin showing deep drill holes and seismic lines (Johnson et al, 2001).	10
Figure 6: Geologic and seismic sections illustrating the structural configuration of the southern portion of the North Albuquerque basin (Russel and Snelson, 1994).....	11
Figure 7: Fault traces near the selected site (Granuch and Hudson, 2007).....	12
Figure 8: Isopach map of the total present day thickness of Tertiary rocks in the Albuquerque Basin using subsurface drill-hole data (Johnson et al. 2001).....	15
Figure 9: Moment Magnitude	19
Figure 10: Effects of hydraulic, thermal and chemical behaviors on annual event rate. .	20
Figure 11: Schematic of a conceptual two-well Enhanced Geothermal System in hot rock in a low-permeability crystalline basement formation (Duchane et al., 1995).....	22
Figure 12: Model grid geometry (side view)	28
Figure 13: Model results at 2018-03-01.....	29
Figure 14: Model results at 2024-09-01.....	30
Figure 15: Model results at 2039-12-01.....	31
Figure 16: Model results at 2044-05-01.....	32
Figure 17: Comparison of CMG and SRM model results and the SRM model.	34
Figure 18: Five spot, and vertically and horizontally stacked reservoir configurations. .	35
Figure 19: Congruence of spherical reservoir (SRM) and parallel fracture (PFM) models to represent deep EGS reservoirs.....	36
Figure 20: Thermal drawdown (TD) with time for sCO ₂ circulation at rates of 100 and 1000 kg/s for fracture spacing within the reservoir of 10m and 100m. Reservoir is 0.125 km ³	37
Figure 21: Scaled rates of drawdown for recovery at 1000 and 100 kg/s for the prototypical reservoirs considered here and for prior demonstration projects at Fenton Hill (USA) and at Rosemanowes (UK) (Elsworth, 1990).	38
Figure 22: Phase Diagram for Pure Water (Mogk 2011).....	41
Figure 23: Phase Diagram for CO ₂	42
Figure 24: Binary Heat Exchanger Raster Technologies (2011)	42
Figure 25 (a) & (b): Wall Thickness Effect on Heat Flow	43
Figure 26: Double Flash Power Plant (Dagan 2007)	45
Figure 27: Supercritical Carbon Dioxide Power Plant	46
Figure 28: T-s and P-v Diagrams of an Ideal Brayton(Cengel 2010).....	52

Figure 29: Block Diagram for pre-combustion carbon capture IGCC Plant	53
Figure 30: Adsorption	55
Figure 31: Polymeric Membranes.....	56
Figure 32: Ion Transport Membrane.....	57
Figure 33: Cryogenic Separation	58
Figure 34: Entrained Flow Gasifier	Figure 35: Moving Bed Gasifier.....
Figure 36: Equivalence Ratio vs. Equilibrium Mole Fraction	62
Figure 37: Equivalence Ratio vs. Equilibrium Mole Fraction	63
Figure 38: Initial Mole Fraction vs. Equilibrium Mole Fraction	64
Figure 39:Initial Mole Fraction vs. Equilibrium Mole Fraction	64
Figure 40: Initial Mole Fraction of water vs. KJ/mole of Synthesis gas	65
Figure 41: GE Reactor	66
Figure 42: Physical Solvent AGR Process Flow	70
Figure 43: Upstream AGR Placement Temperature Profile	71
Figure 44: Down Stream AGR Placement Temperature Profile	71
Figure 45: Composition of synthesis gas through WGS and AGR	73
Figure 46: Effects of variable dilution methods and inlet temperatures on flame temperature (Chiesa & Lozza, 2005).....	75
Figure 47: Calculated nitrogen requirement for a given inlet temperature.....	77
Figure 48: Nitrogen Oxide (NO _x) formation at various effluent temperatures for a defined gas turbine.....	78
Figure 49: Heat Recovery Operations from Combined Cycle Processes	78
Figure 50: Steam and NO _x produced from the gas turbine, while varying excess oxygen provided	79
Figure 51: Nitrogen Oxide Comparison.	84
Figure 52: Sulfur Dioxide Comparison.....	85
Figure 53: Particulate Matter Comparison.....	85
Figure 54: Carbon Dioxide Comparison.....	86
Figure 55: Price & Volume of Sulfur Dioxide Traded	93
Figure 56: Class VI Wells	Figure 57: Class II Wells.....
Figure 58: Fraction costs of the EGS field development and binary power plant (GETEM results).....	107
Figure 59: Determining Break Even Point for Double Flash Plants 41MW	110
Figure 60: Determining Break Even Point for Double Flash Plants 84MW	111
Figure 61: Determining Break Even Point for Double Flash Plants 125MW	112
Figure 62: NPV of EGS and IGCC Combined Systems.....	120

List of Tables

Table 1: Parameters for EGS model	27
Table 2: Sensitivity Analysis	33
Table 3: Thermophysical material parameters appropriate for sCO ₂ -EGS reservoir modeling.	36
Table 4: Separator Calculations	49
Table 5: Separator Calculations	50
Table 6: Separator Calculations	50
Table 7: Typical Parameters of ASU (Smith, 2001).....	59
Table 8: Calculated data based on system inputs, see appendix table 3	77
Table 9: Assumption Table.....	80
Table 10: Power Summaries	81
Table 11: Specifications for Acid Rain Program	90
Table 12: Specifications for Clean Air Interstate Rule	91
Table 13: Trading prices of SO ₂ allowances.....	92
Table 14: Determining binary power-plant size and cost (GETEM results).	106
Table 15: Double Flash Cost and Production Estimations	109
Table 16: Key Assumptions for IGCC plant.....	114
Table 17: Fixed Operation Cost for IGCC plant.....	114
Table 18: Variable Operational Costs for IGCC plant.....	115
Table 19: Capital Costs for IGCC.....	115
Table 20: Assumptions for Economic Analysis.....	119

List of Abbreviations

AGR:	Acid Gas Removal System
ASU:	Air Separation Unit
BTU:	British thermal unit
CAIR:	Clean Air Interstate Rule
CCS:	Carbon Capture and Storage
CCFE:	Chicago Climate Futures Exchange
DOE:	Department of Energy
EIA:	Environmental Impact Assessment
EGS:	Enhanced Geothermal System
EPA:	Environmental Protection Agency
HDR:	Hot Dry Rock
HRSG:	Heat Recovery Steam Generator
HPST:	High Pressure Steam Turbine
IGCC:	Integrated Gasification Combined Cycle
ITM:	Ion Transport Membrane
LCOE:	Levelized Cost of Electricity
NAAQS:	National Ambient Air Quality Standards
NPV:	Net Present Value
OPEC:	Organization of the Petroleum Exporting Countries
PBT:	Payback Time
PFM:	Parallel Fracture Model
PM:	Particulate Matter
PSD:	Prevention of Significant Deterioration of Air Quality

ROI:	Return on Investment
SDWA:	Safe Drinking Water Act
SRM:	Spherical Reservoir Model
STPD:	Short Ton Per Day
UIC:	Underground Injection Control
USGS:	United States Geological Survey
WGRS:	Water Gas Shift Reactor
WGS:	Water Gas Shift

List of Symbols

E_p :	Elastic Energy
$\Delta\tau$:	<i>Stress Drop</i>
M_0 :	seismic moment
M_S :	moment magnitude
E_T :	Total Energy
ε_i :	Initial strain
ε_f :	Final strain
V:	Volume of the matrix
N_{event} :	Number of seismic events,
E_T :	Total energy
E_p :	Potential energy
T_D	Thermal Drawdown
Q_D :	Flow Rate
t_D :	Time
x_D	Fracture Spacing
q :	Flow rate
ρ :	Density
C :	<i>Specific Heat Capacity</i>
l :	Thermal Conductivity
a:	Reservoir Radius
x_E :	Fracture Spacing

t : Time

d_m = Droplet size

μ : Viscosity of continuous phase

ΔSG : Difference between specific gravities of both liquids

d : Vessel internal diameter

L_{eff} : Effective length of the vessel

$(t_r)_o$: Retention time of carbon dioxide

Q_o : Flow rate of carbon dioxide

$(t_r)_w$: Retention time of water

Q_w : Flow rate of water

α_w : Fractional height of water

α_l : Fractional height of liquid

β_w : Fractional height of water

β_l : Fractional height of liquid

$h_{o \text{ max}}$ Height of oil pad

d_{max} : Maximum separator diameter

t_{corr} : Thickness

Problem Statement: Resource assessment and utilization of geothermal energy potential of the Rio Grande Rift Basin: A technical overview and economic analysis of a combined EGS-IGCC system with CO₂ as the working fluid.

1.0 Introduction

Within the desert southwest of the United States lie significant geothermal resources that possess many of the characteristics that are desirable for enhanced geothermal systems (EGS). These resources are unable to be developed using conventional techniques due to insufficient water to serve as the working fluid. To develop these resources a working fluid of sufficient quantities must be used. The focus of this project is to develop an EGS system that uses carbon dioxide as the working fluid whose source is from an integrated gas combined cycle coal-fired power plant.

Enhanced Geothermal Systems or EGS are systems that do not contain sufficient fluids to transfer the heat to the surface. They therefore require a heat transmission medium to extract heat energy. Conventional EGS operate using water as the working fluid. However, in this project, a novel concept of using CO₂ as heat transmission fluid is proposed. Using CO₂ offers numerous advantages, such as having lower viscosity as compared to water, thus resulting into higher flow velocities. Also, low solubility of CO₂ would decrease the scale precipitation in wellbores and surface equipments. In addition to this, geologic sequestration of CO₂ can also be achieved. Thus, the novel concept of combining IGCC with EGS is proposed and designed.

Majority of power plants around the world runs on coal. As energy demand continues to grow it is realistic that energy generation from coal will be necessary until other technologies become capable of producing significant base load power generation. The next generation of coal based power plants, integrated gasification combined cycle (IGCC) is the advance form of technology to obtain energy from the coal cleanly. In IGCC technology CO₂ gas is separated from the synthesis gas which is produced from the coal and the captured CO₂ can be used for various applications.

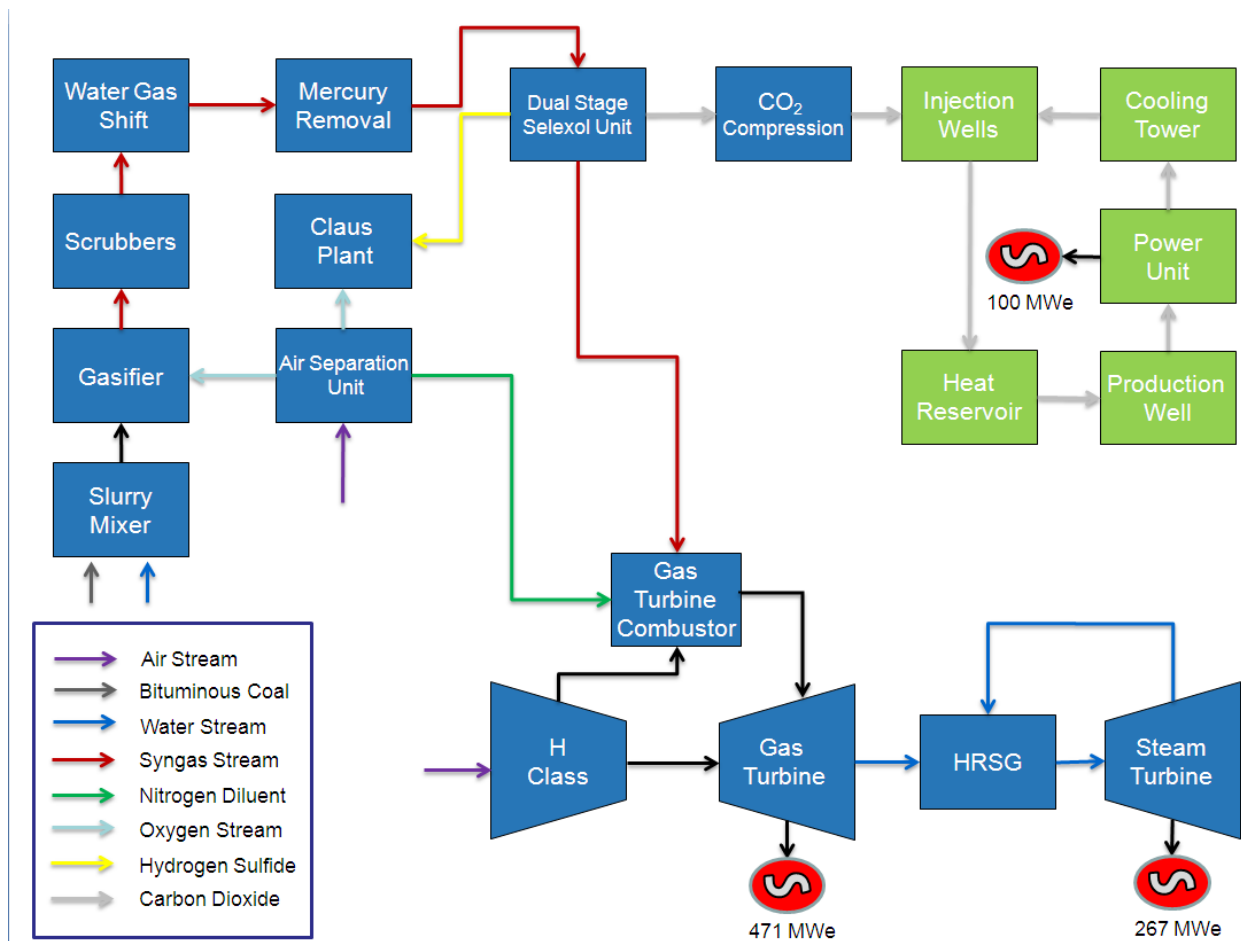


Figure 1: scCO₂-circulated EGS combined with IGCC system

Figure 1 shows scCO₂-circulated EGS combined with IGCC system. The blue block units represent the IGCC system and the green block units represent the EGS system. CO₂ gas is the connecting link between these systems. CO₂ gas is the byproduct of IGCC plant and it is also one of the pollutants responsible for global warming. The combination of EGS-IGCC system will help to significantly reduce CO₂ and other pollutants emissions. This unique combination will be able to tap the geothermal energy which is the renewable energy using CO₂ gas.

New Mexico comes under semi-arid region of USA. Optimal use of water resources should be done for such water scarce region. The proposed scCO₂ circulated EGS-IGCC combined system will maximize energy creation from this volume of water. This combination system will generate more power compared to individual EGS system while minimizing water usage.

2.0 Overview of Region

2.1 Introduction:

The Rio Grande Rift Basin is a prominent geologic feature that stretches from South Central Colorado into Mexico (See Figure 2). The formation of the Rift Basin began approximately 30 MYA and has continued until the present (Morgan et al., 1986). The basin of interest for this enhanced geothermal system (EGS) feasibility study is the Albuquerque Basin. This section of the report will focus on the geology, stratigraphy, structures, and geothermal resources within the basin that are relevant to the study area that is presented on figure 3. The target formations are the Precambrian basement rocks (See Figure 4). Relevant citations are provided for the other non-target formations.

2.2 Geology and Stratigraphy:

The formations within the Albuquerque Basin can be divided into Precambrian crystalline basement rocks, pre-rifting Paleozoic and Mesozoic Sedimentary rocks, and rifting Cenozoic basin fill and volcanics (See Figures 5 and 6). [Citation Note: Relevant formations to study area are referenced to Russel and Snelson (1994). Formation descriptions are referenced to the USGS Mineral Resources On-line Spatial Data for New Mexico.] The geometry of the individual formations is strongly tied to the location within the basin.

The basin filling Cenozoic sediments reach thicknesses on the order of 23,000 feet near the center of the basin. This basin fill serves as a municipal water supply source for many of the cities located throughout the basin (Jiracek et al 1983). A detailed description of the Tertiary rocks is presented by Kelley (1977). In his work, Kelly divides the basin deposits into two types. The first type is the subsiding trough deposits that are not related to the Late Pleistocene and Holocene deposits. The second type is those that are directly related. The formation that makes up a great part of the basin fill and is directly related rifting processes is the Sante Fe Group (Kelley 1977).

The older Paleozoic and Mesozoic sedimentary rocks have been the target of numerous exploratory oil and gas wells but as of yet remains an undeveloped resource due to economic restrictions (Johnson et al. 2001). Detailed analysis of the Mesozoic; Jurassic, Triassic, and Cretaceous systems are presented by Mankin (1958) in NM OFR 49. Detailed analysis of the Mississippian, Pennsylvanian, and Permian aged rocks are presented by Siemers (1973) in NM OFR 54. These reports should provide relevant detailed information for the Albuquerque Basin because these formations were deposited across the region and are present unless they were eroded or cut out by faulting (Molenaar 1988).

The Precambrian basement rocks are granites, gneiss, schists, greenstones, and quartzites that have been through considerable tectonic stresses through geologic time. These rocks typically form the rim around the basin and occur at depth within the basin (Kelley 1977). Within the basin proper either Mississippian aged or Pennsylvanian aged limestones and marine shales rest unconformably on top of these basement rocks.

These basement rocks have been studied in detail by Stark (1956), Myers and McKay (1974), and Bauer (1983) on the surface. In Bauer's 1983 report, he focused on a region near the Cibola National Forest and the Manzano Wilderness area. This region is approximately 50 miles to the southeast of Albuquerque, NM. In Bauer's (1983) report he mentions directly on the difficulty of assigning relative ages to the individual formations, "No stratigraphic order is implied with these names." These different formations correspond to different rock types that are encountered and are known to be Precambrian in age. Detailed formation descriptions are included in Appendix 2.A to assist in understanding how these formations may respond to potential stimulation and geochemical reactions associated with EGS development.

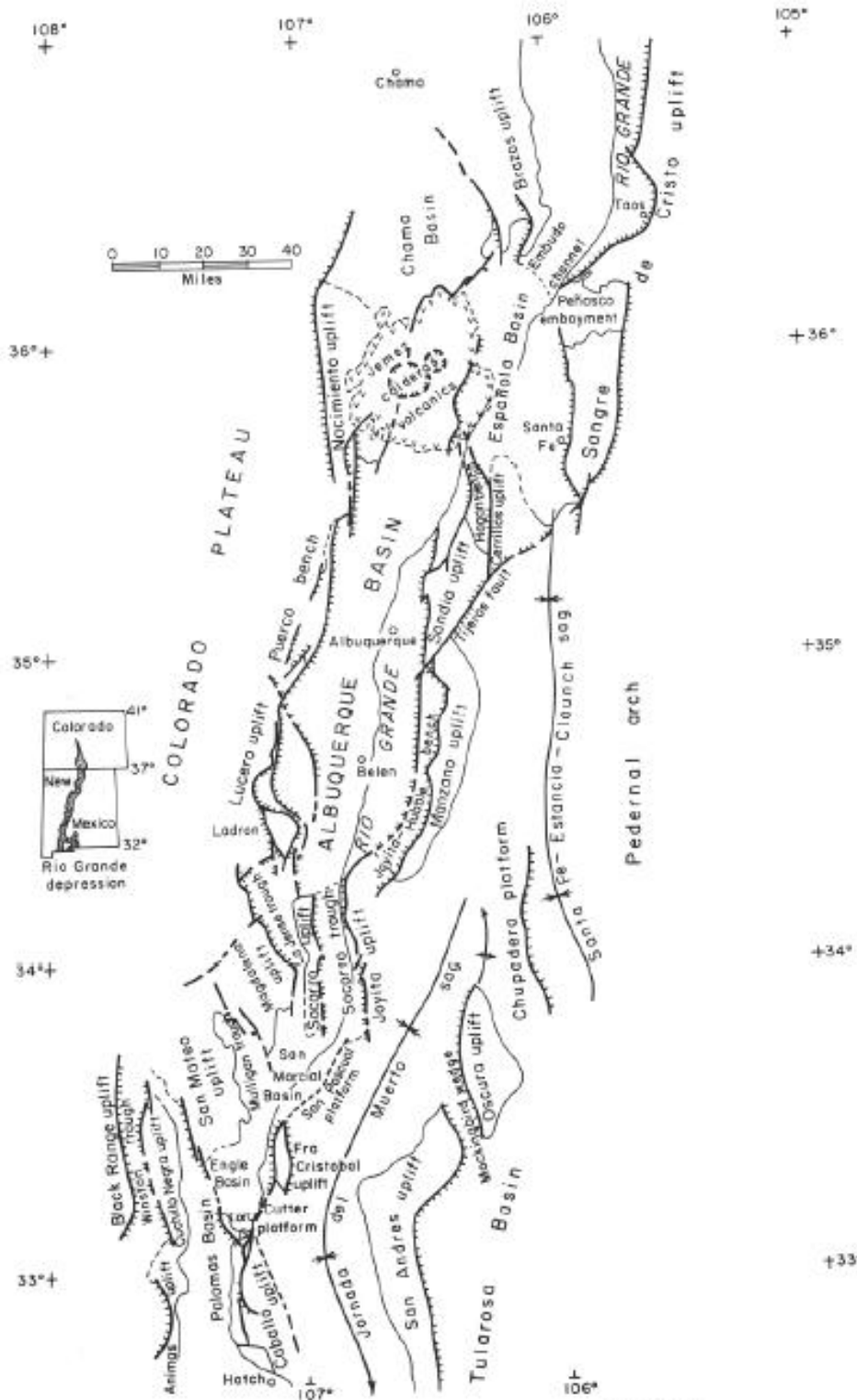


FIGURE 13—TECTONIC MAP OF RIO GRANDE RIFT SYSTEM IN NEW MEXICO.

Figure 2: Tectonic Map of the Rio Grande Rift Basin in New Mexico (Kelly 1977)

[Red star denotes approximate location of Albuquerque, NM and
blue star denotes approximate study area]

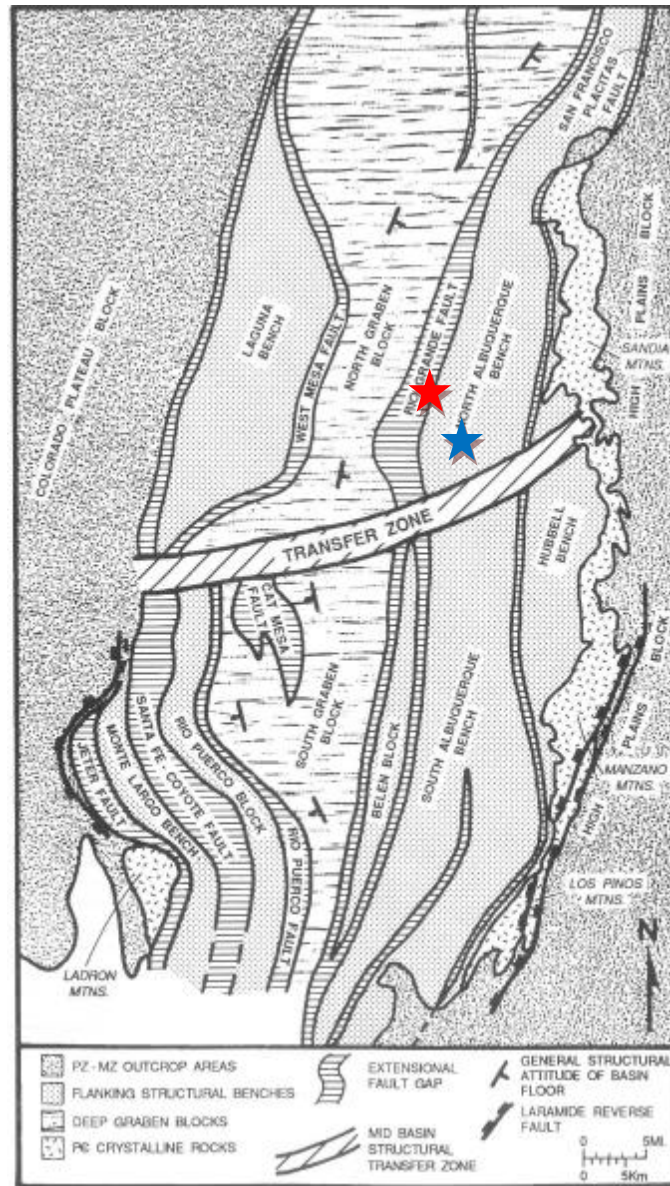


Figure 3: Generalized Structural Framework

Generalized structural framework map of the Albuquerque basin depicting the structural configuration of the pre-Tertiary “basement” (Russel and Snelson 1994).

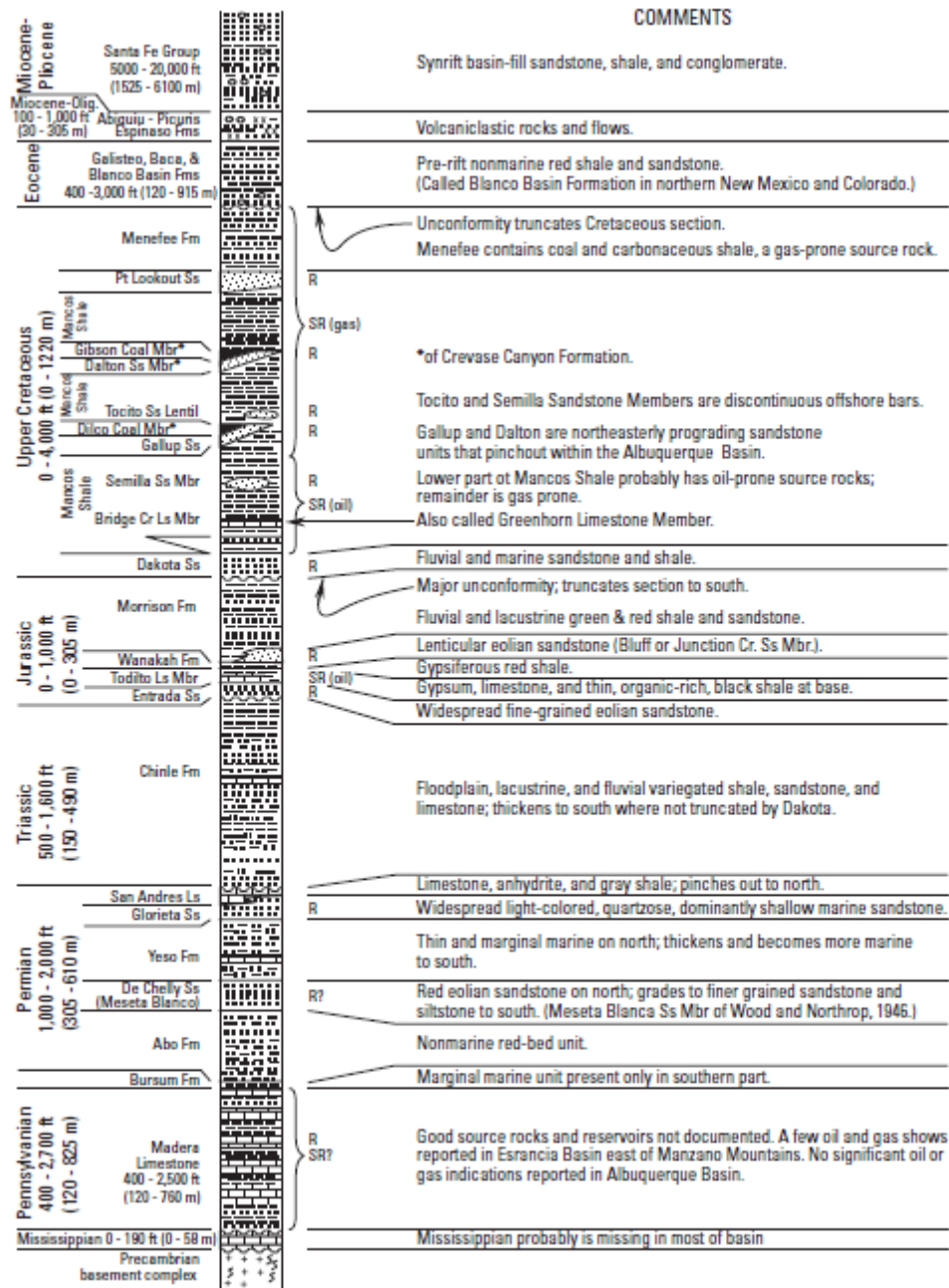


Figure 2. Generalized stratigraphic chart for the Albuquerque Basin (from Molenaar, 1988b). R, potential reservoir rock; SR, potential source rock.

Figure 4: Stratigraphic Column (Molenaar, 1988)

2.3 Structure:

The structure of the Albuquerque Basin is dominated by the rifting events in the greater geographic region. Specifically, the Albuquerque Basin is divided into two sub-basins termed the north basin and the south basin (See Figure 3). The two basins are the product of two different down-dropped grabens. The partition between the two basins is a transfer zone as termed by Russel and Snelson (1994). The northern basin is controlled by a west-dipping listric normal fault (Russel and Snelson 1994). The southern basin is controlled by the east dipping Sante-Fe, Cat Mesa, and Jeter Faults (Russel and Snelson 1994).

The site location (Figure 3) is located within the Northern Albuquerque Bench near the Transocean Isleta-1 exploratory hydrocarbon well (Figures 5 (Plane view) and 6 (Cross section view)). As depicted in Figure 6 it can be seen that the attitude of the beds in the area of the Northern Albuquerque Bench exhibit a more gentle westward dip than the beds found closer to the center of the basin. This rotation is a product of the tectonic history of the rift system (Russel and Snelson, 1994). Furthermore it can be observed that there is a deep detachment surface dominates the seismic section with smaller grabens existing within the larger slip feature.

This area is very close to the Rio Grande Fault and the Hubbell Springs Fault. Near the proposed site location, exists both seismic reflection profiles and petroleum wells that terminate at the top of the basement rocks (Russell and Snelson, 1994). Furthermore additional work completed by Granuch and Hudson (2007) captures the larger faults and the smaller faults with high resolution aeromagnetic surveys that have surface expressions (Figure 7). There is a strong likelihood that there are more faults in the subsurface that possess weak to no surface expression that could significantly affect subsurface flow.

2.4 Geologic concerns associated with the EGS system

Within the basin, most large faults completely penetrate from the crystalline bedrock into the synrift sediments of the Sante-Fe Group. The formations that rest directly upon the crystalline bedrock are marine limestones and shales. There are two main formations that are thought to exist in the study area. The oldest is the Late Mississippian or Earliest Pennsylvanian-aged Sandia Formation. The younger, second formation is the Pennsylvanian-aged Madera Limestone. From Siemers (1973) the depositional environment for Sandia Formation is a shore line complex and the Madera Limestone is shallow marine shelf. These two formations have the potential to act as an imperfect seal.

Siemers (1973) describes the Sandia Formation consisting mostly of shale with interbedded quartzites and micritic limestones. He further describes the Madera Limestone as a homogenous micritic limestone formation with local beds of quartzite. While no mention of porosity or permeability is mentioned directly in this report it can be inferred that these two

formations should act as a no flow boundary but locally may be more permeable as a result of the rifting and faulting processes.

If the flow of carbon dioxide from the targeted crystalline bedrock into these formations occurs there is a distinct possibility that locally the seal may not perform as expected. It is well documented that limestone will undergo dissolution when exposed to carbonated brines. If limestone is exposed to super-critical carbon dioxide the effect can be expected to be similar or higher than carbonated brines. The carbon dioxide that flows through these fractures will enhance the permeability of the fractures and may create a positive feedback loop where the permeability continues to increase over time.

To deal with this potential issue it is recommended that wells be completed in such a way that the fractures and faults that are thought to be in communication with overlying sedimentary rocks are avoided. While not all fractures can be avoided the first and second order fracture systems should be able to be avoided.

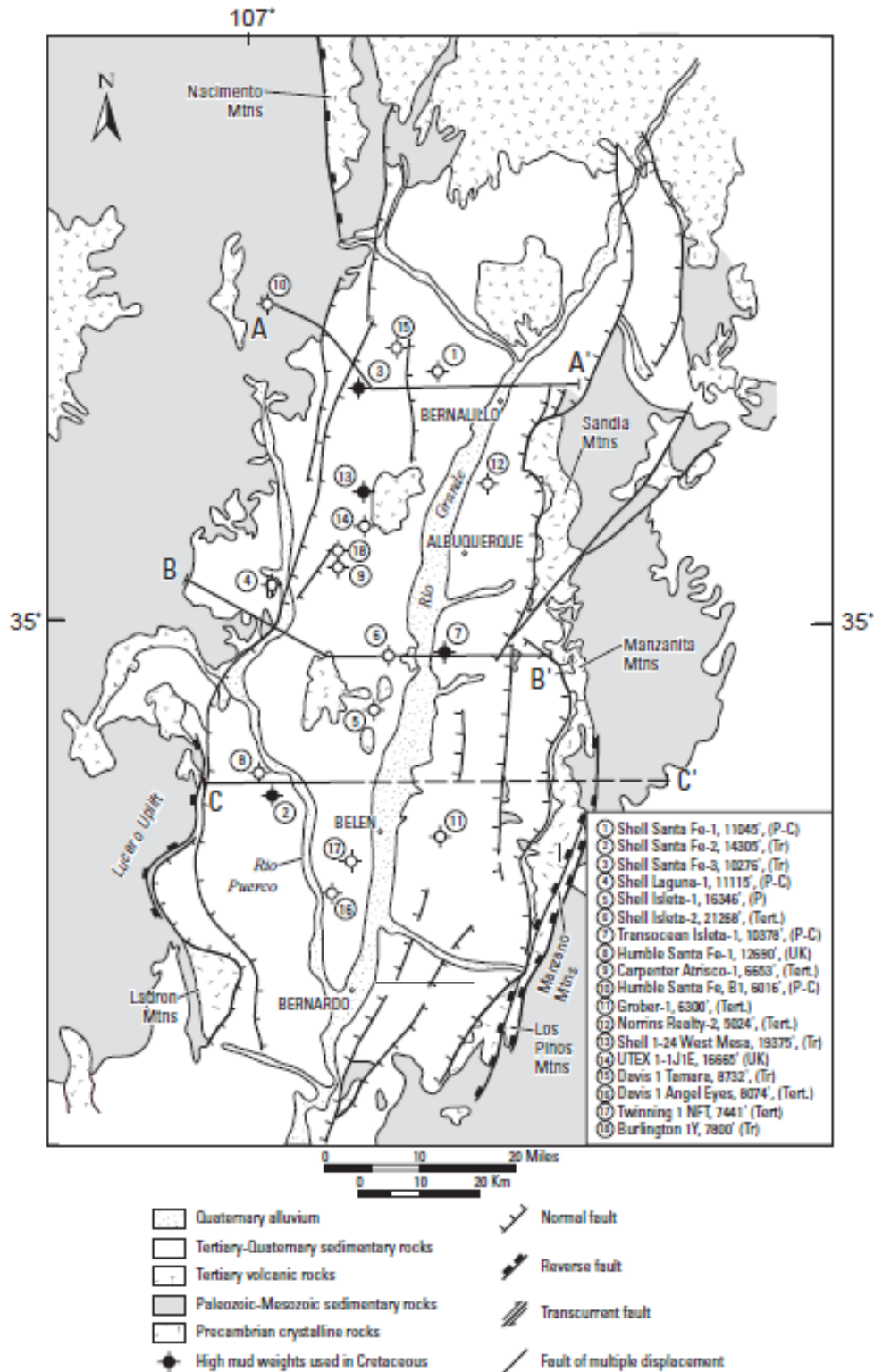


Figure 5: Generalized geologic map of Albuquerque basin showing deep drill holes and seismic lines (Johnson et al, 2001).

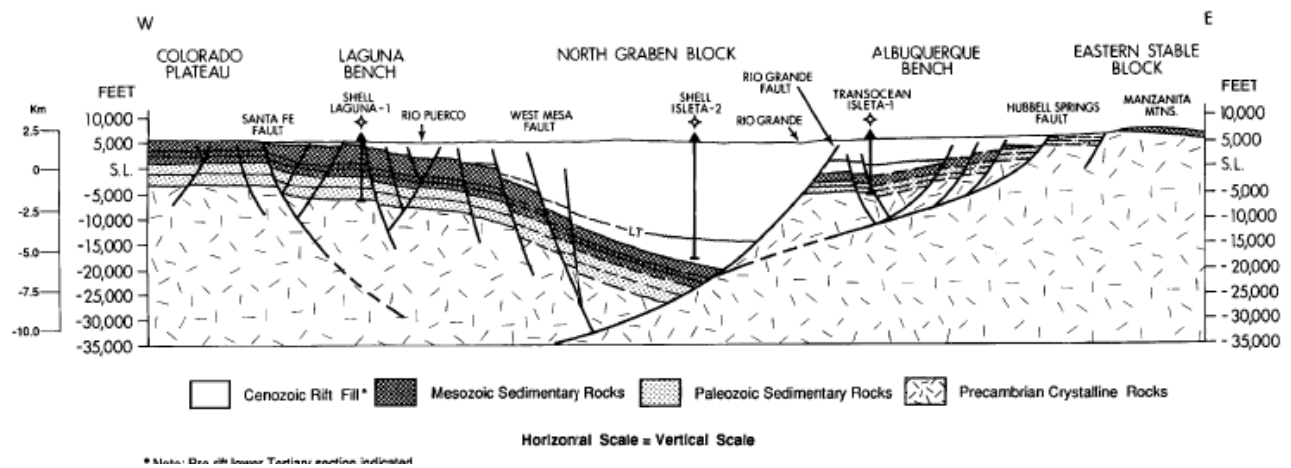


Figure 6: Geologic and seismic sections illustrating the structural configuration of the southern portion of the North Albuquerque basin (Russel and Snelson, 1994).

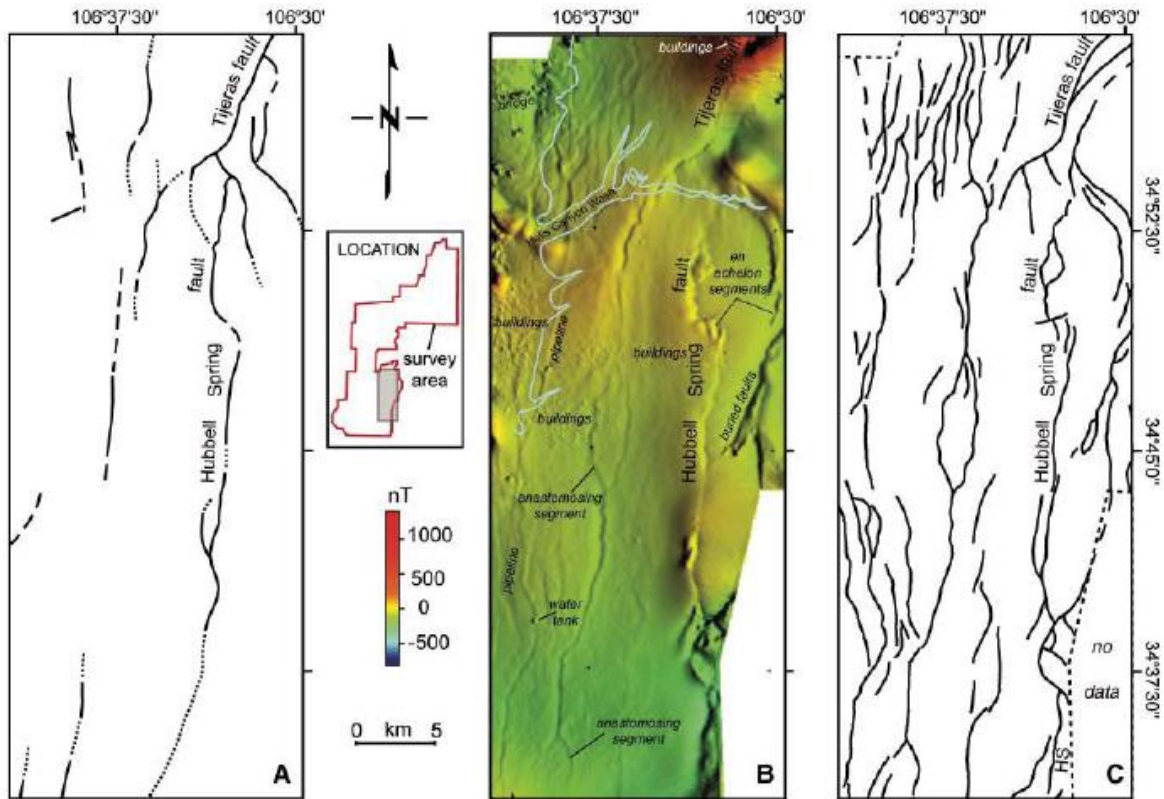


Figure 3. Geologically versus aeromagnetically mapped faults for an area surrounding the Hubbell Spring fault, south of Albuquerque (see inset for location). Except for isolated exposures of Paleozoic sedimentary rocks in the extreme northeastern corner, the area is mapped as Santa Fe Group and younger surficial deposits (Love et al., 1996; Kelley, 1977). (A) Faults mapped before the aeromagnetic data were available are from Machette (1982) and Kelley (1977). (B) Color shaded-relief aeromagnetic image illuminated from the east, with selected features labeled. Note the numerous north-trending linear anomalies, showing apparent en echelon and anastomosing patterns. Compare these to the near lack of expression of the 15- to 50-m-high walls of Hells Canyon Wash (light blue outline). (C) Faults inferred from aeromagnetic data indicating numerous concealed faults and revealing the complexity of faulting in the area. Fault interpretation for the apparent dendritic pattern in the northwest corner of the area is supported by geologic mapping (Love et al., 1996).

Figure 7: Fault traces near the selected site (Granuch and Hudson, 2007).

2.5 Geothermal Resources:

The New Mexico Rio Grande Rift Basin has been the subject of much geothermal exploration with the data organized into many different formats [Blackwell and Richards, 2004; Duffield and Sass, 2003; Jiracek et al., 2003; Reiter et al., 1975, Stone and Mizzell, 1977] with many other reports on spring temperatures, spring chemistry, geothermal municipal wells, geothermal oil and gas wells etc. As geothermal technology has advanced some of the first geothermal studies in the state of New Mexico that concluded that certain resources were uneconomical may now warrant a second look. On technology in of particular note are the systems that were developed by Raster Technologies©. These systems are capable of generating power from geothermal temperatures as low as 165°F using their Binary Cycle Power Plant (Raster Tech., 2011).

The solution to the ultimate question for the proper location of an EGS depends on several factors that include but are not limited to the following:

1. Thermal gradient
2. Temperature of the reservoir
3. Depth to reservoir
4. Volume of reservoir
5. Permeability of the reservoir
6. Fracture Connectivity
7. Presence or absence of water in the reservoir
8. Rock-fluid Interactions
9. Reservoir Pressures

2.5.1 Thermal Gradient and Temperature of the Reservoir:

The thermal gradient within the Albuquerque Basin has been the subject of a number of reports. Some researchers have focused on shallow drill holes and municipal wells and have found shallow (20°C/km) and steep gradients (75°C/km) near Albuquerque, NM (Jiracek, 1983). Other researchers (Reiter et al., 1975; Johnson et al., 2001) have focused on the thermal gradients determined from the oil and gas wells found that the average thermal gradient for the basin approximately is 36.7°C/km. Both sources of data are very useful but care must be taken to not become overly optimistic about extremely steep thermal gradients.

From the work completed by Jiracek (1983) he surveyed the surrounding well fields of Albuquerque, NM in search of shallow thermal waters. His reported bottom-hole temperatures for these wells ranged from 20°C to 46°C however these wells ranged in depths from 300 to

600m in depth. These wells all terminate within the Sante Fe Group and serve as the water supply for the city of Albuquerque. The deeper oil and gas wells commonly penetrate the Mesozoic-aged formations and a few go as deep the Precambrian basement rocks. The bottom-hole temperatures for these oil and gas wells range from 130 °C to almost 200 °C (Johnson et al., 2001). The well depths for these oil and gas wells range from 2000 to 5000m.

2.5.2 Depth and Volume of the Reservoir:

The depth to the reservoir and the volume of the reservoir go hand in hand for site selection after an appropriate temperature has been found. Current thought is that an appropriate depth range for a viable geothermal resource should be on the order of 3 to 5km in depth (MIT Report 2006; Blackwell and Richards, 2004). Conventional thought is that the reservoir thickness should be greater than the spacing of the wells (Ellsworth Per. Comm. 2011). While there are several target sedimentary formations within the basin that may yield suitable temperatures, they are not thick enough and will likely react with the carbon dioxide that is the proposed working fluid for this project. For this reason the Precambrian basement rocks will be the target formation for the EGS system. To get to this resource the site will need to be located away from the center of the basin where the depth to the Precambrian basement rocks is prohibitively deep (Figure 8) [While this figure does not show the true depth to the Precambrian basement rocks it does show the thicknesses of the Tertiary rocks. The Mesozoic and Paleozoic rocks are more uniform in thickness across the basin therefore relative depths can be inferred.] Following the recommendations from the MIT report (2006), a site will be chosen that will allow for 1 to 2 km of penetration into the Precambrian basement for reservoir development of the EGS for a total well depth of approximately 5 km.

2.5.3 Permeability of the Reservoir:

In enhanced geothermal systems there has to be sufficient permeability to allow for economic quantities of fluids to be recovered and injected into the reservoir to maintain the resource (MIT Report, 2006). Typically initial porosities and permeabilities are very low in crystalline basement rocks but substantial fracture permeability may exist if the fractures are under tensional stresses. In the case of the Albuquerque Basin a site can be selected that can take advantage of an existing local network of fractures and faults. It will more than likely be necessary to stimulate the fractures to insure adequate fracture connectivity within the reservoir. Care will need to be taken to limit the possibility of connecting to the more regional network of fractures that will allow the injected fluids to migrate out of the reservoir and adversely impact the surrounding environment. This can be accomplished by staying within the half-graben fault blocks that are currently thought to exist on the Albuquerque Bench near Transocean Isleta-1 exploratory well or through optimized positioning of injection and production wells.

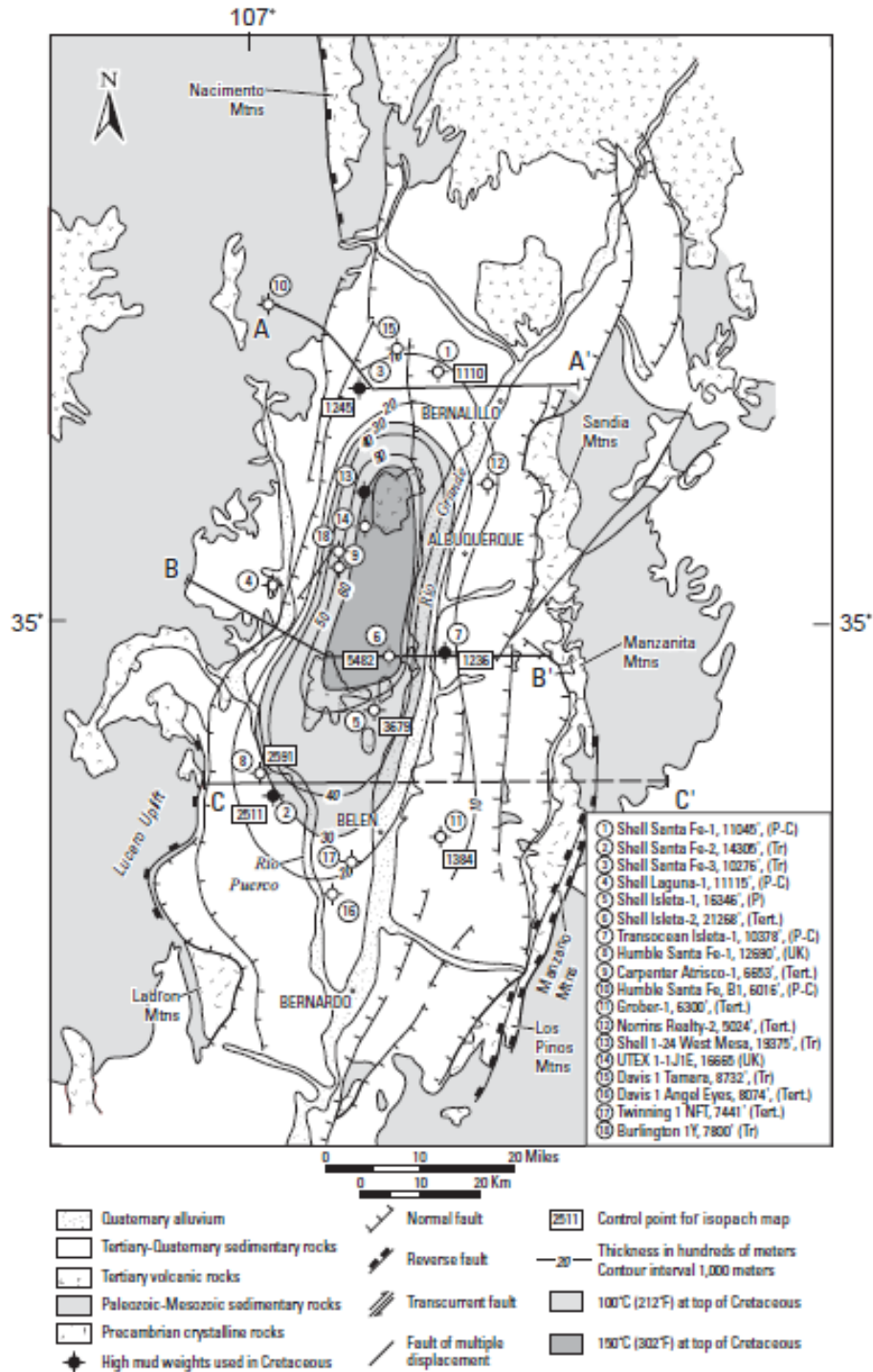


Figure 8: Isopach map of the total present day thickness of Tertiary rocks in the Albuquerque Basin using subsurface drill-hole data (Johnson et al. 2001).

2.5.4 Presence or Absence of Water:

The presence or absence of water within these local fracture systems will depend on whether or not they are sealed. According to Kelley (1977) only the youngest fractures and faults are not sealed due to fracture infilling over geologic time. In either event these fracture systems whether open or closed will become open after the stimulation phase of the reservoir development because they will be the weakest zones within the crystalline bedrock and should deform before other unfractured crystalline rocks.

2.6 Evolution of Energy Release and Moment Magnitude in EGS Reservoirs

To predict the moment magnitude and measure the earthquake size in EGS reservoir, during induced seismicity, we represented a numerical modeling to define small/large fractures. These models allow us to calculate the potential release of energy for different fracture spacing within reservoirs based on measurement of the elastic energy released from failure of a single penny-shaped crack. In this model we also assumed the fracture distribution in whole reservoir with multiple orientations (0 to 90°). For any arbitrary size of fractures failure calculated from finite difference method with FLAC^{3D} and timing of failure is defined base on size of crack which located in such elements. We also considered critical zones in the model and it means that between injection and production wells fracture network is denser. This model was setup with 160 fractures of size 200m with ~100m spacing, 64 fractures of size 500m with ~150m spacing and 12 fractures of size 1000m with ~500m spacing. All fractures distributed in different orientations. The potential release of energy for different fracture spacing within reservoirs is defined based on the evaluation of the elastic energy released from repeating failure of a single large penny-shaped crack. The elastic energy release, E_p , for failure of a penny shaped crack due to a stress drop $\Delta\tau$ is given as

$$E_p = \frac{2\Delta\tau^2 a^3}{3G}. \quad 2.1$$

2.6.1 Moment Magnitude

Energy release from fractures is most conveniently represented as a Moment Magnitude (Aki, 1967; Kanamori, 1977; Keylis-Borok, 1959). The moment magnitude relation is defined as (Purcaru and Berckemer, 1978):

$$\log M_0 = 1.5M_s + 9.1 \quad 2.2$$

where,

M_0 = seismic moment

M_s = moment magnitude.

In this model M_0 is seismic energy which is derived from the elastic energy released by shear on pre-existing fractures. This relation allows us to determine both the spatial and temporal evolution of moment magnitude in EGS reservoirs for the ensemble arrangement of large fractures (200-900m).

First we consider a large single fracture. The moment magnitude for large- and small-spaced fractures (~1-500m) within the reservoir for a spectrum of crack sizes (1m-900m) is calculated. Comparing the effects of the small and large spaced fractures - significant changes of moment-magnitude occurs for the larger cracks (>200m). Also we note that the early moment is higher for closely-spaced fractures, because shear stress reaches the peak strength earlier and stress drop is greater. In closely-spaced fractures, shear stress builds up and fails earlier in time compared to larger fractures.

We initially consider the specific times at which seismic activity occurs as a function potential and total energy. This is then implemented within the THMC simulator to describe the seismic behavior within the reservoir in both the short and long term. The THMC simulator is run to enable the evolution of effective stresses to be determined as a result of HM, TM and CM effects. The model is seeded with fractures and the timing of failure and the strain energy release evaluated. This is then used to show the evolution of seismicity with reservoir development. The distribution of moment magnitudes with time, due to combined thermal, mechanical and chemical effects for a reservoir seeded with 200m fractures is illustrated in **Figure 9**. This outcome indicates that the potential energy within the reservoir containing fracture networks is released with time and goes far from injection. In this simulation we defined 36 zones and in each zone there are 360 fractures with 200m length and 100m spacing and also based on observation, by comparison between the various fracture spacings we can conclude that smaller

spaced fractures generate more events but with smaller energy release and more widely spaced fractures may fail as one or two much larger events.

2.6.2 Global Energy Balance for Fracture Networks

During the rupture process the shear stress drops an amount $\Delta\tau$ from an initial value of τ_i to a final value τ_f . Then we can define an expression for total energy E_T as

$$E_T = \int \Delta\tau^T \Delta\varepsilon dV \quad 2.3$$

$$E_T = \int (\tau_f - \tau_i)^T (\varepsilon_f - \varepsilon_i) dV \quad 2.4$$

where;

ε_i = initial strain

ε_f = final strain

V = volume of the matrix

Potential energy released with the failure of each fracture and the total energy stored within the matrix block allow us to determine the number of events in both the short and long term for varied spaced fracture networks. Here we introduce a relation to obtain the number of events which occur during the failure process based on potential and total energy as

$$N_{event} = \frac{E_T}{E_p} \quad 2.5$$

where;

N_{event} = Number of seismic events,

E_T = Total energy

E_p = Potential energy.

Based on these previous results we define the relation to obtain the number of events per year that occur for different fracture sizes and different location within the reservoir. During triggering, three individual influences of the HM, TM and CM effects may be followed to define their relative influence (although not completed here). These ensemble effects are shown over a period of 10 years production in an IGS reservoir in Figure 9

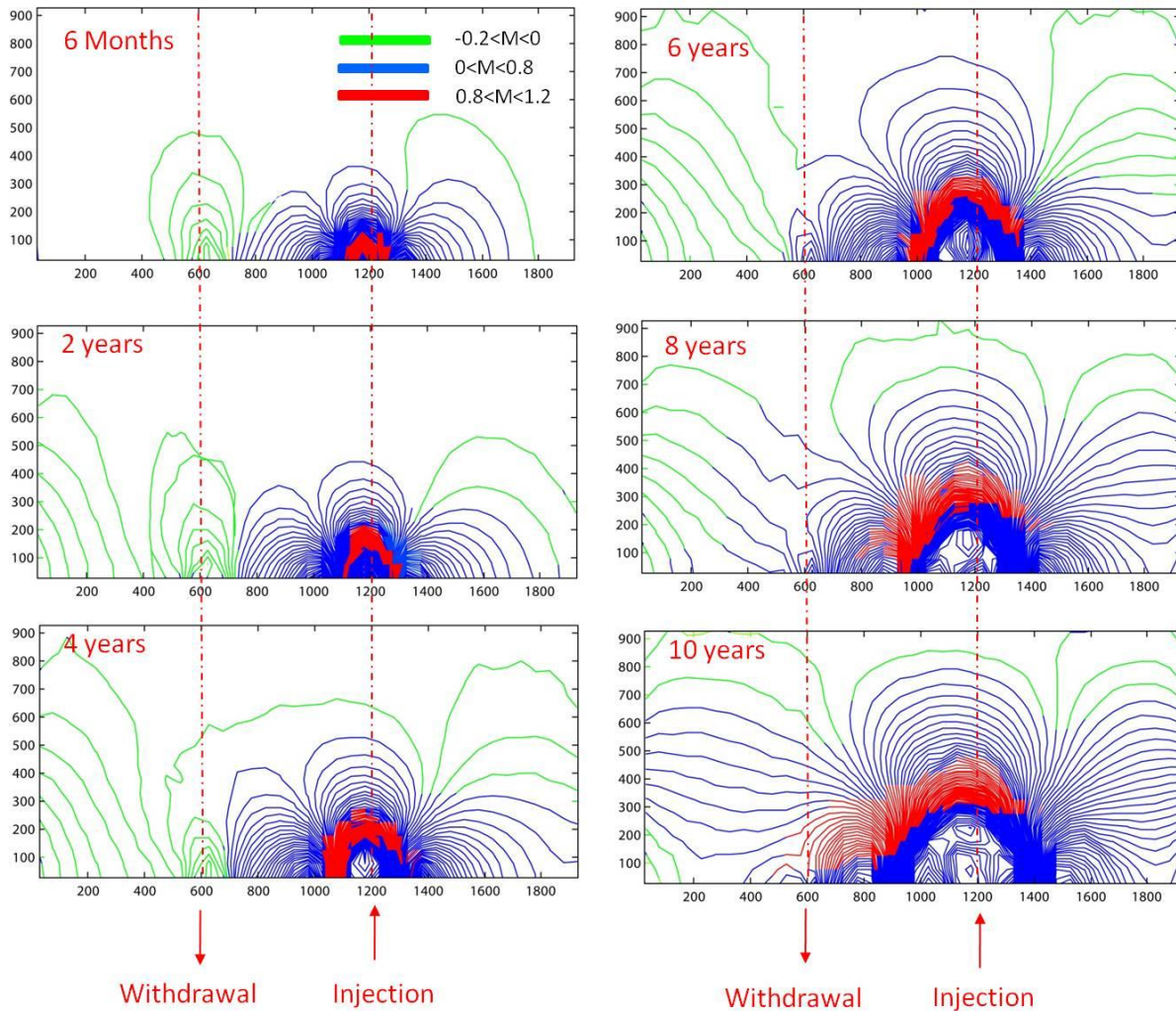


Figure 9: Moment Magnitude

The evolution of moment magnitude in an EGS reservoir with 200m fracture size in 10 years simulation. Solid lines illustrated the failure in each location of reservoir. Green region illustrates smallest event magnitude and red region illustrates the largest potential energy that is released in different locations due to thermal, mechanical and chemical effects. Migration in strain energy occurs within reservoirs.

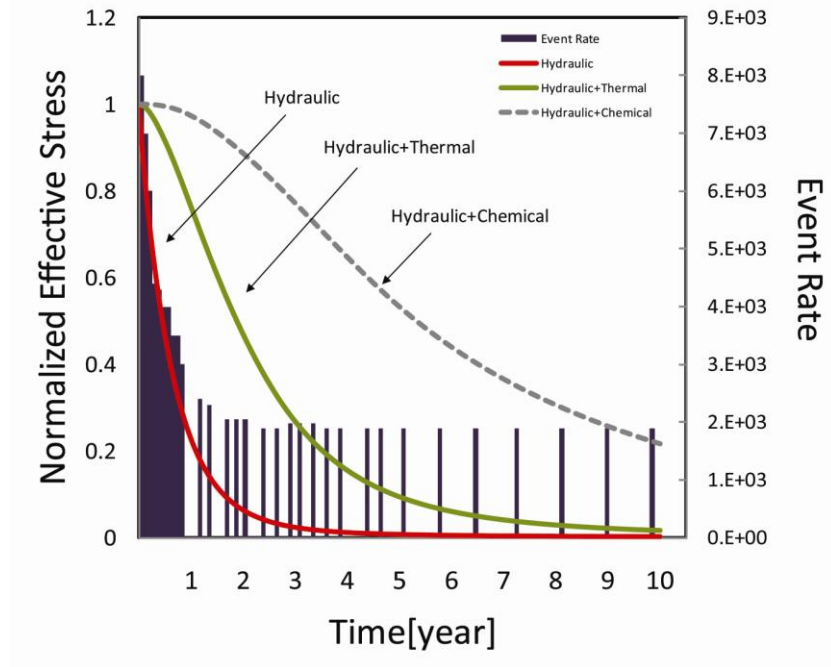


Figure 10: Effects of hydraulic, thermal and chemical behaviors on annual event rate.

2.7 Conclusions and Recommendations:

The site that is selected for this project was selected based on the available literature at the time of the literature survey. The location near Transocean Isleta-1 was selected due to satisfactory depth to Precambrian basement rocks (~3.2 km), geothermal gradient (39°C/km), bottom-hole temperature (131°C), and thickness of the Precambrian basement rock that could be penetrated to create a reservoir (~1.8km) (Johnson et al., 2001). If the geothermal gradient that was determined for the Transocean Isleta-1 well holds true than a bottom-hole temperature of ~200°C is expected at a depth of 5km.

In addition to this the EGS system could be located within a local fault block that could be isolated from the larger fault system that surrounds the site. This will be an important part of the induced seismicity mitigation strategy during site operations. At the time of the literature survey there was an expectation that the Transocean Isleta-1 well could be reconditioned to become one of the EGS wells which would provide considerable cost savings to the project.

3.0 Enhanced Geothermal System (EGS)

3.1 Introduction

Reservoir simulation is the modeling of flow behavior, be it mass, energy or momentum, to predict the future performance of the system under consideration. Typically, this is done for the prediction of the flow of oil, gas and/or water through porous media. However, the basic principles used in these simulations and the ones required for geothermal reservoir simulations are the same.

In 1980 the results of a Code Comparison Study for geothermal reservoir simulators, were published (O'Sullivan, 1985). This study, sponsored by the U.S. Department of Energy, showed that all the codes tested produced very similar results for six carefully selected idealized geothermal reservoir problems. Therefore the study confirmed that the numerical techniques for simulating the movement of heat and mass through a geothermal reservoir were satisfactory, provided that the basic physical assumptions made in setting up the mathematical model, such as the validity of Darcy's law, were accepted.

In the following text, an overview of Enhanced Geothermal System (EGS) is provided. Also, since the main theme of this project is the utilization of CO₂ as a working fluid for EGS, certain important advantages of using the same are provided. A brief review about what are important aspects in geothermal reservoir engineering, differences in geothermal and petroleum reservoir simulation is given. Finally, the approach taken towards modeling the reservoir using CMG STARS™ simulator is provided.

3.1.1 What is Enhanced Geothermal System (EGS)?

In a broad sense, geothermal energy can be defined as the natural heat content of the earth. The geothermal systems can be classified under four main types (Parlaktuna, 1995):

1. Vapor dominated reservoirs: Vapor phase is the continuous phase determining the pressure regime of the reservoir, although hot water and water vapor can co-exist in this reservoir.
2. Liquid dominated reservoirs: Liquid phase is the continuous, pressure determining phase in these reservoirs. The heat recovery from these reservoirs is higher compared to vapor dominated ones because of the boiling of the reservoir fluids and reinjection of produced fluids.
3. Geo-pressured reservoirs: These systems contain fluids having pressures higher than hydrostatic. They generally occur in the zones covered with an impermeable layer.
4. EGS (or formerly known as Hot dry rock): These systems do not contain sufficient fluid to transfer the heat to the surface. The only way to utilize these systems is to

extract the heat energy of the rock by a working fluid, which in our case is CO₂. The fluid is circulated along an artificial fracture between two wells.

Conventional geothermal technology entails the production of useful energy from natural sources of steam or, much more commonly, hot water (Tester et al., 2006). These hydrothermal resources are found in a number of locations around the world, but they are the exception rather than the rule. In most places, the earth grows hotter with increasing depth, but mobile water is absent. The vast majority of the world's accessible geothermal energy is found in rock that is hot but essentially dry -- the so-called hot dry rock (HDR) resource.

The total amount of heat contained in HDR at accessible depths has been estimated to be on the order of 10 billion quads. This is about 800 times greater than the estimated energy content of all hydrothermal resources and 300 times greater than the fossil fuel resource base that includes all petroleum, natural gas, and coal. Like hydrothermal energy resources already being commercially extracted, HDR holds the promise for being an environmentally clean energy resource.

EGS concepts would recover thermal energy contained in subsurface rocks by creating or accessing a system of open, connected fractures through which water can be circulated down injection wells, heated by contact with the rocks, and returned to the surface in production wells to form a closed loop (Figure 11).

A pilot project was conducted at Fenton hill, New Mexico by Los Alamos National Laboratory between 1970 and 1995 (Duchane et al., 1995). The objective of the project was to develop a heat-extraction system in a high-temperature-gradient area with a large volume of uniform, low-permeability, crystalline basement rock on the margin of a hydrothermal system in the Valles Caldera region of New Mexico.

3.1.2 Advantages of using CO₂ as a working fluid

Responding to the need to reduce atmospheric emissions of CO₂, Brown et al. (2000) suggested an EGS concept of utilizing supercritical CO₂ instead of water as a heat transmission fluid. Brown noted certain physical and chemical properties of CO₂ would be advantageous in its operation of an EGS. The following are certain advantages that were proposed (Pruess, 2006; Atrens et. al, 2009):

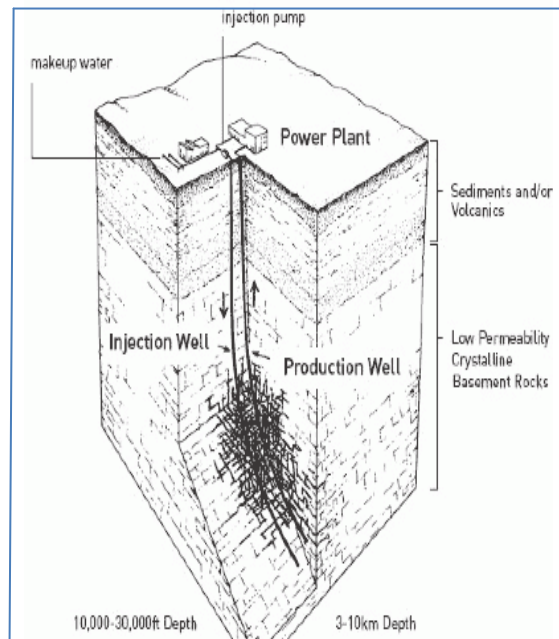


Figure 11: Schematic of a conceptual two-well Enhanced Geothermal System in hot rock in a low-permeability crystalline basement formation (Duchane et al., 1995)

1. Large expansivity, which would generate large density difference between the cold CO₂ in the injection well and the hot CO₂ in the production well, and would provide buoyancy force that would reduce the power consumption of the fluid circulation system.
2. Lower viscosity as compared to water, which would yield larger flow velocities for a given pressure gradient.
3. Low solubility of salts, thus decreasing the potential for scale precipitation in wellbores and surface equipment.
4. Potential for chemical and geological sequestration of CO₂ within the reservoir.
5. Possibility of direct use of produced CO₂ in turbo machinery, instead of using a binary design.

Thus, CO₂ as a working fluid offers numerous advantages over conventional water based EGS. Another important point in favor of CO₂ is that, by using CO₂, the water supply of nearby region will not be affected. Therefore, combining IGCC with EGS seems to be a viable option for generating power without endangering the environment and societal needs.

3.2 Reservoir Simulation

3.2.1 Geothermal reservoir engineering concepts

Geothermal reservoir engineering starts with the determination of well locations and continues with several measurements within the wellbore (well logging, production rates, etc.), interpretation of these data, determination of production mechanisms and performance prediction studies of reservoir behavior. The ultimate goal of these studies is to determine the optimum production conditions to maximize the recovery of heat from the reservoir under suitable economic conditions. The main activity of a reservoir engineer is the prediction of the long-term behavior of the wellbore and/or reservoir under study. In this context, the important questions to be answered are:

1. What is the most suitable development plan of the reservoir?
2. How many wellbores should be drilled to reach the most suitable development plan? What would be the well pattern?
3. What will be the production rates of the wellbores?
4. How much heat will be recovered?
5. How will the change in reservoir temperature be?
6. Will there be a need to apply enhanced recovery techniques to increase the heat recovery from the reservoir?

In order to find answers to those questions, reservoir engineers must pursue a continuous study with a great care from the beginning of production. Reservoir engineers can have a chance to revise his/her studies and a better representation of the reservoir with the addition of new data during production. Unfortunately, the best information about the reservoir is generally available at the latest stage of production from the reservoir. Reservoir engineers must define physical processes of a geothermal system. This can be achieved in three steps:

1. First of all the physical processes that are related to the geothermal system must be defined. Those processes should be used to develop the conceptual model of the reservoir.
2. Secondly, physical and chemical properties of reservoir rock and fluid must be determined.
3. Lastly, mathematical and physical models of the reservoir must be developed with the help of existing data. This model must contain the initial and boundary conditions of the reservoir. The model must be refined with the addition of new data as production continues. The response of the reservoir to production must be matched.

Although there are certain similarities between the oil and natural gas reservoirs and geothermal reservoirs, there are differences that are specific to geothermal reservoirs alone:

- Relatively high reservoir temperatures
- Volcanic origin of reservoir rocks with highly fractured characteristics
- Chemical precipitation of solids within the reservoir during production
- Boiling of water within the reservoir and/or wellbore

3.2.2 CMG STARS™ Simulator

CMG STARS™ is a thermal, K-value compositional, chemical reaction and geomechanics reservoir simulator (CMG STARS™ manual, 2008). It is well suited for modeling geothermal systems, taking into account thermal as well as geomechanic effects.

There are 9 different parts for which information must be fed in order to generate a model:

- i) *Input/Output Control*
Parameters that control the simulator's input and output activities are defined. No significant changes are introduced in this section.
- ii) *Reservoir Description*
This section contains data describing the basic reservoir definition and the simulation grid used to represent it. These data can be classified into simulation grid and refinement grid options, choice of natural fracture reservoir options, well discretization option, basis reservoir rock properties and sector options. For EGS, dual porosity and dual permeability model is used.
- iii) *Other Reservoir Properties*
This section contains data describing other reservoir properties. These data can be classified into rock compressibility, reservoir rock thermal properties and overburden heat loss options. This section is particularly important for EGS simulation since it incorporates heat balance into simulation. Both, overburden and underburden, heat effects are taken into consideration.
- iv) *Component properties*
This section indicates number of each type of component in preparation for fluid data input. In short, we have to provide how many components are present in each phase so that their properties might be calculated. For EGS, it initially assumed that only CO₂ is present in liquid as well as vapor phase.
- v) *Rock-fluid data*
Relative permeabilities, capillary pressures and component adsorption, diffusion and dispersion are defined. Since this data is not available at this time, suitable

values are assumed for k_{rel} and P_c . Adsorption, diffusion and dispersion are taken to be zero.

vi) *Initial conditions*

Initial conditions for pressure, saturation and temperature are provided. Matrix and fractures will have different values for each property. It is here that we make the oil and water saturation to be equal to zero so that the simulator will be modified to a geothermal reservoir simulator.

vii) *Numerical methods control*

Parameters that control the simulator's numerical activities such as time stepping, iterative solution of non-linear flow equations and the solution of resulting system of linear equations are defined. Default parameters are used in this section.

viii) *Geomechanical model*

There are two separate model options available: Plastic-nonlinear elastic deformation model and single-well boundary unloading model. The plastic deformation model performs a finite-element elasto-plastic stress analysis of the reservoir formation using a specific set of displacement and traction boundary conditions. The boundary unloading model is restricted to an axisymmetric radial grid analysis where the wellbore is located at the axis. This section is currently being modified to match the EGS simulation.

ix) *Well and recurrent data*

This section contains data and specifications which may vary with time.

The key information which will be required for simulation and which will be obtained from the geology part of the project is:

- a) Initial reservoir temperature
- b) Initial reservoir pressure
- c) Depth
- d) Fracture spacing

Other important data (which may be approximated, if necessary):

- e) Permeability
- f) Porosity
- g) Grain type
- h) Reservoir Dimensions
- i) Reservoir fluid specifications (whether water or any other component may be present)
- j) Rock-fluid data

3.3 Model Preparation and Results

3.3.1 Model Parameters

Model preparation assumed certain key assumptions:

1. Thermal equilibrium exists everywhere at all times.
2. Injection fluid is pure CO₂. Although in reality, this fluid is about 90-95% CO₂.
3. Dual porosity model. The porosity depends both, on pressure and temperature.

There were other key assumptions such as permeability, porosity, fracture spacing, initial reservoir composition. These values were varied to compare different model results and to determine which variables the model was most sensitive to. This analysis allows for future money to be directed towards defining the variables that would affect reservoir simulation the most .

The following table shows the typical parameters taken for a model:

Table 1: Parameters for EGS model

Parameters	Values
Initial formation temperature	392 °F (200 °C)
Initial formation pressure	5000 psia
Total formation thickness	4921.2 ft (1500 m)
Reservoir depth	8000 ft(2439 m)
Matrix porosity	0.1
Fracture porosity	0.1
Matrix permeability	0.01 md
Fracture permeability	0.6 md
Fracture spacing	32.8 ft (10 m)
Injector – Producer distance	1640.4 ft (500 m)
Injection temperature	60 °F
Initial water saturation	0.5
Residual water saturation (Bennion D., 2007)	0.3
Rock thermal conductivity	0.00034 BTU/ft/sec/°F (2.1 W/m/°C)
Rock specific heat	0.239 BTU/lb/°F (1000 J/kg/°C)

The parameters indicated in green color are varied for different models and then the results are compared. Other parameters are fixed either because they are known from the geology section or because a reasonable assumption has been made in their case.

The model generated in CMG is shown below:

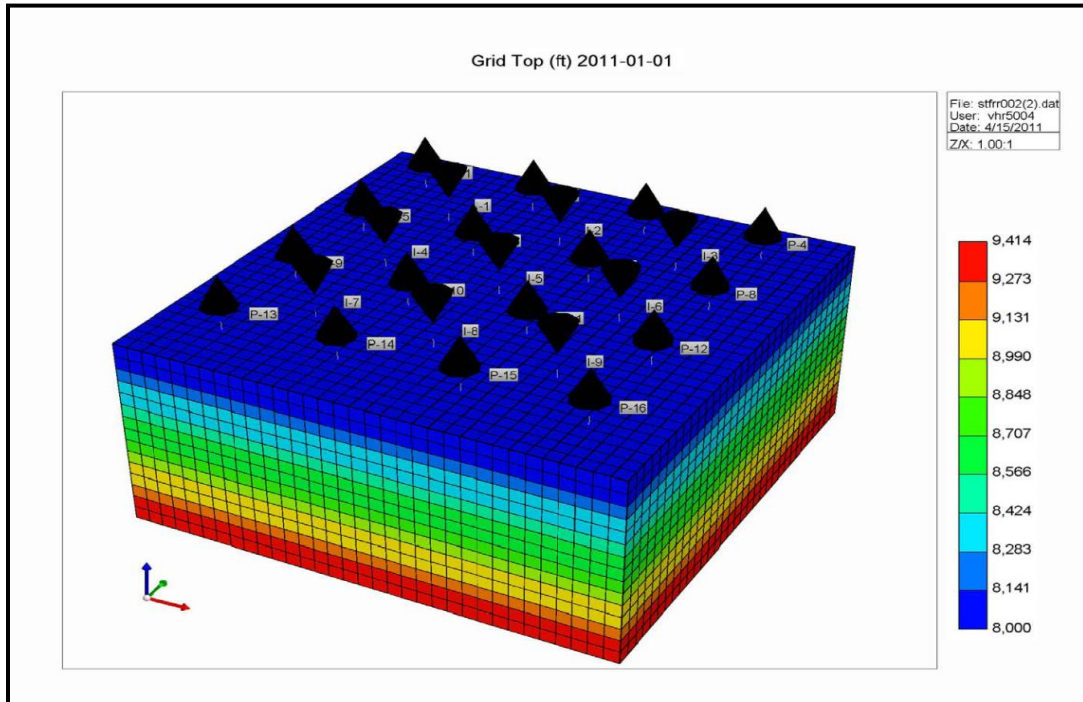


Figure 12: Model grid geometry (side view)

The reservoir geometry can be summarized below:

- 9 Injection and 16 Production wells
- 5-spot pattern for well spacing
- Injector–Producer distance: 1640.4 ft (500 m)
- Additional 1312.3 ft (400 m) space for CO₂ migration

3.3.2 Model results

The following results have been shown for the parameters listed in the table 1 above.

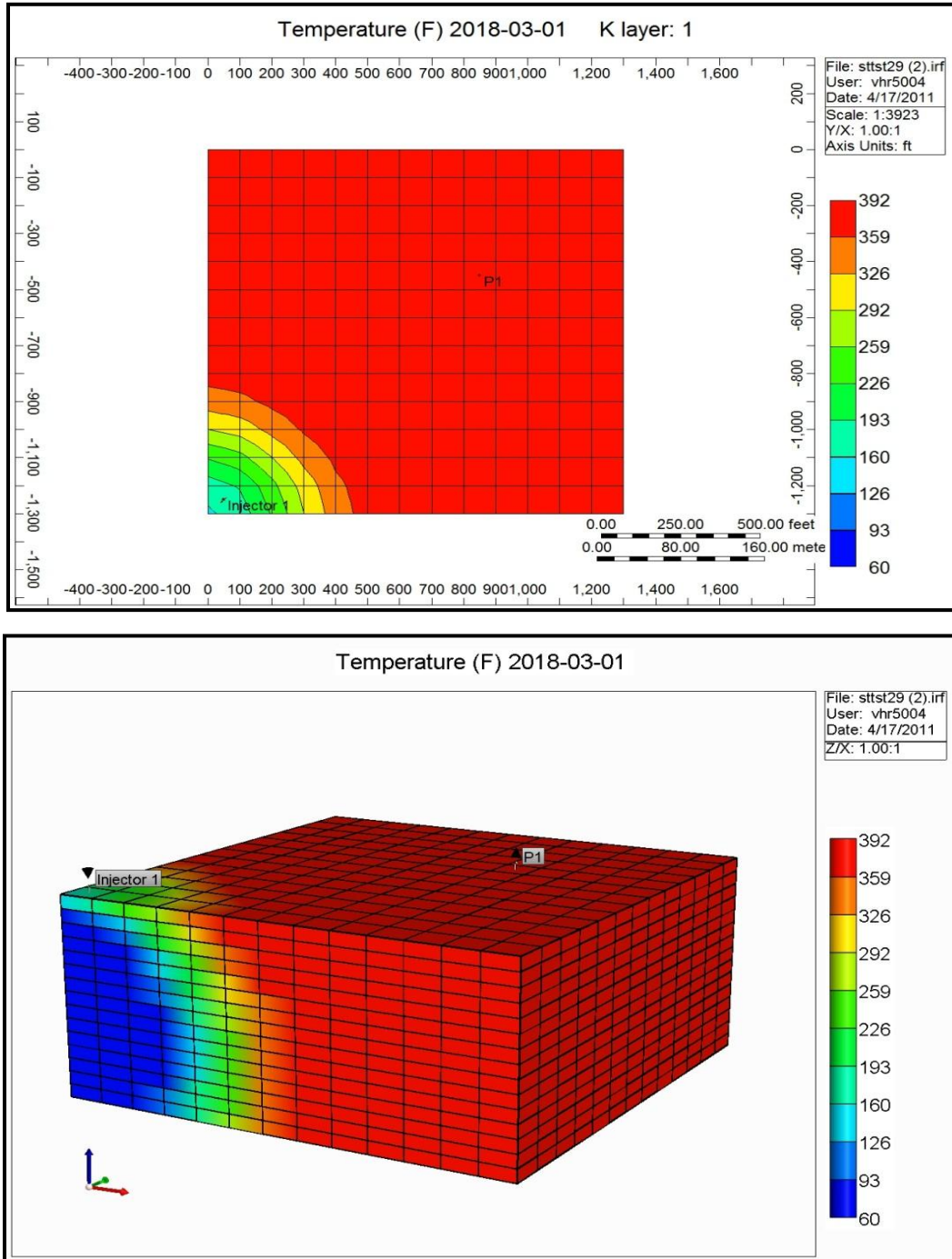


Figure 13: Model results at 2018-03-01

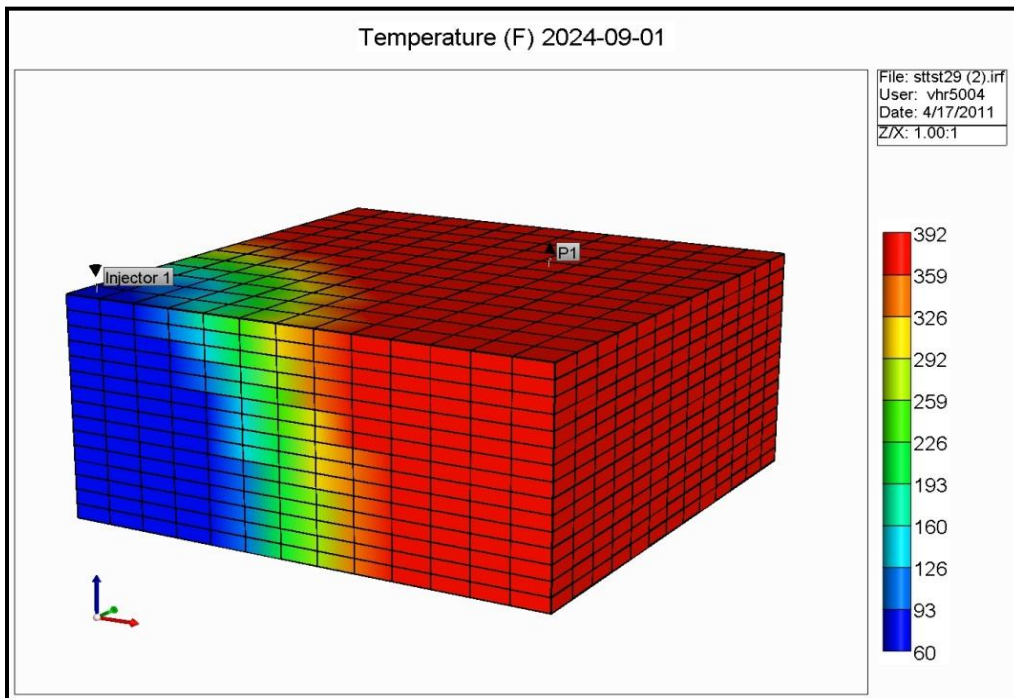
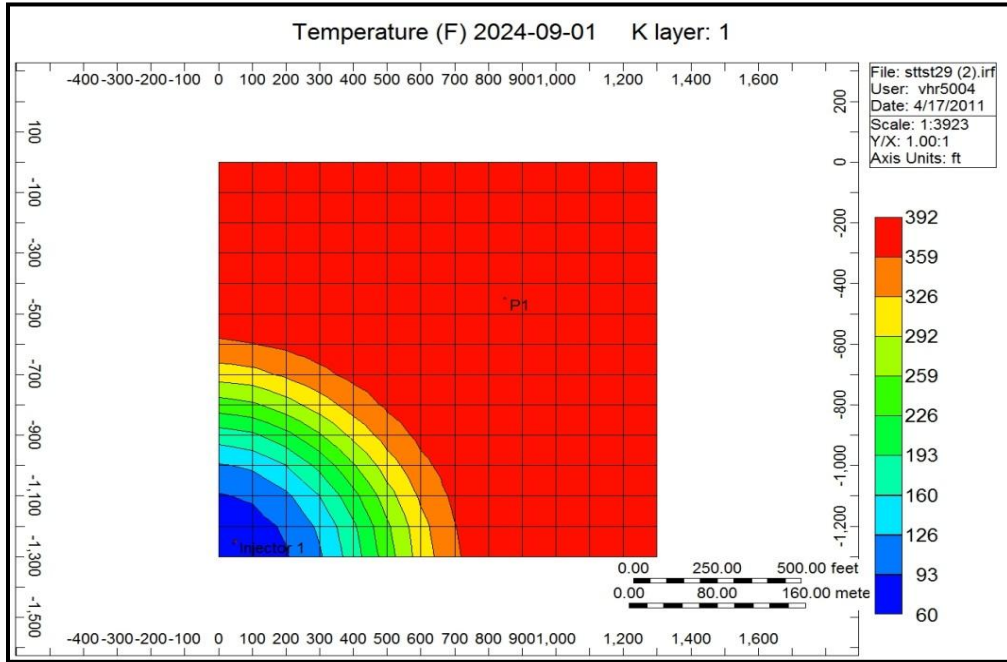


Figure 14: Model results at 2024-09-01

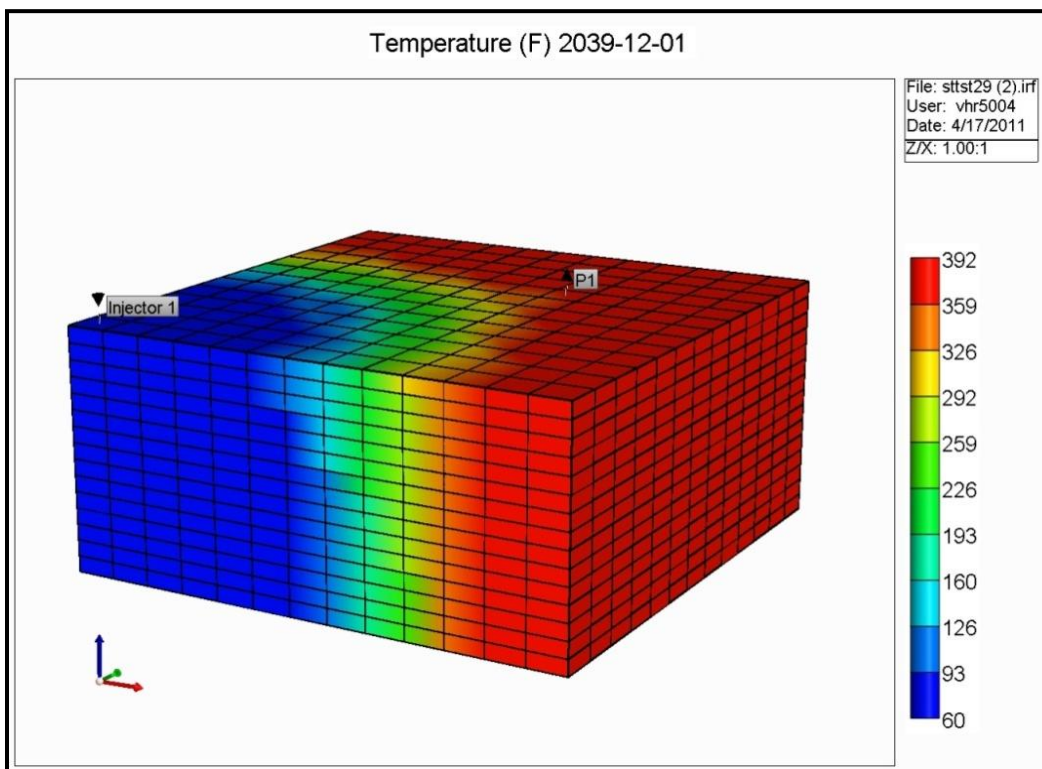
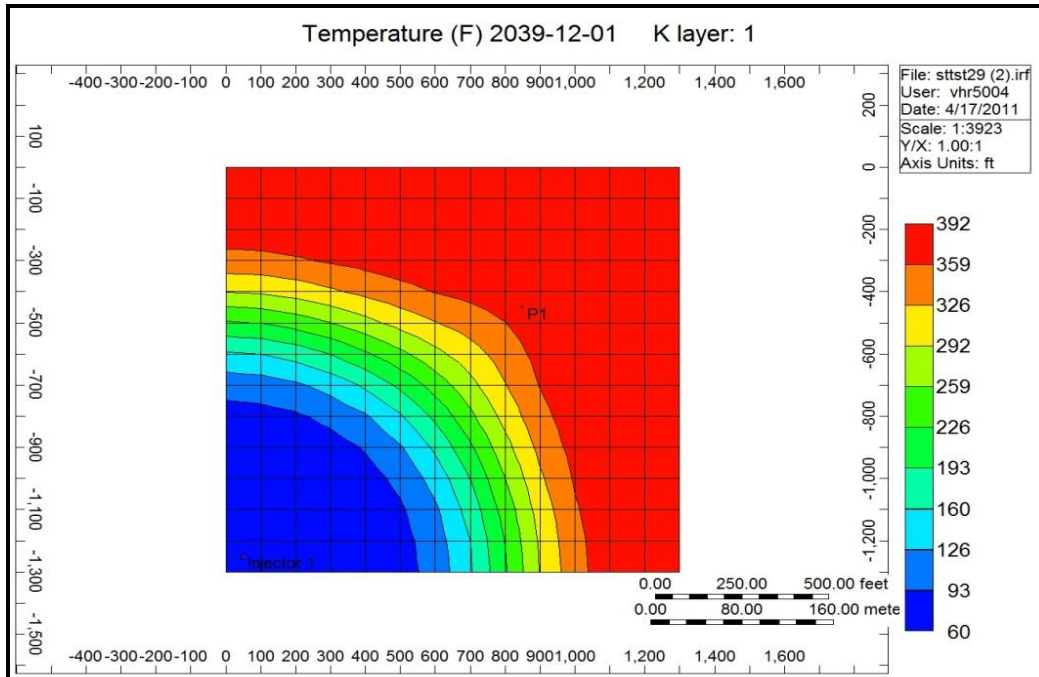


Figure 15: Model results at 2039-12-01

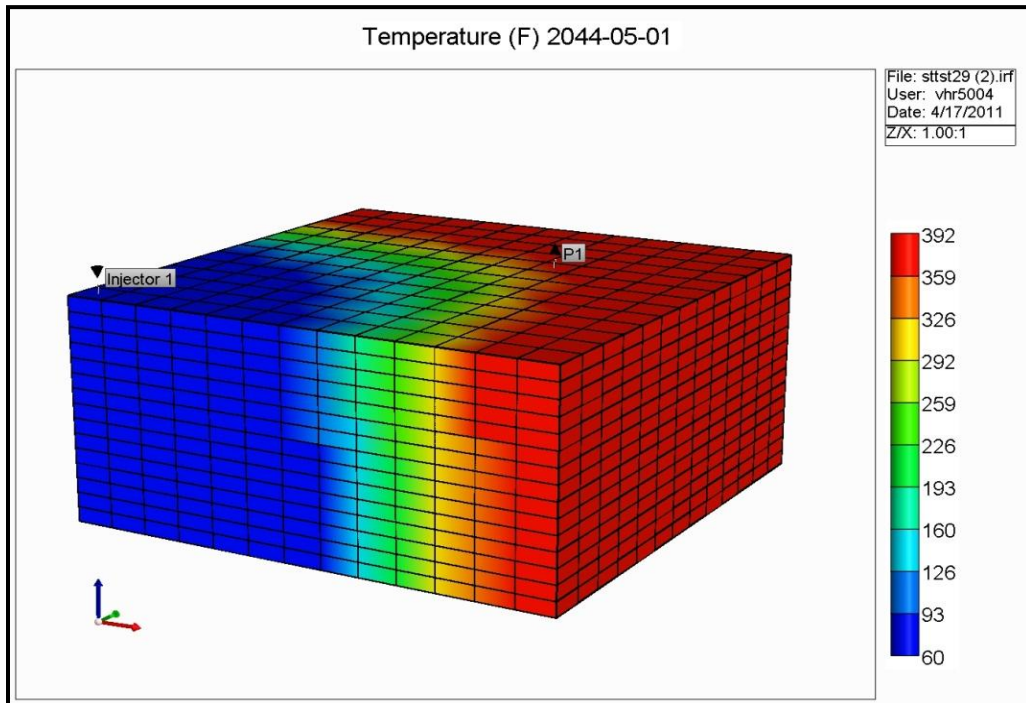
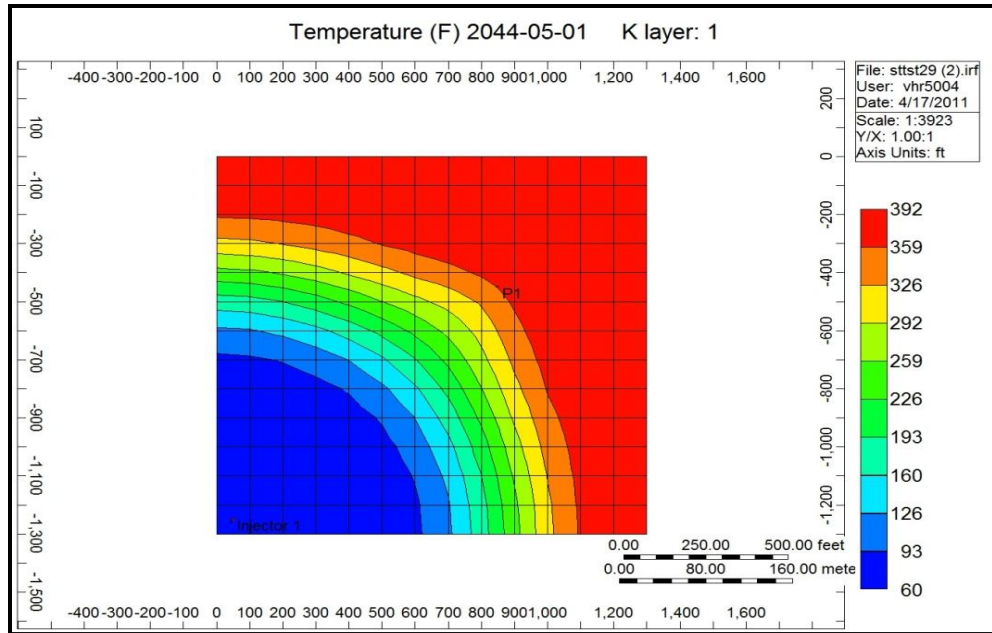


Figure 16: Model results at 2044-05-01

In the figures 13 – 16 above, only a part of the overall 5 spot pattern has been shown. This was done to have a better look at the thermal breakthrough with time. As can be seen, the thermal breakthrough for this case occurred at about 2044 i.e. after about 33 years of operation.

The following table shows the comparison of this breakthrough with different water saturation and fracture spacing.

Table 2: Sensitivity Analysis

Initial water saturation	Fracture Spacing (m)	Temperature Breakthrough (years – rounded off)
0.5	10	33
0.75	10	24
0	10	36
0.5	50	48
0.5	100	72

An important note is that, when water is present and its initial saturation is more than 30% water is produced. However, once the water saturation drops to 30%, only CO₂ will be produced leaving an irreducible water saturation of 30% in the reservoir (Bennion D., 2007).

A general trend that can be observed in Table 2 is that as the fracture spacing increases, the overall permeability of the formation decreases, leading to a delayed temperature breakthrough. Also, the presence of water decreases the breakthrough time. The comparison of the model results with the Spherical Reservoir Model (SRM) is done in next section.

3.4 Thermal Drawdown

SRM is a thermal drawdown model (Elsworth D., 1990) accommodating heat supply from the external geologic formation to a spherical production zone. The circulating fluid and the formation rock are assumed to be in thermal equilibrium. The model is semi-analytical and represents continuum behavior of the reservoir or a representative portion of the reservoir.

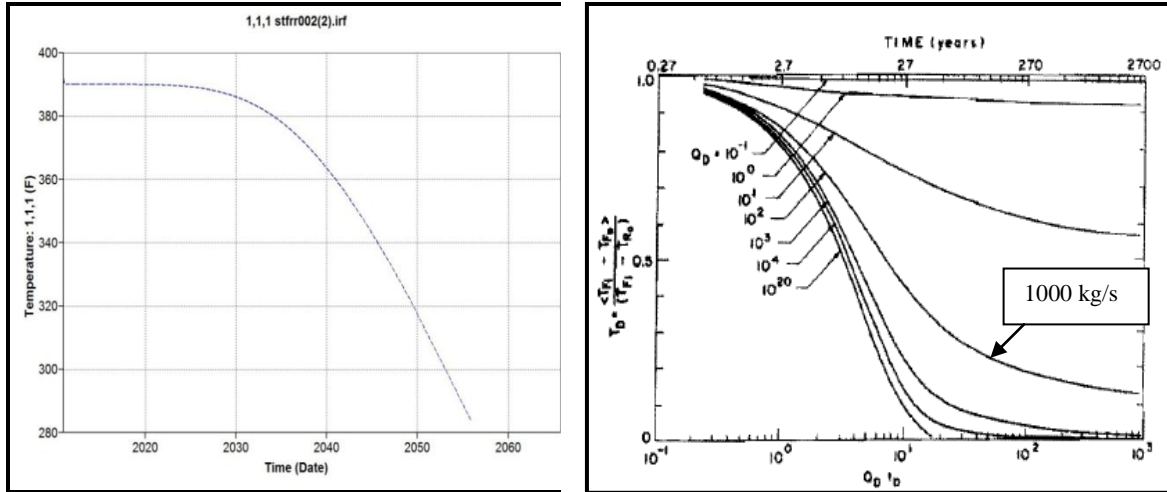


Figure 17: Comparison of CMG and SRM model results and the SRM model.

The comparison shows that the CMG model follows the trend predicted by SRM model. Important point to note at this time is that the injection rate for CMG model is about 880 kg/s while that shown in SRM model is 1000 kg/s. Hence, the curve in SRM model is shifted slightly to the left i.e. thermal breakthrough in SRM occurs at an earlier time.

3.5 Simplified Thermal Drawdown Calculations

A variety of issues relate specifically to interfacing scCO₂-EGS with IGCC. These include all the reservoir interaction behaviors important in ensuring the viability of EGS: viz. reservoir stimulation and development concurrent with developing heat-transfer area within the reservoir. For scCO₂-EGS these include the important and poorly defined role of fluid-rock interactions and their impact on permeability, heat-transfer area and strength characteristics of the reservoir. The latter is ultimately related to production-induced seismicity and the related development of permeability by hydroshears. Although these issues are crucial and relate fundamentally to the viability of scCO₂-EGS they are beyond the scope of this work. Here we limit ourselves to the highest-level linkages between scCO₂-EGS and IGCC – these relate to anticipated thermal output from such a system and mechanism of interfacing the output stream with IGCC via surface plant. We discuss only the issue of thermal output in the following in particular related to anticipated thermal drawdown within the reservoir. This analysis relies on the selection of (i) an appropriate reservoir configuration and (ii) appropriate mechanistic models for thermal drawdown.

3.5.1 Reservoir configurations

A variety of potential configurations exist for reservoir development. For the demonstration-level projects currently observed, these configurations have typically been a doublet (single injector and producer) or flanked doublet (single injector flanked by dual

producers split from a single surface hole). This configuration is peculiar to demonstration projects as it provides the most effective and lowest-cost access to a deep reservoir. However, for large-scale development, this configuration is likely to be supplanted by other well configurations [Figure 18]. Typical within the petroleum field is the repeating “five-spot” pattern (Pruess, 2006). This regular grid is common in shallow regular reservoirs but is disadvantaged where the reservoir is deep as it requires multiple deep wells to access the reservoir zone. Alternative configurations are to examine vertically stacked reservoirs (Elsworth, 1989) or horizontally aligned reservoirs, now feasible with advances in horizontal drilling technology. It is not clear whether drilling technology in hard rock is sufficiently advanced to allow the latter.

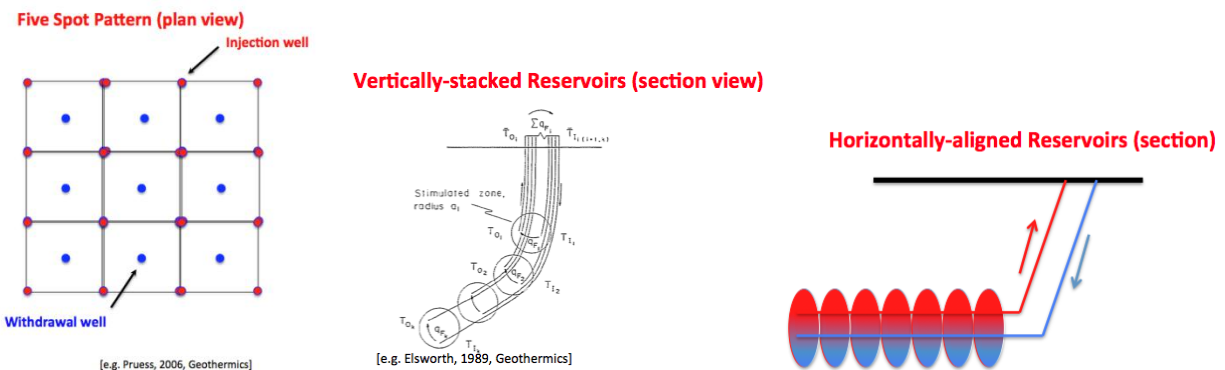


Figure 18: Five spot, and vertically and horizontally stacked reservoir configurations.

3.5.2 Thermal drawdown analysis

Somewhat independent of the well configuration thermal drawdown within the reservoir may be evaluated with knowledge of the thermophysical properties of the reservoir rocks and circulated fluid and the geometry of the transport connections within the reservoir. For first order analysis spherical reservoir and parallel flow models are reasonable candidates to represent behavior [Figure 19]. The spherical reservoir model (SRM) assumes that both the reservoir and circulated fluids are at thermal equilibrium with temperatures augmented by heat supply from the far-field by conduction (Elsworth, 1989a&b). This model gives adequate estimates for heat supply where fracture spacing within the reservoir is small but overestimates thermal output where spacing is large. Where fracture spacing is large the parallel fracture model (PFM) provides better estimates of thermal output and of thermal drawdown although the boundary of the reservoir is assumed thermally isolated and no supplemental heat supply is possible (Gringarten and Witherspoon, 1973; Gringarten et al, 1975). In practice this latter constraint is of second-order importance and thermal drawdown may be evaluated from knowledge of the previous thermophysical properties supplemented by reservoir volume, fracture spacing and fluid throughput (Elsworth, 1990).

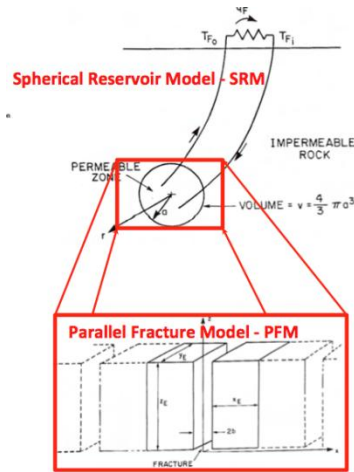


Figure 19: Congruence of spherical reservoir (SRM) and parallel fracture (PFM) models to represent deep EGS reservoirs.

The appropriate thermo-physical properties for the reservoir and fluids are given in Table 3. The non-dimensional thermal drawdown (T_D) scales with three other non-dimensional parameters of flow rate (Q_D), time (t_D) and fracture spacing (x_D) (Elsworth, 1990). These are:

$$T_D = \frac{T_{Fi} - T_{Fr}}{T_{Fi} - T_R}; Q_D = \frac{q_F \rho_F c_F}{\lambda_R a}; t_D = \frac{\lambda_R t}{\rho_R c_R a^2}; x_D = \frac{x_E}{a} \quad 3.1$$

where subscripts are for fluid (F) and rock (R), reservoir inlet (i) and outlet (r), flow rate (q), density (ρ), specific heat capacity (c), thermal conductivity (λ), reservoir radius (a), fracture spacing (x_E) and time (t).

Table 3: Thermophysical material parameters appropriate for sCO₂-EGS reservoir modeling.

Property	Rock	Water	CO ₂ (200C)	Units
Thermal Conductivity	2.1	0.6	0.015	W/m.K
Density	2600	1000	231	kg/m ³
Specific Heat Capacity	1000	4181	1364	J/kg.K
Thermal Diffusivity	8.1E-07	1.4E-07	4.8E-08	m ² /s

Where the thermo physical parameters of Table 3 are used, the thermal drawdown of candidate sCO₂-EGS reservoirs may be evaluated. We assume doublet well spacing of 500m as a reasonable candidate separation, fracture spacing in the range 10-100m and fluid circulation rates of 100 and 1000 kg/s of sCO₂. The resulting rates of thermal drawdown are shown in Figure 20 for the SRM and PFM models.

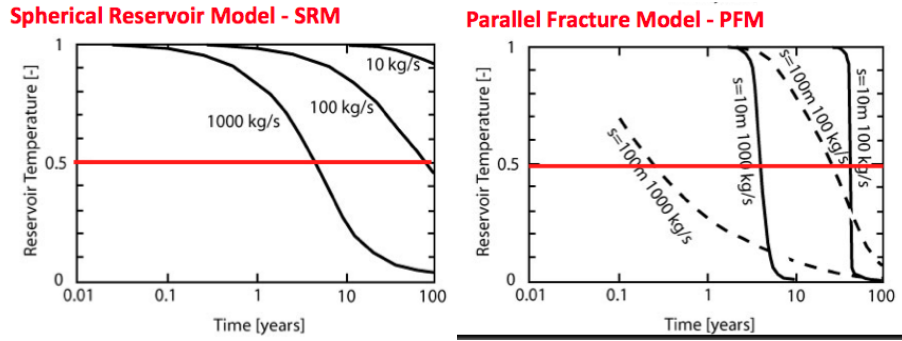


Figure 20: Thermal drawdown (TD) with time for sCO₂ circulation at rates of 100 and 1000 kg/s for fracture spacing within the reservoir of 10m and 100m. Reservoir is 0.125 km³.

3.5.3. Thermal output

With feasible limits placed on circulation rates to ensure a long-lived reservoir, the thermal output may be straightforwardly evaluated from the product of mass flowrate, injection-to-withdrawal temperature differential and specific heat of the working fluid. Thus, the thermal output (W_{th}) is defined as

$$W_{th} = q_F \rho_F (T_{Fi} - T_{Fo}) c_F \quad 3.2$$

where all terms are as defined previously. Since the IGCC plant is merely supplying the make-up CO₂ to replace leak-off losses, then the circulation rate of the sCO₂-EGS system is in direct proportion to the make-up volume rate. For presumed losses of 5%-10% the ultimate reservoir circulation volumes are in the proportion of 20-10 times the IGCC output rates, respectively. Thus IGCC-sCO₂ production rates of the order of 80 kg/s (Table 3) translate to sCO₂-EGS circulation rates of the order of 800 kg/s (10% loss) to 1600 kg/s (5%). For a presumed reservoir temperature of 200 °C and a reinjection temperature of 60 °C the thermal drop across the system is 140 °C. This results in an augmented upper bound (geo)thermal output of ~150-300 MW_{th} (5%-10% loss) to supplement the 550 MW_e from the IGCC.

3.5.4 Thermal drawdown in prototypical reservoir

Thermal drawdown within the PFM occurs most rapidly for circulation at 1000 kg/s. Where the fractures are widely spaced (100 m) thermal supply to the circulating fluid is conduction-limited and the reservoir cools rapidly - the reservoir lifetime is of the order of months. Reservoir lifetime is extended for more narrowly spaced fractures and the reservoir approaches a condition of being flowrate limited as evident in the steep decline curve of Figure 21. In this configuration, the thermal drawdown is similar to that of the SRM as in each instance the fluid and average rock temperatures are in equilibrium. However, at this rate of circulation the thermal drawdown is still too severe to be commercially viable limiting the reservoir lifetime to only a few years. However the reservoir lifetime is extended where the circulation rate is reduced. Where the circulation rate is reduced to 100 kg/s the reservoir approaches a state of thermal equilibrium

even for widely spaced fractures (100m) and reservoir lifetimes (50% drawdown) are congruent for SRM and PFM as of the order of 20-50y. Thus, limiting rates of circulation (100 kg/s), reservoir volumes (one-eighth of a cubic kilometer) and fracture spacing (<100m) are defined as feasible for reservoir lifetimes of the order of 30 years.

These estimates are consistent with observations scaled from other demonstration projects, most notably the drawdown rates observed at Fenton Hill (USA) and at Rosemanowes (UK) as illustrated in Figure 21.

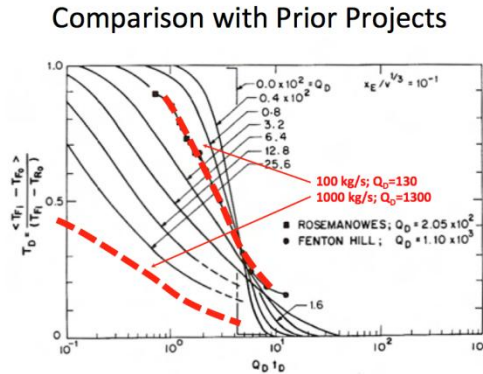


Figure 21: Scaled rates of drawdown for recovery at 1000 and 100 kg/s for the prototypical reservoirs considered here and for prior demonstration projects at Fenton Hill (USA) and at Rosemanowes (UK) (Elsworth, 1990).

3.6 CO₂ Corrosion

A review from oil and gas industries shows that carbon dioxide systems are one of the most common environments where corrosion occurs. Carbon dioxide forms a weak acid known as carbonic acid (H₂CO₃) in water, a relatively slow reaction. However, CO₂ corrosion rates are greater than the effect of carbonic acid alone. Cathodic depolarization may occur, and other attack mechanisms may also be at work. The presence of salts is relatively unimportant.

Corrosion rates in a CO₂ system can reach very high levels (thousands of mils per year), but it can be effectively inhibited. Velocity effects are very important in the CO₂ system; turbulence is often a critical factor in pushing a sweet system into a corrosive regime. This is because it either prevents formation or removes a protective iron carbonate (siderite) scale. Conditions favoring the formation of the protective iron carbonate scale are elevated temperature, increased pH (bicarbonate waters) and lack of turbulence. Magnetite scales are also formed in CO₂ systems, and corrosion product scales often consist of layers or mixtures of siderite and magnetite. CO₂ corrosion products include iron carbonate (siderite, FeCO₃), Iron oxide, and magnetite. Corrosion product colors may be green, tan, or brown to black.

In this EGS system, although elevated temperatures are present, increases of pH and laminar regime cannot occur, which are essential to the creation of the protective layer. Hence, another inhibition method is required to match the operational conditions found at the site. One such method is the use of austenitic grades of stainless steel. These steels were developed for use in both mild and harsh, corrosive environments. They are a chromium-nickel alloy. The name austenitic is derived from the type of crystal structure from which it is comprised. 304 stainless (18% Cr – 8% Ni) is the basic material and is used more than any other stainless steel. Because of their chromium content, austenitic stainless steels form a passive film to provide protection against corrosion. The addition of nickel stabilizes the austenitic crystal structure and interacts with chromium to maintain the passive film. The material is non-magnetic. There are many grades of austenitic stainless steels which are alloyed for various applications. Thus, the material of construction for piping system is suggested to contain a high percent of Chromium and Nickel for the prevention of CO₂ corrosion.

3.7 Geothermal Energy Conversion Systems

3.7.1 Introduction:

The geothermal resource at the selected site is at the cusp of either a binary or a double flash energy conversion system if the working fluid was only water. The expected pressures and temperatures within the reservoir are firmly within the liquid phase envelope of water (See Figure 22). However, the expected pressures and temperatures within the reservoir are firmly within the supercritical region of carbon dioxide (See Figure 23). In addition to the phase behavior of the water and carbon dioxide mixture, its corrosive nature must be accounted for within any conversion system due to lifespan concerns. This suggests that there are two general solutions, either the geofluid is used as is or it goes through a separation process that creates a scCO₂ stream and a water stream.

For either fluid there is a limit on the amount of energy that can be recovered. This maximum value for complete energy conversion is described by thermodynamics. A calculation similar to Dagdan (2007) shows that for a flow rate of 180 kg/s of water will result in approximately 150MW of power. The same flow rate for scCO₂ will result in approximately 30MW. If the flow rate of 1000 kg/s as proposed for the circulation rate for this project the resulting power is 834MW for water and 164 MW for scCO₂. The difference between the two conditions may not seem significant but the opportunity to realize an additional 14MW (scCO₂; 1000kg/s versus water; 180kg/s) of power is similar to a capacity increase of nearly 10% in a turbine.

3.7.2 Binary Conversion Systems

The binary conversion system converts heat to electricity by transferring the heat from the geothermal fluid to a secondary fluid which is then in turn used to drive a turbine. This method will use the geofluid as it is produced from the reservoir with no separation processes. A schematic of a typical binary system is presented in figure 24. The net thermal efficiency for a system is typically between 5 and 15% with lower thermal efficiencies at lower temperatures and higher thermal efficiencies at higher temperatures (Tester et. al., 2006). The binary system is most applicable for use with geothermal reservoir temperatures below 250°C and at moderate pressures (Tester et. al., 2006).

There are several advantages for the use of binary conversion systems for use with mixtures of water and scCO₂. Firstly there is a limit on the exposure of the corrosive mixture of fluids with expensive working parts. By containing the geofluid to a pipe, the corrosion can be controlled with appropriate coatings, and the corrosion that does occur can be predicted. After the appropriate time duration the pipe can be replaced. A second advantage is that a greater proportion of heat energy can be capture through the use engineered secondary heat transfer fluids. A third advantage for this system that is related to plant design is the use of a water based cooling tower instead of an air-based system. This will increase the conversion efficiency of the plant by approximately 0.2% and will help control cost (Mendrinis et al. 2011). As presented by Mendrinis et al. (2011) the “cost of a high conversion efficiency air-cooled tower may cost 10 times more than the wet-cooled tower, which may result in raising overall plant costs by 50%.”

Upon closer inspection of the binary energy conversion system there are doubts about the efficiency of the system that must be used to capture the energy potential of the scCO₂. To deal with the estimated produced fluids pressures of ~3000 psia (thermo-siphon) will require thicker walled pipes within the heat exchanger. This introduces a substantial inefficiency in the heat exchanger. This inefficiency is presented in Figures 25(a) and 25(b). From this plot it can be see that thicker walled pipes have significant heat transfer inefficiencies associated with them. This inefficiency increases as pipe diameter increases. For a 24 inch diameter pipe the differences approximate an order of magnitude in energy that can be transmitted across the pipe. This inefficiency becomes less pronounced (Figure 25 (b)) as the pipe diameters decrease because the pipe wall thickness differences between the three schedules of pipe become less. (Please refer to the appendix at the end of this section for additional details.)

There is an additional inefficiency in the system that is directly related to the nature of the scCO₂. Following the calculations presented by Dagdan (2007) the maximum energy rate of scCO₂ is approximately 30,000 KW while the maximum energy rate of water is 150,000 KW for an initial temperature of 210°C and a mass flow rate of 180 kg/s. Once the net thermal efficiency is considered the 30,000 KW becomes approximately 5,000 KW and after the heat transfer efficiency is considered are combined the likely power to be generated will be 500KW for the

schedule 180 pipe at a 15 cm diameter pipe. These combined inefficiencies suggest that an alternative energy conversion system should be used that makes better use of the produced scCO_2 energy.

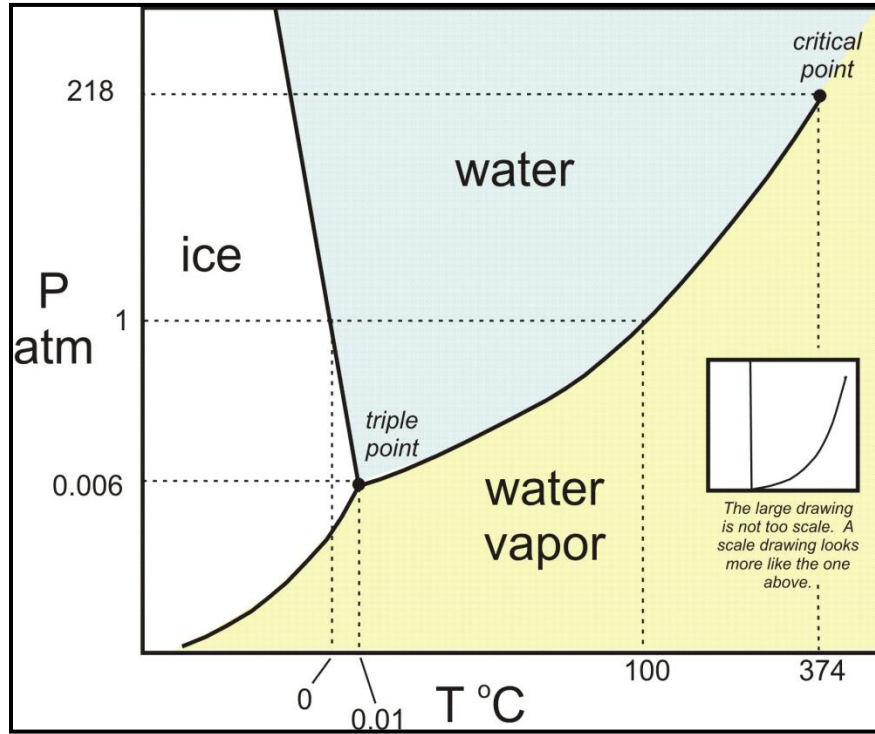


Figure 22: Phase Diagram for Pure Water (Mogk 2011)

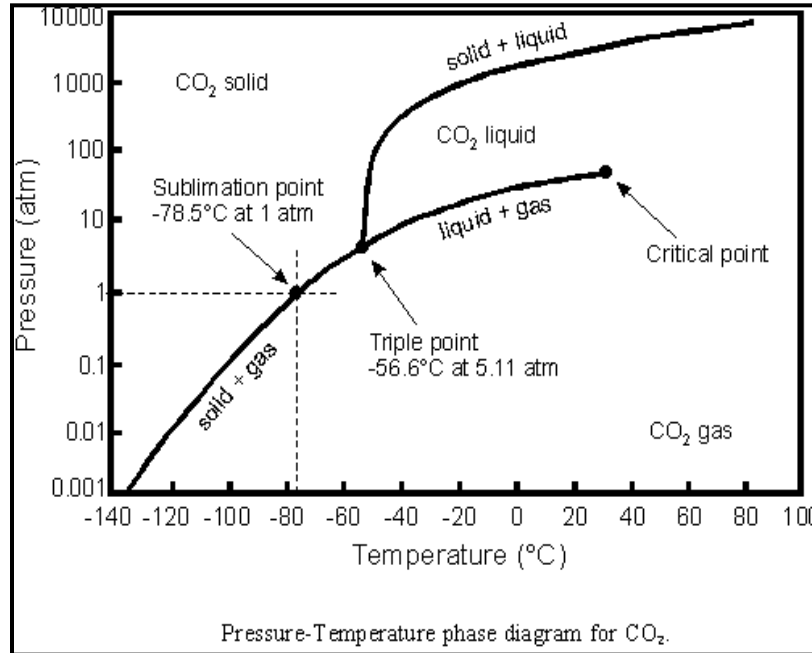


Figure 23: Phase Diagram for CO₂

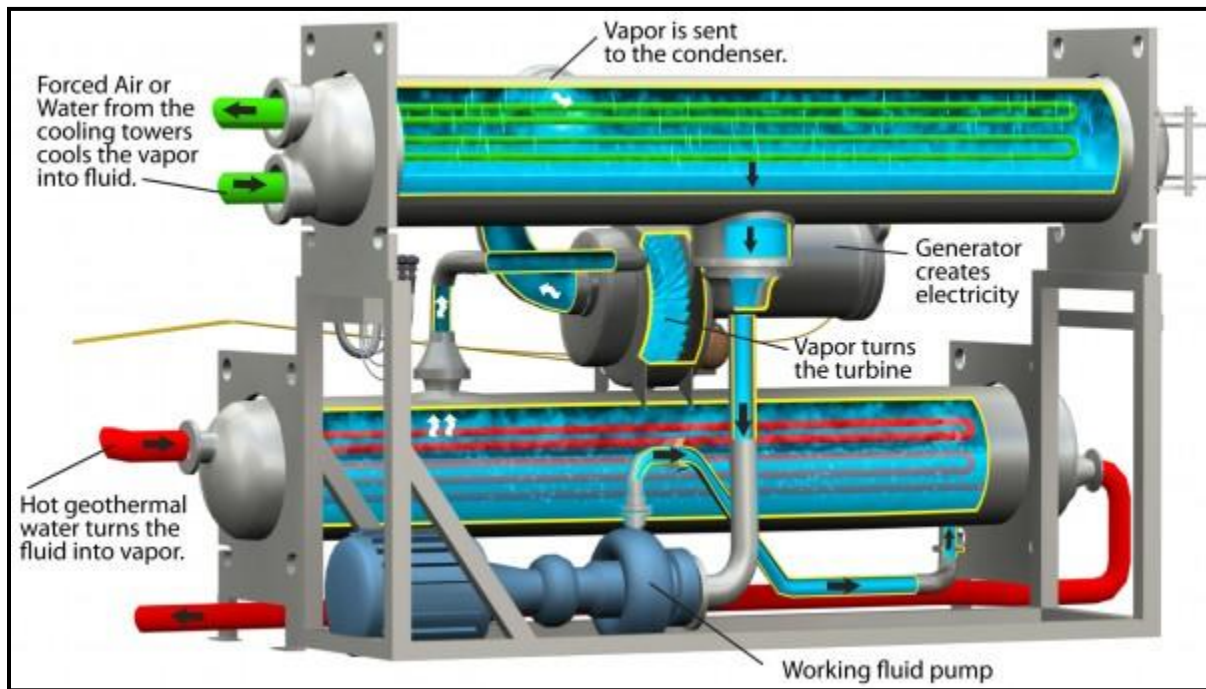


Figure 24: Binary Heat Exchanger Raster Technologies (2011)

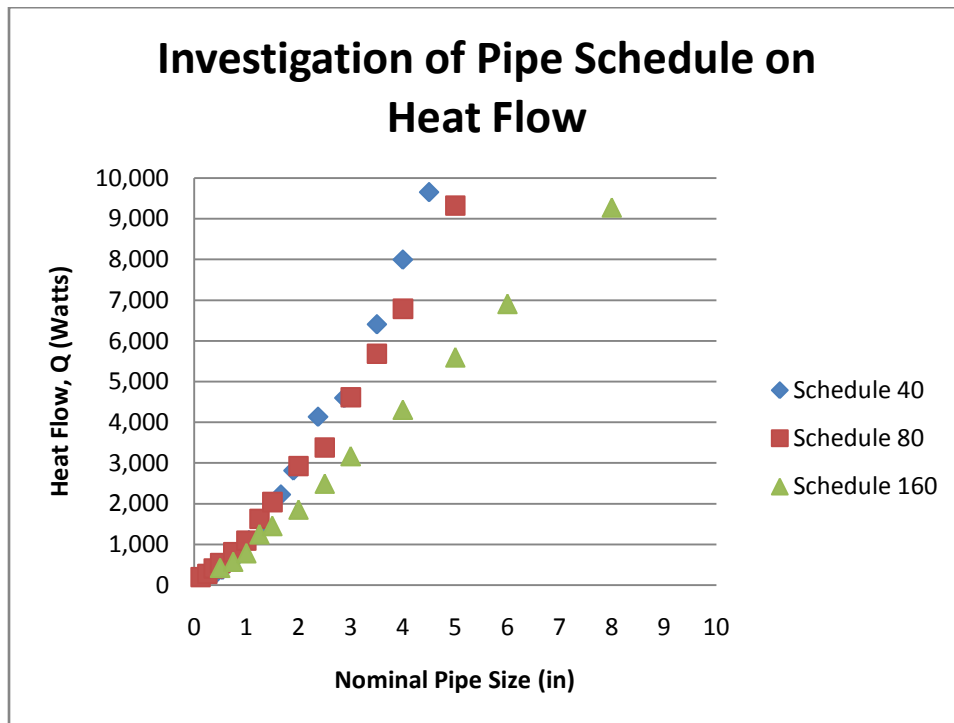
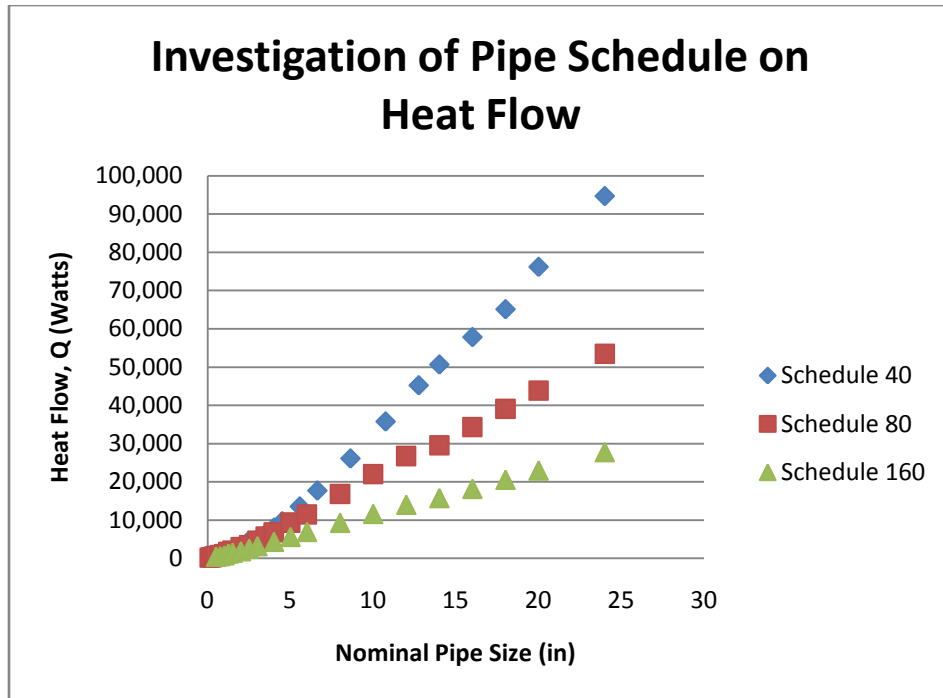


Figure 25 (a) & (b): Wall Thickness Effect on Heat Flow

3.7.3 Flash Conversion Systems

The flash conversion system converts heat to electricity by allowing the produced geofluid's pressure to decrease at constant enthalpy which produces steam which in turn drives a turbine. There are three different types of flash conversion systems. There are single, double, and triple flash systems. Single flash and double flash systems are typically used for subcritical conditions while the triple flash system is a proposed system for supercritical geofluids (Tester et. al., 2006). All three systems operate in a similar manner. A single flash system has one constant enthalpy pressure decrease while the double has two and the triple has three such pressure decreases.

The double flash system is more efficient at extracting workable heat energy for electricity generation than a single flash system (Tester et. al., 2006). A double flash conversion system uses two constant enthalpy pressure decreases to create steam at a high pressure and at a lower pressure (See Figure 26). Typically the outflow of the high pressure is fed into the lower pressure steam flow. This allows for additional electricity to be generated. An order of magnitude estimate is that a single flash system sized for 50MW requires 1000kg/s fluid circulation and 200°C (Tester et. al., 2006). A double flash system can produce the same 50 MW at 1000kg/s fluid circulation rate at 180°C (Tester et. al., 2006). This additional efficiency will be required to maximize energy conversion during the initial field development until scCO₂ begins to be produced.

By itself a flash system is not appropriate for a geofluid that contains both water and scCO₂. In addition to scaling issues from phase changes from water there will also be significant corrosion of the turbines which will adversely affect their performance and lifespan. At the pressures and temperatures experienced within the reservoir water and scCO₂ are expected. If the flash pressures are determined for either fluid without consideration of the other fluid significant energy losses will occur.

An additional caveat for energy conversion in this system is the strong desire to keep the scCO₂ in the super critical state throughout the entire process including reinjection. Through the flashing approach the scCO₂ will become a gas. The parasitic loading of reforming the scCO₂ will represent a significant inefficiency that will affect net power to the grid. To produce significantly more power and decrease operation costs the two fluids need to be separated and processed according to their own physical and phase behaviors.

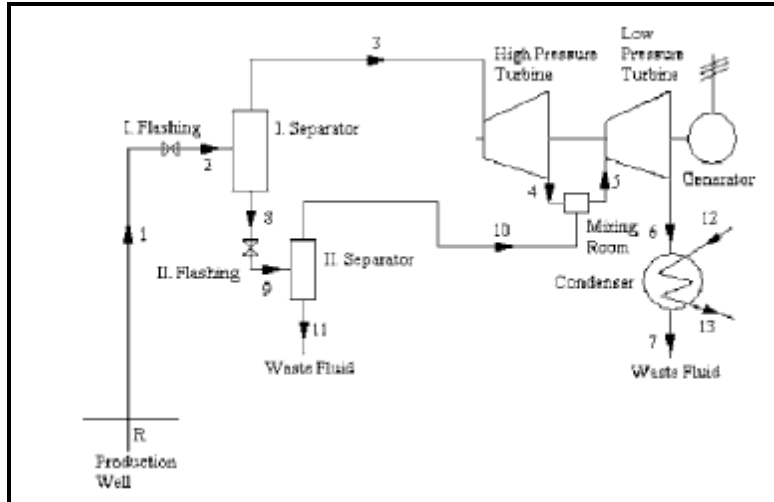


Figure 26: Double Flash Power Plant (Dagan 2007)

3.7.4 Gravity Separation- scCO₂-Double Flash Conversion System

This proposed energy conversion system is the result of the literature survey associated with this project. To maximize energy conversion from both produced liquids they must be first separated into different energy conversion streams to take advantage of their very different phase behaviors. While it is desirable to bring the water stream to near standards conditions it is not desirable to do the same for the scCO₂ stream. For this plant it is necessary to inject carbon dioxide into the reservoir at supercritical conditions. By allowing the scCO₂ to remain in the supercritical state though out the energy conversion process will minimize parasitic loads associated with changing the phase of non-critical carbon dioxide to the supercritical conditions prior to reinjection. The proposed power conversion system is presented in Figure 27. The individual components are discussed below in the order that they are presented in the figure.

3.7.4.1 Gravity Separation

The first and most important step in this proposed energy conversion system is to separate the scCO₂ from the water. This will be accomplished by using the density differences between the two fluids. This type of separator is known as a gravity separator and is common to the oil and gas industry. The gravity separator that is required for this site must be very flexible in order to match the changing produced fluids conditions. Broadly the produced fluids can be divided into three distinct time periods. These periods are:

- Early times: Only water is produced
- Middle times: A water dominated mixture of water and scCO₂ will be produced.
- Late times: A carbon dioxide dominated mixture water and scCO₂ will be produced.

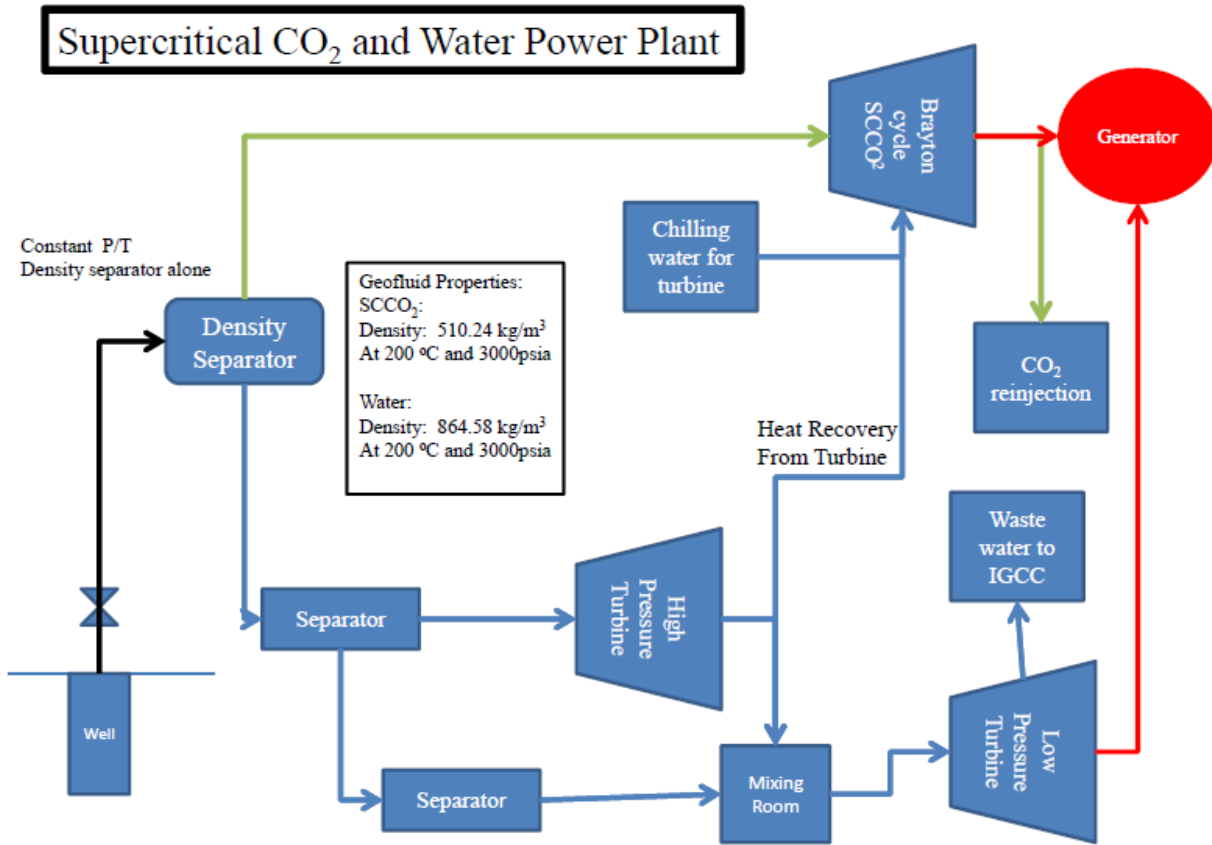


Figure 27: Supercritical Carbon Dioxide Power Plant

Of these three different times the latter two present more of an engineering problem. To determine the correct size of the separator that will be required the following assumptions were made.

- Pressure: 3000 psia
- Temperature: 200 °C
- 100% fluids will be produced over the lifespan of the reservoir.
- No gas capacity constraint
- scCO₂ retention time is similar to that of gas condensate at 3 minutes at a minimum (Steward and Arnold 2009).
- Water retention time is 10 minutes as recommended (Steward and Arnold 2009).
- Mass flow of combined fluids always equals 1000kg/s
- Specific gravity of water at above conditions: 0.86458
- Specific gravity of scCO₂ at above conditions: 0.5124
- scCO₂ droplets in water are similar in size to oil droplets
- Water droplets in scCO₂ are similar in size as those found in oil.

- The equations used to size hydrocarbon/water separators hold true for scCO₂/water separators.

To determine the appropriate size for the separator, the following calculations must be completed (All formulas for separator sizing are attributed to Steward and Arnold 2009):

scCO₂-Water Settling:

$$V_t = \frac{5.56 \times 10^{-7} (\Delta SG) d_m^2}{\mu} \quad 3.3$$

where:

d_m= droplet size [microns]

μ = viscosity of continuous phase [Pa S]

ΔSG = difference between specific gravities of both liquids

Retention time constraint,

$$d^2 L_{eff} = 21 * \frac{(t_r)_o Q_o + (t_r)_w Q_w}{1.4\alpha} \quad 3.4$$

where:

d= vessel internal diameter [mm]

L_{eff}= effective length of the vessel [m]

(t_r)_o= retention time of carbon dioxide [minutes]

Q_o= flow rate of carbon dioxide [m³/h]

(t_r)_w= retention time of water [minutes]

Q_w= flow rate of water [m³/h]

α =1

Settling time constraint,

$$\alpha_w = \frac{\alpha_l Q_w (t_r)_w}{Q_o (t_r)_o + Q_w (t_r)_w} \quad 3.5$$

where:

α_w= fractional height of water

α_l= fractional height of liquid

Height of oil pad (mm)

$$(h_o)_{max} = 0.033 * \frac{(t_r)_o (\Delta SG) d_m^2}{\mu} \quad 3.6$$

where:

ΔSG =difference in specific gravity between the two liquids [D]

μ = viscosity of the continuous phase [Pa s]

Maximum separator diameter (mm),

$$d_{max} = ((h_o)_{max})/(\beta_l - \beta_w) \quad 3.7$$

where:

β_w = fractional height of water

β_l = fractional height of liquid

To determine the appropriate size of separator for the reservoir the flow rate of both scCO₂ and water were varied uniformly across conditions that mirrored middle and late times as described above. From this analysis it was determined that the droplet size of the scCO₂ in water is directly proportional to the size of the separator that is required. From this analysis the result is an optimized separator sized on a produced fluid that is 90% scCO₂ and 10% water at a total flow rate of 1000kg/s and a droplet size of 500 microns result in a maximum diameter of 223,000 meters. Any horizontal gravity separator smaller than this diameter can efficiently separate the two fluids at the residence times of 3 minutes for scCO₂ and 10 minutes for water.

The separator dimensions were sized to match the 1000kg/s flow rate of fluids plus a safety factor to account for potential increases of flow rates over the lifetime of the reservoir. To match the prevailing volume required to contain the 3 minutes and 10 minutes worth of fluid production a container of approximately 700 m³. The dimensions of the separator will be 4 meters in radius and 20 meters in length on the inside. For a sensitivity analysis the container volume was varied by +/- 300 m³.

The gravity separator that is presented here has to be operated at considerable pressure and elevated temperatures. This will directly affect the wall thickness and the overall weight of the separator. There are two components of any tank. The first is the cylindrical tanks and the second is the head of the tank. For this project the head of the tank is a 2:1 ellipsoidal head. The

effect of pressure on wall thickness and weight was investigated and is presented in Tables 3, 4, and 5. The material used in this investigation was a carbon steel plate, SA-516 Grade 70 with a safety factor of 3.5. It is apparent that a different material and/or multiple separators will have to be used due to the exceedingly prohibitive wall thicknesses for a single separator.

Table 4: Separator Calculations

Volume of 400m³ is presented for wall thickness calculations.

Volume [m ³]	P [psia]	P_calc [psia]	Wall Thickness		2:1 Ellipsoidal Heads		Total Wt [kg]
			t_corr [mm]	Wt [kg]	t_corr [mm]	Wt [kg]	
400	1000	1050	578	1.36E+07	524	1.55E+05	1.38E+07
400	2000	2100	1311	3.10E+07	1062	3.15E+05	3.13E+07
400	3000	3150	2287	5.40E+07	1621	4.80E+05	5.45E+07
400	4000	4200	3647	8.61E+07	2202	6.52E+05	8.67E+07
400	5000	5250	5675	1.34E+08	2807	8.31E+05	1.35E+08
400	6000	6300	9024	2.13E+08	3437	1.02E+06	2.14E+08
400	7000	7350	15609	3.68E+08	4093	1.21E+06	3.70E+08
400	8000	8400	34500	8.14E+08	4778	1.41E+06	8.16E+08
400	9000	9450	59084	1.39E+10	5492	1.63E+06	1.39E+10

Table 5: Separator Calculations

Volume of 700m³ is presented for wall thickness calculations.

Volume [m ³]	P [psia]	P_calc [psia]	Wall Thickness		2:1 Ellipsoidal Heads		Total Wt [kg]
			t_corr [mm]	Wt [kg]	t_corr [mm]	Wt [kg]	
700	1000	1050	768	2.42E+07	697	3.65E+05	2.46E+07
700	2000	2100	1746	5.50E+07	1415	7.40E+05	5.57E+07
700	3000	3150	3047	9.59E+07	2160	1.13E+06	9.70E+07
700	4000	4200	4860	1.53E+08	2935	1.53E+06	1.55E+08
700	5000	5250	7564	2.38E+08	3741	1.96E+06	2.40E+08
700	6000	6300	12030	3.79E+08	4581	2.40E+06	3.81E+08
700	7000	7350	20810	6.55E+08	5456	2.85E+06	6.58E+08
700	8000	8400	45997	1.45E+09	6368	3.33E+06	1.45E+09
700	9000	9450	787797	2.48E+10	732	3.83E+06	2.48E+10

Table 6: Separator Calculations

Volume of 1000m³ is presented for wall thickness calculations.

Volume [m ³]	P [psia]	P_calc [psia]	Wall Thickness		2:1 Ellipsoidal Heads		Total Wt [kg]
			t_corr [mm]	Wt [kg]	t_corr [mm]	Wt [kg]	
1000	1000	1050	769	3.46E+07	697	3.65E+05	3.49E+07
1000	2000	2100	1747	7.85E+07	1415	7.40E+05	7.93E+07
1000	3000	3150	3047	1.37E+08	2160	1.13E+06	1.38E+08
1000	4000	4200	4861	2.19E+08	2935	1.53E+06	2.20E+08
1000	5000	5250	7565	3.40E+08	3741	1.96E+06	3.42E+08
1000	6000	6300	12031	5.41E+08	4581	2.40E+06	5.43E+08
1000	7000	7350	20811	9.36E+08	5456	2.85E+06	9.39E+08
1000	8000	8400	45998	2.07E+09	6369	3.33E+06	2.07E+09
1000	9000	9450	787797	3.54E+10	7321	3.83E+06	3.54E+10

3.7.4.2 Brayton Open Cycle Super-Critical CO₂ Turbine

As the scCO₂ flows from the gravity separator it flows towards the Brayton cycle turbine. This turbine is a high efficiency turbine that is designed to operate with super-critical carbon dioxide as the working fluid. Recent work by Sandia National Lab (2011) suggests that this turbine will be capable of performing within the prevailing conditions of the system at the site with substantial benefits such as the ability to remove the compressor and combustion sources from the system because the scCO₂ exits the reservoir preheated and at elevated pressures and after water separation arrives at the Brayton turbine ready for power generation. Compared to other gas turbines the scCO₂ turbine could increase the electrical power produced per unit of fuel by 40 percent or more (Wright et al. 2010).

The classical brayton cycle turbine undergoes four processes. These are an isentropic compression, a constant heat addition, isentropic expansion, and a constant heat rejection (Wright et al. 2010) (See Figure 27). All four of these processes occur at steady state flow. Only two of these processes are of interest for this project. These are the isentropic expansion and the constant heat rejection. For the system proposed here the isentropic expansion will occur under a pressure decrease from 3000psia to near the critical point at 1200 psia. The heat rejection phase will occur from 200 to 40°C.

A rough estimate of energy production can be accomplished by up scaling the results presented by Wright et al. 2010. The turbine that was presented in their report produced approximately 53KW at a flow rate of 3.5 kg/s and a pressure ratio of 1.8. If a flow rate of 1000 kg/s scCO₂ is considered with similar pressure ratios then a rough power production of 15MW could be expected. In addition to this power an additional from the heat rejection from the turbine would result in approximately 100 MW if there is a conversion efficiency of 50%. A similar binary power plant would alone be able to capture the 100MW of power while leaving the additional 15MW of power lost and then only if approximately 1800 psia was lost prior to the heat exchanger to allow the pipes within the heat exchanger to be of similar size as those after the turbine.

A brayton cycle engine has not been applied to scCO₂ associated with geothermal resources as of yet but in the opinion of the author of this section, a serious design concern for the turbine is the mass flow rate of scCO₂ over the lifetime of the reservoir. The size of the turbine will be based on the mass flow rate of scCO₂. During initial times it is expected that the flow rate of scCO₂ will be less than flow rates at later times. This may require a low mass flow turbine as well as a high mass flow turbine to efficiently generate power.

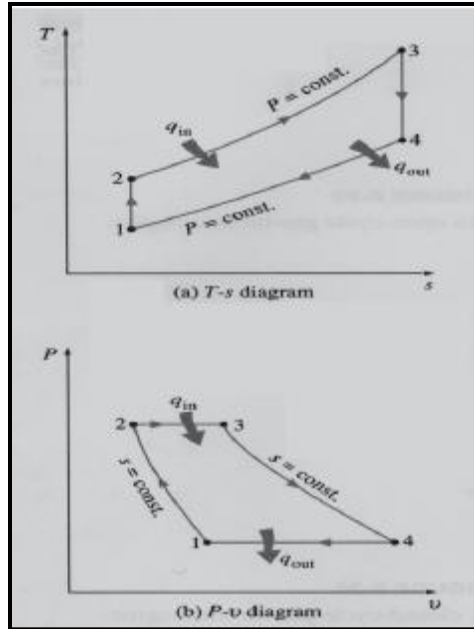


Figure 28: T-s and P-v Diagrams of an Ideal Brayton(Cengel 2010)

3.7.4.3. Flash System

The necessity of a double flash system will be directly related to the volumes of water that are produced over the early and middle times of the reservoir development. The amount of water that will be produced is very dependent upon the initial water saturation of the reservoir. From simulation work conducted within this project it appears that the cut off saturation is approximately 30%. If the saturation is above this value then water will be produced but if it is below this value no water will be produced. If no or minimal water is produced then the double flash system will not be required. If significant water is produced then a double flash system may be worthwhile. To decide the feasibility of a double flash power plant the costs of the plant and the power generated must be considered together. This feasibility study is presented within the EGS Economics section of this report.

4.0 IGCC

4.1 Introduction

IGCC plant is used as the source of CO₂ for this project. Our approach is to capture the maximum amount of CO₂ produced from the coal. IGCC plant consists of gasifier where coal is burnt and converted into synthesis gas and carbon monoxide. This mixture of gas is passed through various processes under different units and gets cleaned. The pure synthesis gas is burnt in the combustion chamber. The heat generated through the combustion chamber is used to run the gas turbine and generate power. The byproducts of clean gas are (i) Pure sulfur which can be used for industrial purpose (ii) CO₂: can be used for various purposes.

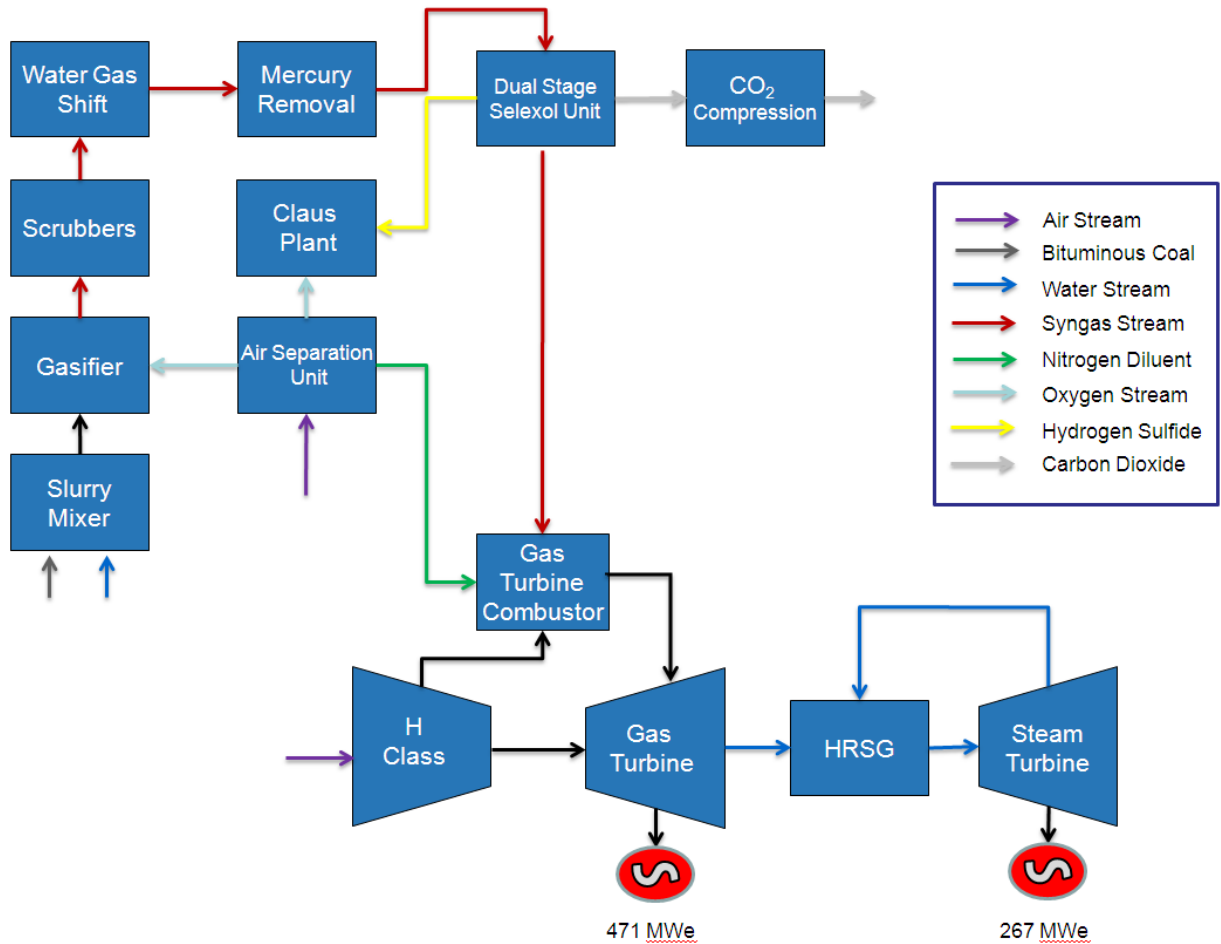


Figure 29: Block Diagram for pre-combustion carbon capture IGCC Plant

The Integrated Gasification combine cycle consist of

- 1) Air Separation Unit(ASU)
- 2) Gasifier
- 3) Gas Cleaning Unit
- 4) Gas Turbine
- 5) Steam Turbine

Coal Slurry is fed into the gasifier where it gets converted into synthesis gas and CO. This mixture of synthesis gas and CO is passed through scrubber in order to remove particulate. Further it is passed to WGRS and AGS where H₂ and CO are separated and CO is converted into CO₂. In AGS Sulfur is removed from the gas mixture with the help of catalyst. The clean H₂ gas is burnt into gas turbine and the steam generated from it is used to run the steam turbine

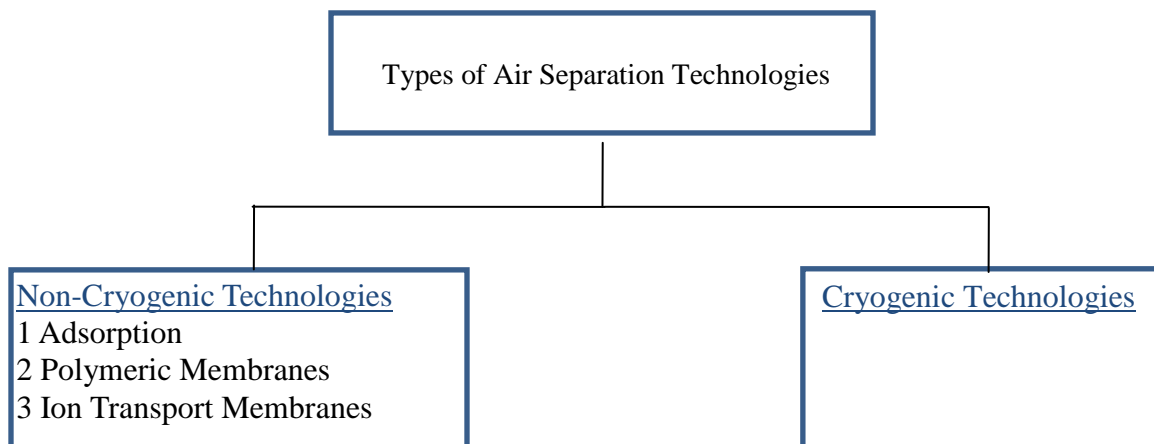
4.2 Air Separation Unit

4.2.1 Introduction

Air Separation unit (ASU) plays vital role in creating clean energy from coal in an IGCC plant. The primary purpose of an ASU is to separate oxygen and nitrogen from air (Smith, 2001). The separated oxygen is sent to the gasifier for the production of synthesis gas and separated nitrogen is sent to turbine where it is used for various other processes.

The other advantages of using ASU in IGCC plant are the gas coming out from the turbines can be purified and also reused for different units of IGCC plant. The final product can be obtained in liquid as well as gaseous form depending on the application.

4.2.2 Types of ASU



Air Separation Technologies can be classified as Cryogenic Technology and Non-Cryogenic Technologies.

Cryogenic Technology is a conventional technology which has been successfully implemented for many years. It operates at very low temperature. The advantages of cryogenic technology are the purity level of obtained products are very high and even by-product obtained is very clean and can be used directly without undergoing any further process. The limitation of this technology is its capital cost.

Non-Cryogenic Technologies are upcoming technologies. Some of the non-cryogenic technologies have very high purity level. Product output is completely dependent on bed size of the plant. Capital cost is low compared to cryogenic technology. For some cryogenic technologies by-product obtained cannot use and some of them cannot be integrated with IGCC plant.

4.2.2.1 Adsorption Process

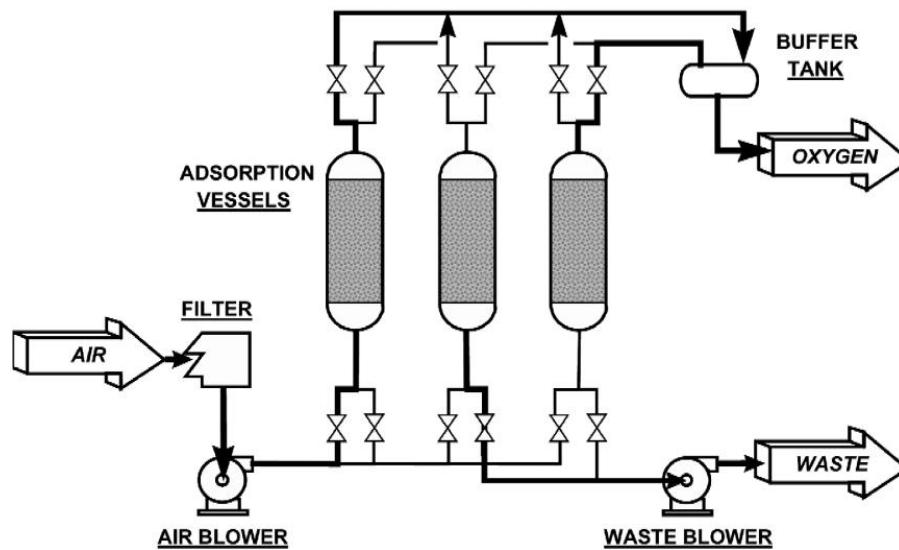


Figure 30: Adsorption

In adsorption process, some natural and synthetic materials are used to adsorb nitrogen in air separation, nitrogen molecules are more strongly adsorbed than oxygen or argon molecules. The pore sizes of carbon molecular sieves are of the same order of magnitude as the size of air molecules. Oxygen molecules are slightly smaller than nitrogen molecules; they diffuse more quickly into the cavities of the adsorbent. Thus, carbon molecular sieves are selective for oxygen and zeolites are selective for nitrogen.

Figure 30 shows that air is filtered first and then it is pressurized with the help of a blower. Pressurized air enters a vessel containing the adsorbent. Nitrogen is separated from air by adsorption and an oxygen-rich effluent stream is produced until the bed has been saturated with nitrogen. At this point, the feed air is switched to a fresh vessel and regeneration of the first bed can begin. Regeneration can be accomplished by heating the bed or by reducing the pressure

in the bed, which reduces the equilibrium nitrogen holding capacity of the adsorbent (Smith, 2001).

Characteristics

- Separate pretreatment of the air is required in order to remove water and carbon dioxide, Oxygen purity is typically 93–95 vol%.
- Due to the cyclic nature of the adsorption process, bed size is the controlling factor in capital cost.
- Production is proportional to bed volume, capital costs increase more rapidly as a function of production rate compared to cryogenic plants.

4.2.2.2 Polymeric Membranes

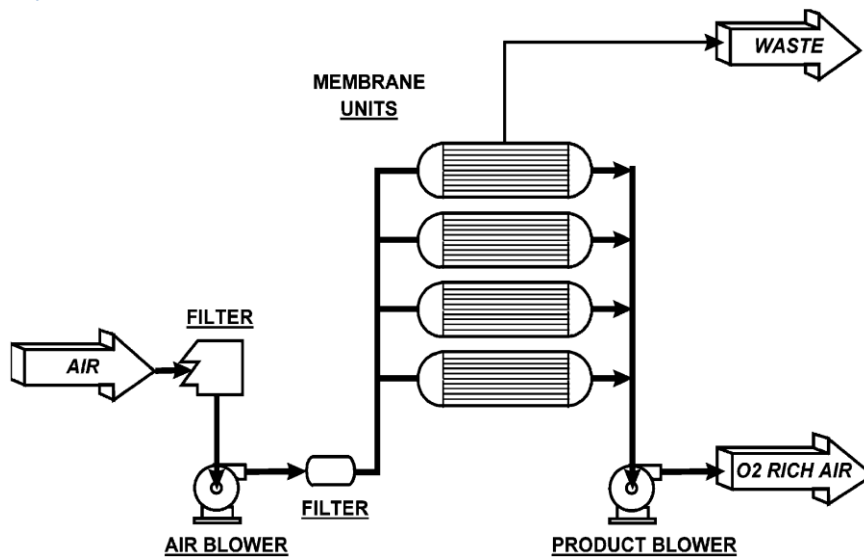


Figure 31: Polymeric Membranes

Polymeric membranes work on the differences in rates of diffusion for oxygen and nitrogen through a membrane, which separates high-pressure and low-pressure process streams. The economics of membrane systems are determined by flux and selectivity. Flux determines the membrane surface area, and is a function of the pressure difference divided by the membrane thickness.

As oxygen molecules are smaller in size compare to nitrogen, most membranes are permeable to oxygen than to nitrogen. Active or facilitated transport membranes, which incorporate an oxygen-complexing agent to increase oxygen selectivity, are a potential means to increase the oxygen purity from membrane systems, assuming oxygen compatible membrane materials are also available.

Figure 31 Filtered air is passed through blower in order to overcome the pressure drop through membrane tubes and piping. Air is then passed through the membrane materials which are usually assembled into cylindrical modules that are joined together to provide the required production capacity. Oxygen permeates through a fiber or through sheets and is withdrawn as product. A vacuum pump typically maintains the pressure difference across the membrane and delivers oxygen at the required pressure (Smith, 2001).

Characteristics

- Separate treatment require to separate CO₂ and water from the oxygen enrich stream.
- It is simple in operation
- Continuous nature of the process and operation at near ambient conditions
- Limited oxygen production (25–50%)

4.2.2.3 Ion Transport Membrane

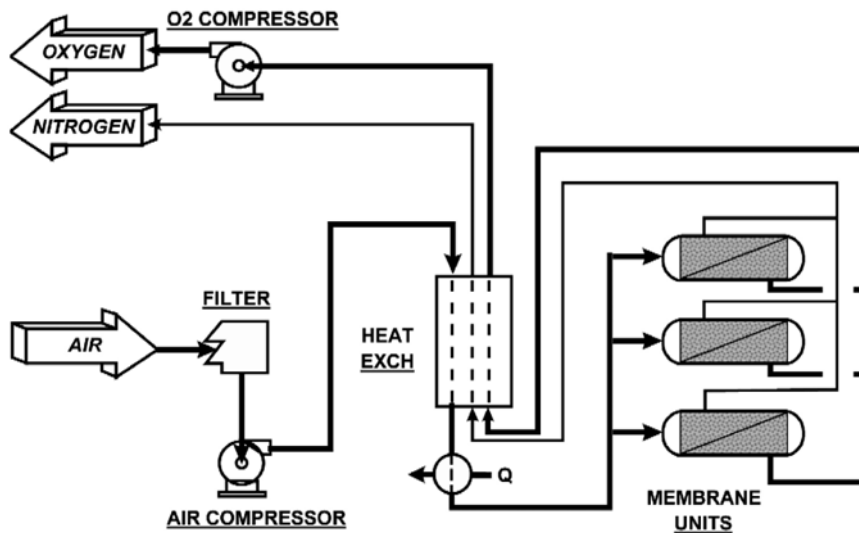


Figure 32: Ion Transport Membrane

ITMs are made up of solid inorganic oxide ceramic materials that produce oxygen by the passage of oxygen ions through the ceramic crystal structure. It operates at high temperatures. Oxygen molecules are converted to oxygen ions at the surface of the membrane and transported through the membrane by an applied electric voltage or oxygen partial pressure difference, then reform oxygen molecules after passing through the membrane material. Membrane materials can be fabricated into flat sheets or tubes. For large energy conversion processes the pressure difference transport driving force is the method of choice.

The oxygen ions travel at very high flow rates and produce nearly pure oxygen on the other side of the membrane. The oxygen can be separated as a pure product, or another gas can be used to sweep on the permeate side of the membrane to produce a lower purity product.

From figure 32 Filtered air is compressed and then heated to operating temperature in heat exchanger. In general, the heating of air can be done by either indirect heat exchange or direct firing of fuel. The heated air is passed through the ITM where oxygen and nitrogen get separated. The oxygen stream is compressed to delivery pressure for use in IGCC or other applications (Smith, 2001).

Characteristics:

- The ITM oxygen process is suited to integration with power generation and energy conversion processes that require oxygen as a feedstock for combustion or gasification, or in any oxygen-based application with a need for power or an export power market.
- The pressurized nitrogen enriched non-permeate stream is used elsewhere in balance of the energy conversion process, for instance, expanded in an integrated gas turbine cycle to generate electric

4.2.2.4 Cryogenic Separation

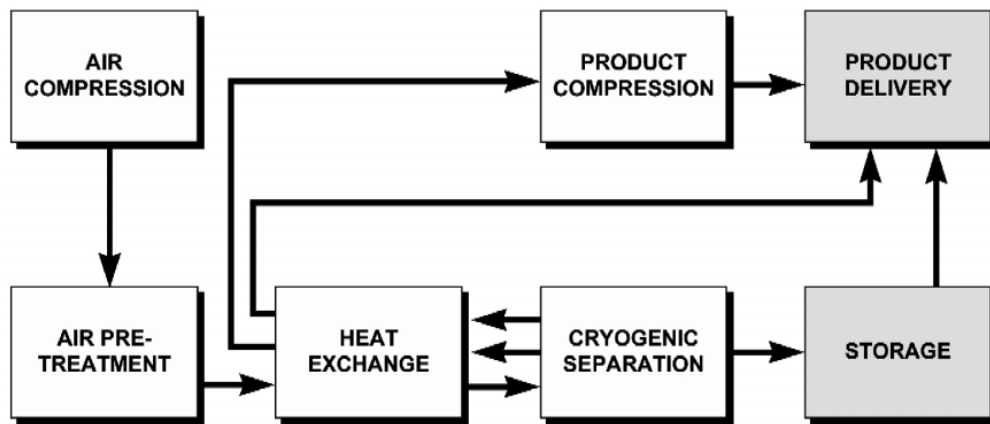


Figure 33: Cryogenic Separation

In Cryogenic Separation the air is compressed first and then it is sent to a pretreatment process whereby air is cooled in order to remove contaminants, including water, carbon dioxide, and hydrocarbons. The air is then cooled to cryogenic temperatures and distilled into oxygen, nitrogen, and, optionally, argon streams. Warming these product streams against the incoming air feed conserves refrigeration, with any deficit made up by expanding a small portion of

pressurized air or nitrogen. Numerous configurations of heat exchange and distillation equipment can separate air into the required product streams (Smith, 2001).

Characteristics:

- High purity level
- Byproduct nitrogen can be used for other applications.
- Can be integrated with other facility units.
- Capital cost and power consumption are high
- Can produce products in large quantities.

Selection Criteria

Air Separation units are selected basis on

1. Purity
2. Pressure
3. Use pattern
4. Specific rate
5. Integration opportunities with other process

Table 7: Typical Parameters of ASU (Smith, 2001)

Process	Status	Economic range(sTPD)	Byproduct capability	Purity limit (vol%)	Start-up time
Adsorption	Semi-mature	<150	Poor	95	Minutes
Membrane	Semi-mature	<20	Poor	40	Minutes
ITM	Developing	undetermined	Poor	99+	Hours
Cryogenic	mature	>20	excellent	99+	Hours

4.2.3 Conclusion:

Nitrogen is used as a diluent for gas turbines in order to improve efficiency. NO_x emissions can be reduced as injected nitrogen inside turbine helps in controlling adiabatic flame temperature of the combustion products. From Table 6 it is observed that adsorption process and polymeric membrane process are not capable of producing nitrogen so they are not suitable for IGCC plant. ITM cannot be used for mass production. Cryogenic Technology is preferred as it can be integrated with other process as well as the byproduct obtained can be used for other applications. Two gear production cryogenic air separation units will be used. The air separation units will provide 4400 tons/day of oxygen to the gasifier and Claus plant (DOE Report, 2010).

4.3 Gasifier

4.3.1 Introduction

A primary component in coal power plant system's success is the gasification reactor located in the heart of the IGCC plant. While gasification can make use of many fuel types, the abundance of coal reserves in New Mexico makes coal the logical choice. The product of interest in coal gasification is known as synthesis gas. This refers to a gaseous mixture which can vary greatly depending on the gasification reactor, coal type and operational parameters. Therefore, a primary objective is to identify a gasification configuration which best satisfies the demands of a power plant that produces a gross power output greater than 700 megawatts.

Commercial gasification reactors are commonly classified into three groups; moving bed, entrained flow and fluidized bed. Of these, the entrained flow and the moving bed are most common in industrial applications. The fundamental differences between the reactor types are represented in the figures below.

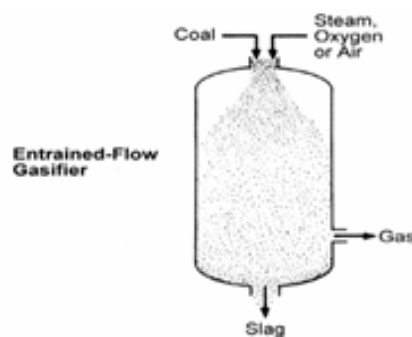


Figure 34: Entrained Flow Gasifier

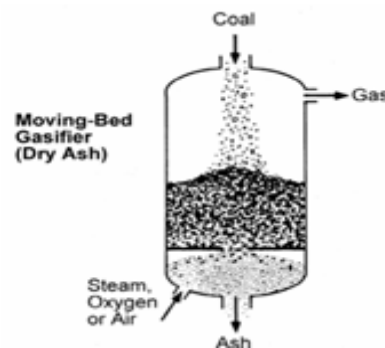


Figure 35: Moving Bed Gasifier

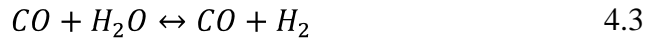
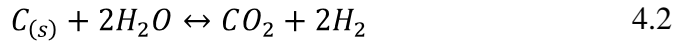
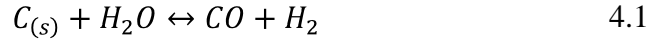
In relation to IGCC, the best reactor type would consist of a short residence time with the least available energy lost in the gasification process. Advantages of the entrained flow reactor type are high temperature, relaxed coal type restrictions and short residence times. (Jeffrey, NETL Reference Shelf)

Based on these conditions, an entrained flow system has the potential to be an excellent candidate for supplying synthesis gas in an IGCC plant. This analysis will explore the theoretical effects of select reactor conditions and reactant concentrations on synthesis gas quality in order to identify if this gasification design is conducive to power generation.

4.3.2 Methods

The key to successful gasification is maximizing the heat of combustion present in the synthesis gas. An analysis of typical synthesis gas composition from the Tampa Florida IGCC plant owned by TECO electric reveals that the two largest sources of chemical energy are

molecular hydrogen and carbon monoxide. This is due to the heat of combustion possible from both species. Therefore, the formation of these two molecules holds high priority. CO and H₂ formation from coal is a combination of exothermic and endothermic reactions with oxygen and water. The most pertinent of these are listed below.



Both oxygen and water streams must be carefully adjusted to ensure that the formation of hydrogen gas and carbon monoxide is thermodynamically favored. Using relevant reactions listed in the GRI mechanism, a series of calculations were performed to test the theoretical effects of oxygen and water inputs on the thermodynamic equilibrium concentrations.

Synthesis gas composition depends on the internal reactor conditions and the concentrations of the reactants. One aspect that sets the entrained flow reactor apart is the elevated operating temperature. This is a result of operating above the coal's ash fusion temperature. A combination of this dramatic increase in operating temperature and a highly pressurized reactor will greatly increase the coal's chemical reaction rates (Liu 2009). Therefore, the assumption that gas-phase equilibrium is reached will be implemented when testing the reactor's sensitivity to select parameters.

Since coal is a complex heterogeneous solid, the fuel input needed to be simplified to conduct reasonable calculations. Therefore the molecule CH was used to represent the coal feed. The oxidizing stream consisted entirely of oxygen accomplished with an air separation unit. Actual reactor conditions and synthesis gas composition was collected from the final technical report on the Tampa Florida IGCC plant owned by TECO electric.

The typical reactor conditions of the TECO plant were mimicked in the following cases studies with an initial reactor temperature of 1300 Celsius and five megapascals (Mc Daniel 2002). In each case, both the mole fractions of oxygen or water were varied over a select range and equilibrium concentrations were then calculated.

The estimates on mass and energy flows through the theoretical system were calculated to estimate the quantities of reactants and theoretical efficiencies of the New Mexico gasifiers. Coal composition Illinois No. 6(Herrin) is used as a basis for calculations and synthesis gas

composition was taken from the Cost and Performance Baseline for Fossil Energy Plants (Haselbeck 2010). Gasification efficiency is calculated using the cold gas efficiency method. This is calculated by dividing the lower heating value of the synthesis gas by the higher heating value in the coal (McDaniel 2002).

Each parameter study varied one component of the gasifier's reactant feed while holding the others constant. Cases one and two were set to observe the influences of oxygen and water respectively. For case one the equivalence ratio was varied and the default water to fuel ratio in the fuel stream of 63% remained constant. For case two the default equivalence ratio was held at a constant value of three, while the water to fuel ratio was varied.

4.3.3 Results

The results of each parameter study are presented in four plots. Each plot displays the influence of a parameter on the hydrogen and carbon containing species which are dominant in the synthesis gas. In case one, the first parametric study was designed to test the sensitivity of higher heating value chemicals to fluctuations in the equivalence ratio. As the equivalence was varied the following trends were observed.

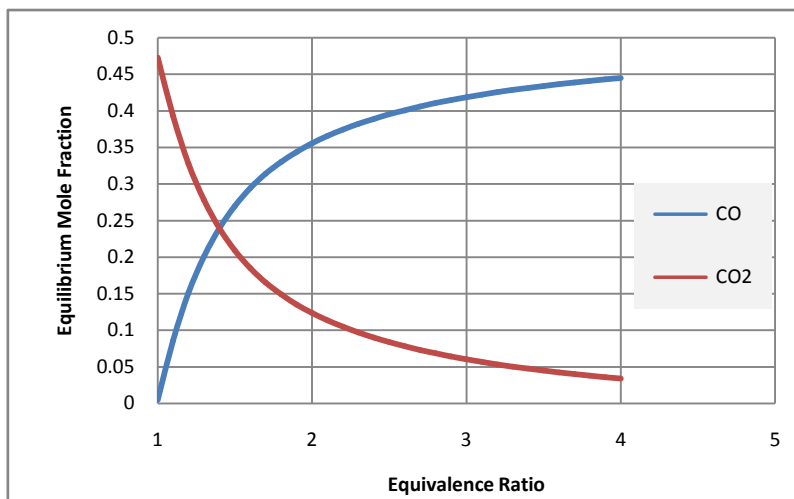


Figure 36: Equivalence Ratio vs. Equilibrium Mole Fraction

The trends in Figure 36 follows the same equilibrium trends observed with fuel rich conditions in a typical combustion reactor. As the fuel rich conditions increased, so does the mole fraction of carbon monoxide. However, in a gasification reactor carbon monoxide is not a pollutant but a desired product.

Figure 36 shows these increases in production with the decreasing oxygen concentration. As an entrained flow gasifier operates at higher temperatures, this typically implies lower equivalence ratios. Therefore, this explains the lower cold gas efficiencies reported when compared to the lower equivalence ratios of moving bed reactors. What this graph does not

demonstrate is the advantages of higher oxygen concentrations and likewise higher operating temperatures. Although the equilibrium values favor lower oxygen inputs, the benefits in operation seen from elevated temperatures in the areas of kinetics and mass transfer offset the losses in cold gas efficiency. These factors aside, this calculation proves the merit of partial oxidation in relation to carbon monoxide formation.

Figure 37 shows the effects of equivalence ratios on the hydrogen gas and steam concentrations. The increase in hydrogen gas is best explained by an increased use of water in coal oxidation. As the oxygen supply continues to decrease, the water molecules present in the coal water slurry oxidizes a higher percentage of the fuel source.

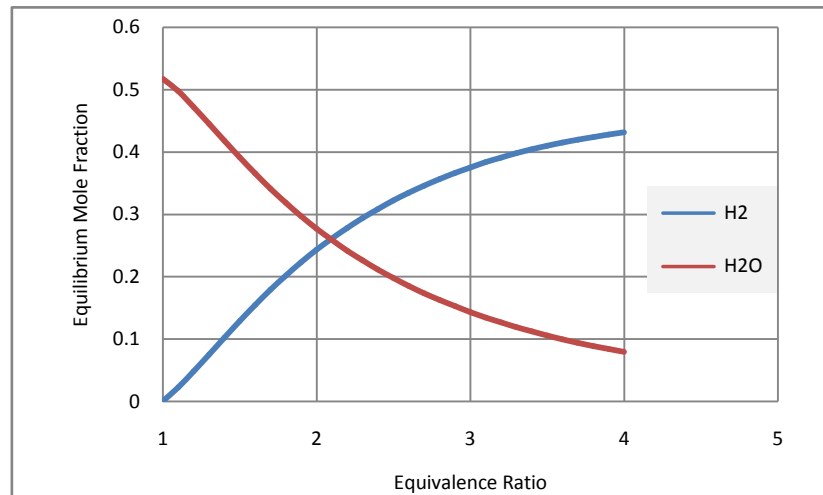


Figure 37: Equivalence Ratio vs. Equilibrium Mole Fraction

When water comes in contact with the coal, this oxidation process emits hydrogen gas as one of its products.

Overall, Figure 36 and Figure 37 adequately show the effects of partial oxidation and steam reformation on an equilibrium synthesis gas composition. Still, this case does not account for the changes in the time required to achieve equilibrium. In practice, the advantages of increased product gases are often rejected in favor of faster reaction rates at the lower equivalence ratios.

The second parametric analysis was designed to demonstrate the composition effects seen at thermodynamic equilibrium when the water concentration is varied in the coal water slurry. As the initial mole fraction of water was varied the following trends were observed.

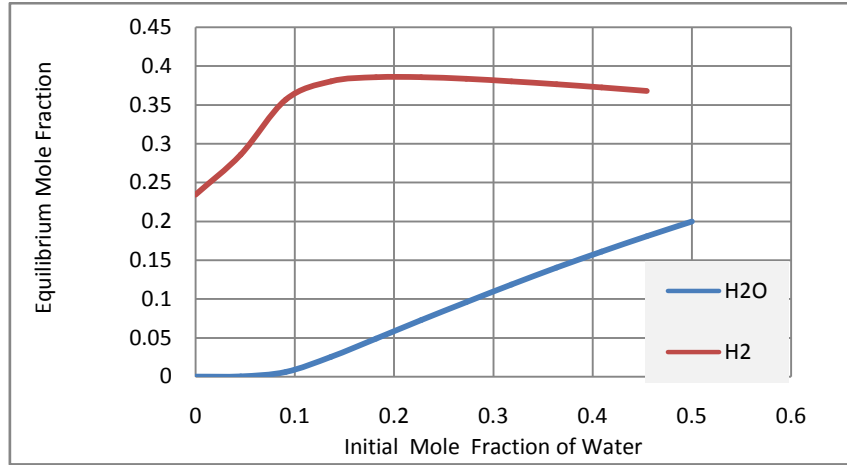


Figure 38: Initial Mole Fraction vs. Equilibrium Mole Fraction

The first trend of interest is the initial increase in hydrogen production seen at low water concentrations. This steep increase in hydrogen, verifies the role of water as an oxidizer under fuel rich conditions. Likewise, it demonstrates the benefits of using partial oxidation in conjunction with steam reformation. Another point of significance occurs as the water concentrations approach 20%. The advantages in hydrogen production gradually decline after 0.01 mole fractions. At the same time, steam emerges in higher concentrations within the synthesis gas. Therefore, as the water concentration approaches a mole fraction of 0.2, the additional water is not oxidizing.

Figure 38 illustrates the effects of the water concentration in the coal water slurry on carbon monoxide formation. The trends observed in the two chemicals, verify the conclusion that water is being used as an oxidizing species. Assuming that water is an oxidizing species, then as the concentration of water increases the reactor becomes fuel lean and equilibrium will shift in favor of carbon dioxide. This logic is justified with the increase in the present of carbon dioxide after 0.1 moles of water.

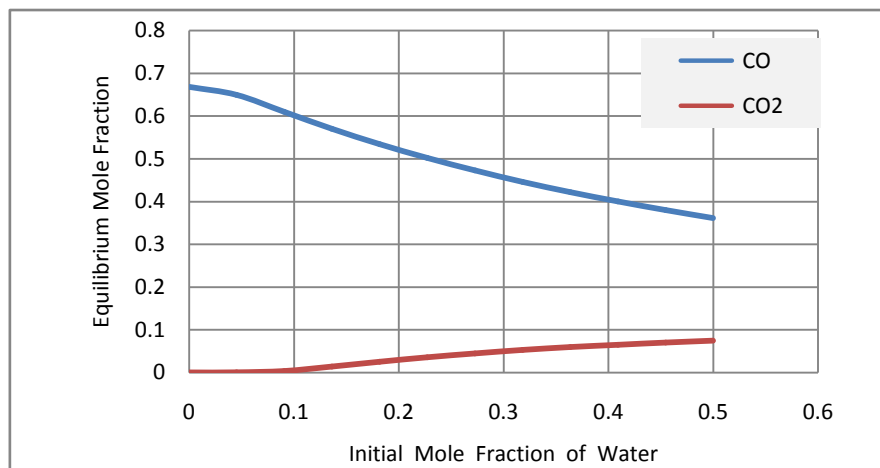


Figure 39: Initial Mole Fraction vs. Equilibrium Mole Fraction

One important difference in the effects of water concentration on hydrogen species verses carbon species is the water's effect on heating value. Unlike Figure 38, every addition of water lowers the equilibrium heating value that is available from carbon species. Though this is often done intentionally in later stages such as the water gas shift reactor, excess concentrations of water have the potential to be counterproductive. Endothermic reactions, like the water gas shift, in excess can slow down the coal gasification kinetics which may decrease the overall percent of carbon conversion.

4.3.4 Coal Water Slurry Preparation

To accomplish the required power output, the system will gasify an average of 5500 pound tons of coal per day. Using local railways, the necessary coal can be procured from upstate coal mines and avoid costly transportation methods. Likewise, the coal handling facilities will need coal storage, crushing and slurry prep stations that can accommodate this magnitude of coal. One distinct advantage to the Texaco design is its ability to gasify all ranks of coal (Jeffrey, NETL Reference Shelf). This means the plant will have more flexibility in relation to fuel supplies in the coming decades. However, any given coal feed dictates the reactors operational parameters and limits the power output. For this reason, the plant will place preference on local bituminous coal. This coal type is successfully used in the Tampa Florida IGCC plant with high efficiency results (McDaniel 2002).

The coal water slurry concentration will maintain the ratio of 63% solids. This is the recommended parameters to balance the lifespan of the reactors lining with a profitable power output (McDaniel 2002). This goes past the optimal ratio if governed solely by thermodynamics as shown in Figure 40

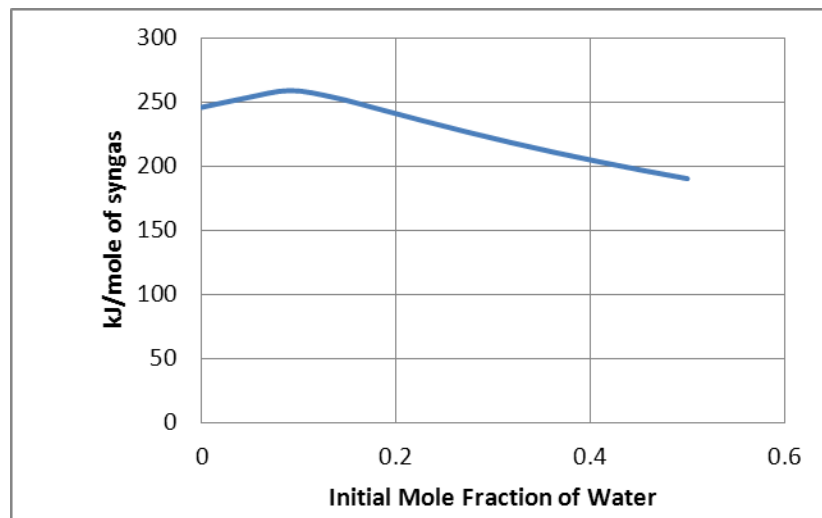


Figure 40: Initial Mole Fraction of water vs. KJ/mole of Synthesis gas

One possible explanation for the elevated water concentrations would be to maintain a lower operating temperature in order to prolong the life of the refractory or minimize damage to the slurry injector.

4.3.5 GE Reactor

One of the largest coal IGCC plants is the TECO plant in Tampa Florida. Using a high temperature entrained flow reactor, the plant gasifies 2500 tons of coal per day (McDaniel 2002). This model maintains an operational range from 1300 - 1500 Celsius and five to eight megapascal (McDaniel 2002).

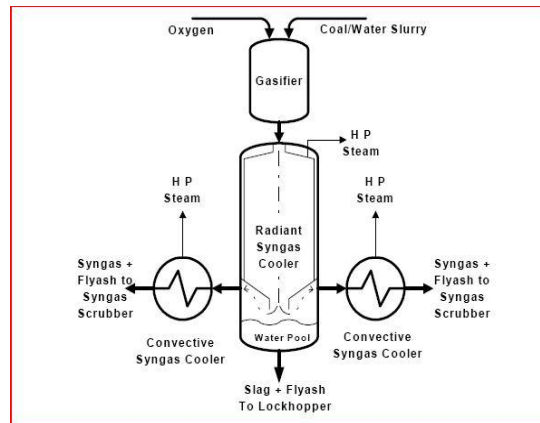


Figure 41: GE Reactor

In order to produce a net power output of 550 megawatts, two entrained flow reactors are needed in the design for the New Mexico plant. The two reactors will operate with an average cold gas efficiency ranging from 70 – 75%, supplying a synthesis gas capable of 1000 megawatts. This will also use the radiant synthesis gas cooler over the water quench systems which is typically used in the ammonia industry (Liu 2009). Radiant synthesis gas coolers are reported to have excellent performance and recover 10% of the fuels heating value in the form of pressurized steam (McDaniel 2002)

4.3.6 Oxygen and Water Supply

A key to successful gasification is optimizing uses of partial oxidation and steam reformation in such a way that the synthesis gas achieves a high level of heating value within the limitations of the reactors design. Without diligent management of the oxygen and water streams, much of the carbon and hydrogen present in the coal will either form carbon dioxide and water or pass through unreacted with the slag. The New Mexico plant will require an average 4000 tons of oxygen per day. This amount should be raised or lowered to maintain a suitable temperature above the coal's ash fusion temperature. For this reason the operating equivalence ratio will be lower than the optimal ratios which hold higher cold gas efficiencies.

4.4 Gas Cleaning Unit

4.4.1 Introduction

The Water Gas Shift (WGS) reaction is commonly utilized as an industrial process for hydrogen production. The WGS is a reaction between carbon monoxide (CO) and water (H₂O) that is reversible and exothermic. Historically and currently, large scale WGS reactions are facilitated by catalysts in conjunction with methanol steam reforming where the hydrogen produced is used in hydrogen-consuming processes such as ammonia production or hydro processing of petroleum fractions (Platon, 2009 & Amphlett, 2004). The WGS reaction is an equilibrium reaction that can be “shifted” to either side depending on the amount of reactants and products present in the system.

WGS reactors are also used in conjunction with Integrated Gasification Combined Cycle (IGCC) plants. The synthesis gas from the gasifier, primarily composed of CO and H₂, undergoes the WGS to form a product stream containing mostly H₂ and CO₂. The hydrogen is separated from the product stream and is fed to a turbine for combustion and electricity production (Amphlett, 2004). There are two general types of WGS reactors: Sour shift or Sweet shift. The type of reactor is based on the synthesis gas stream and whether acid gas removal is performed upstream or downstream of the reactor (Grol, 2009). The catalysts differ for these types based on resistance to sulfur and other acids that could be contained in the synthesis gas stream (Platon, 2009).

The WGS is favored at low temperatures for driving the reaction toward the products but reaction kinetics are favored at high temperatures. For this reason, the WGS occurs in two stages: a high temperature shift and a low temperature shift. The high temperature shift allows for rapid CO conversion, converting the bulk of the CO, while the low temperature shift minimizes the CO-slip through the system (Grol, 2009). The catalysts differ for these two components. An excess of steam (H₂O) is necessary to drive the reaction toward the products of CO₂ and H₂ (Klara, 2007). By varying amount of steam and the temperature of the reaction, the composition of the product stream can be optimized to contain the maximum amount of hydrogen allowable by thermodynamics.

Mercury (Hg) removal is of particular importance as it is a harmful pollutant and will be potentially regulated by the EPA in the near future. By using an activated carbon bed, the mercury will be absorbed and removed from the synthesis gas stream (Klara, 2007).

Acid Gas Removal allows for the removal of acidic gases such as H₂S, COS, and CO₂. This operation is performed to protect downstream catalysts (depending on its location within the plant) and meet environmental standards/regulations for emissions set by the government. There are three types of solvents used in the AGR process: chemical, physical, and hybrid. A shift from using chemical solvents such as MDEA to physical solvent such as Selexol and Rectisol is

occurring throughout the industry as the physical solvents are more economical due to efficient separation of acid gases from the solvent (Klara, 2007).

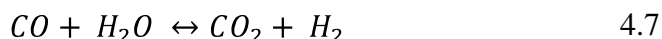
Selexol, a physical solvent that is chemically described as Dimethyl ether of polyethylene glycol, has a high selectivity for H₂S as well as CO₂ which makes it a good candidate for sulfur removal as well as CO₂ removal for sequestration (Klara, 2007). Acid gases are absorbed separately at high pressures and low temperatures to increase the absorption of the solvent. The sour gases are then stripped from the catalyst through a series of flash drums and the regenerated catalyst is sent back to the absorber unit for further use (Black, 2010).

The CO₂ rich stream is sent to a compressor to be transported to the Enhanced Geothermal System (EGS) where it will be utilized as a heat transfer fluid instead of water. The H₂S-rich stream is sent to the Claus Plant for sulfur recovery. Elemental sulfur is produced from the H₂S gas and can be sold to the chemical industry.

To maximize the efficiency through an Integrated Gasification and Combined Cycle (IGCC) plant heat recovery and heat utilization is essential. Parameters of particular interest are the location of sulfur removal and where the water gas shift takes place for the synthesis gas stream. To minimize loss in efficiency, the IGCC units were set up to ensure a periodic decrease in temperature. By not reheating gas streams for particular processes such as Acid Gas Removal, more heat was recoverable and not lost during the operation of the plant.

4.4.2 Water Gas Shift

The basic water gas shift (WGS) reaction is an equilibrium reaction that converts carbon monoxide and water in the form of steam to hydrogen and carbon dioxide (Platon, 2009).



Since the WGS reaction is an equilibrium reaction, L'Chatlier's Principle applies meaning that if more reactant is added into the system, the system will drive itself to the products (Klara, 2007). Thus to promote a high production of hydrogen, a 2:1 molar ratio of H₂O to CO is maintained throughout the fixed bed reactors by adding in steam (Black, 2010). There are two stages/shifts for the WGS reaction, a high temperature shift to convert the bulk of the CO and a low temperature shift to convert the remaining CO and minimize the CO slip through the system (Grol, 2009). Various catalysts could be used to aid in the conversion process, but a Co/Mo catalyst is utilized in this case due to its resistance to sulfur because the acidic gases have not yet been removed from the raw synthesis gas stream (Klara, 2007). The Co/Mo catalyst also serves to hydrolyze COS to H₂S thus eliminating the need for a separate COS hydrolysis reactor (Black, 2010). The WGS reaction occurs in two stages that are maintained two temperatures. The high temperature shift (224°C) serves to convert the bulk of the CO to CO₂ (Black, 2010). The WGS reaction is exothermic at a rate 41 kJ/mol and the extra heat is removed and sent to the Heat Recovery Steam Generation (HRSG) (Klara, 2007). The low temperature shift (204°C)

serves to reduce the remaining amount of CO in the synthesis gas stream so that an overall conversion of 97% is reached (Black, 2010).

4.4.3 Mercury Removal

The mercury removal section operates at a temperature of 35°C thus the shifted synthesis gas must be cooled down before passing through a fixed packed bed reactor that contains sulfur-impregnated activated carbon (Black, 2010). The excess heat is extracted and transferred to the HRSG in the form of high and medium pressure steam. At high pressures of 6.2MPa, the activated carbon removes 95% of the mercury in the raw, shifted synthesis gas stream. The bed life is estimated to be between 18 and 24 months but is dependent on the actual amount of mercury contained in the coal. Generally over the carbon bed life, the weight percent increase from mercury removal will be 0.6-1.1wt% however the activated carbon could absorb up to 20wt% maximum but with decreasing rate of ability of absorptivity (Black, 2010).

4.4.4 Acid Gas Removal

Acid gas removal (AGR) serves to remove acidic gases such as H₂S and CO₂ out of the raw synthesis gas stream (Chiesa, 1999). Chemical and physical solvents provide the means of accomplishing AGR, but chemical solvent pose an issue of separation after absorption, thus the physical solvent of Selexol was chosen. Selexol is polyalkylene glycol dimethyl ether (PGDE) (Song, 2009). The more common Rectisol process was not chosen due to the energy requirements to chill the methanol down to temperature of -40 to -60°C (Robinson, 2010). Prior to AGR, the raw synthesis gas stream is cooled down to approximately 25° C and passed through two consecutive physical absorption columns (Song, 2009). The amount of acid gases absorbed into the physical solvent is based on Henry's Law, meaning that at constant temperatures the amount of a given gas that dissolves into a liquid is directly proportional to the acid gases partial pressure (Klara, 2009).

The physical absorption of acid gases into Selexol is favored at lower temperatures (25°) and high pressures (5.1MPa) (Klara, 2007). The reclamation process of procuring the H₂S and CO₂ requires a series of flash drums where the pressure is “flashed” or decreased rapidly thus decreasing the solubility of the physical solution in which the acid gases were captured (Black, 2010). A flow diagram of the removal of acid gases and recovery of the Selexol can be observed in figure 42

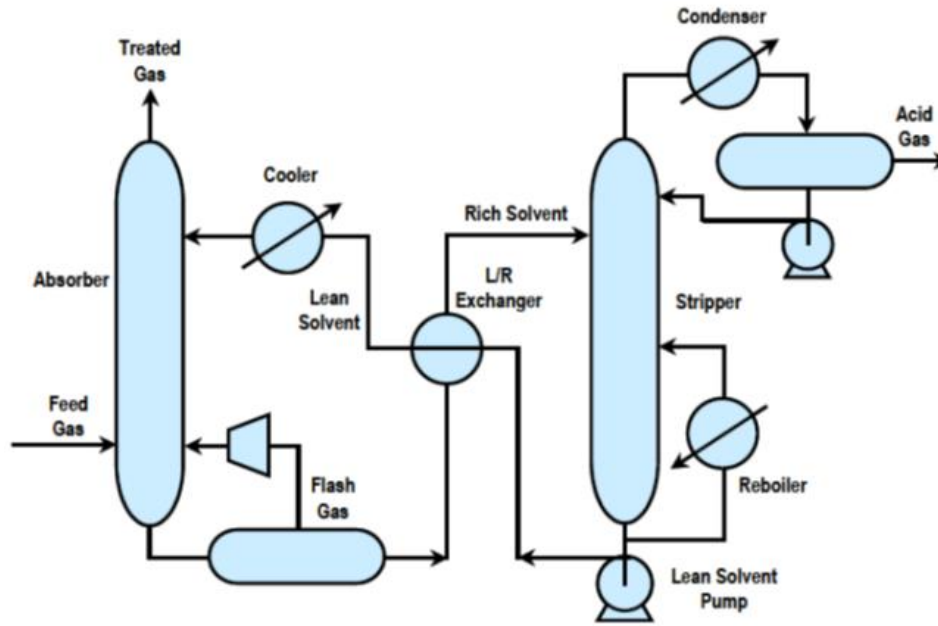
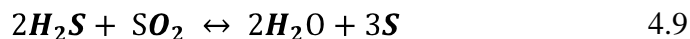
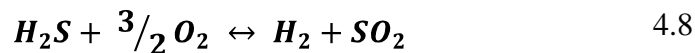


Figure 42: Physical Solvent AGR Process Flow

The dual stage Selexol process removes 99.7% of the H_2S from the synthesis gas stream which is then sent to the Claus Plant for further processing (Black, 2010). 90.3% of the CO_2 is stripped and removed for the acid gas stream then sent to the Enhanced Geothermal System (EGS) plant. The CO_2 stream sent to the EGS is composed of 99.48% CO_2 (Black, 2010). The H_2 -rich synthesis gas stream contains 91.4% hydrogen and is sent to the gas turbine to be utilized for electricity generation (Black, 2010).

4.4.5 Claus Plant

The Claus process converts H_2S to elemental sulfur. The elemental sulfur can be sold to the chemical industry to generate further income for the overall IGCC plant. The following reactions occur in the conversion of H_2S :



Equation 4.8 shows the stoichiometry for the combustion of H_2S to form SO_2 which is required for the 2nd reaction (Equation 4.9). The reaction shown by equation is an equilibrium reaction thus it follows L'Chatlier's Principle. The Claus process works in many stages including a catalytic stage which consists of gas preheat a catalytic reactor, and a sulfur condenser (Black, 2010). Oxygen is required from the Air Separation Unit (ASU) for the first part of the H_2S combustion inside the furnace (Black, 2010). Temperatures typically range from 1100 to 1400°C in the furnace but higher conversions are achieved at higher temperatures (Klara, 2007).

Assuming the H₂S input stream is at least 20-50% H₂S, a sulfur recovery of 94 to 96% will be achieved (Klara, 2007).

4.4.6 Methods

To ensure that the IGCC plant maintained the highest possible efficiency and maximum heat recovery a comprehensive literature review was performed. Variations of each component were considered, including experimental design and operational procedures for the water gas shift and acid gas removal. In particular, the AGR was placed downstream of the WGS so that there would be a consistent step down in temperature instead of reheating the raw synthesis gas to be passed through the WGS. Figures 43 and 44 graphically show the difference in the upstream and downstream placement of the AGR.

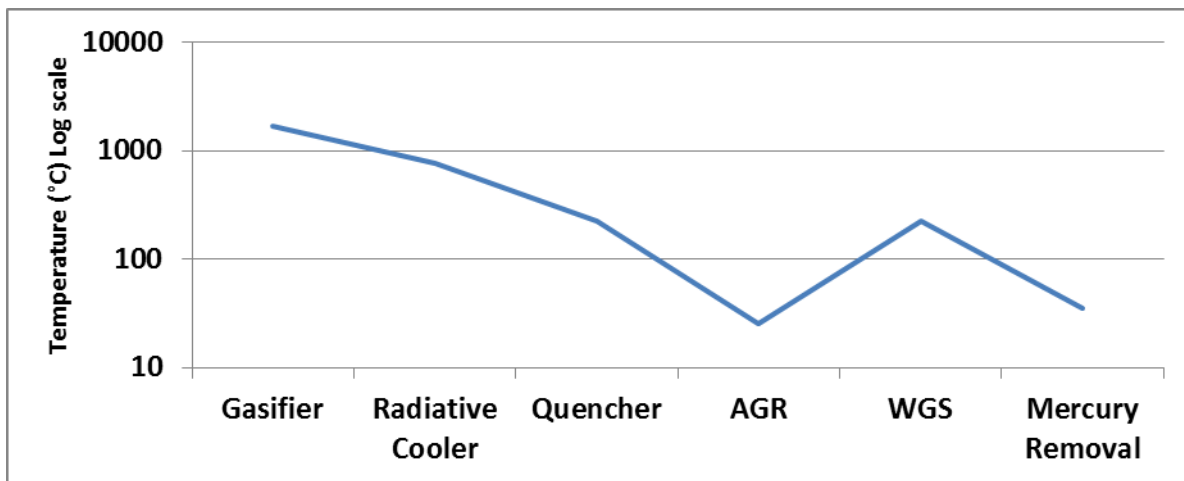


Figure 43: Upstream AGR Placement Temperature Profile

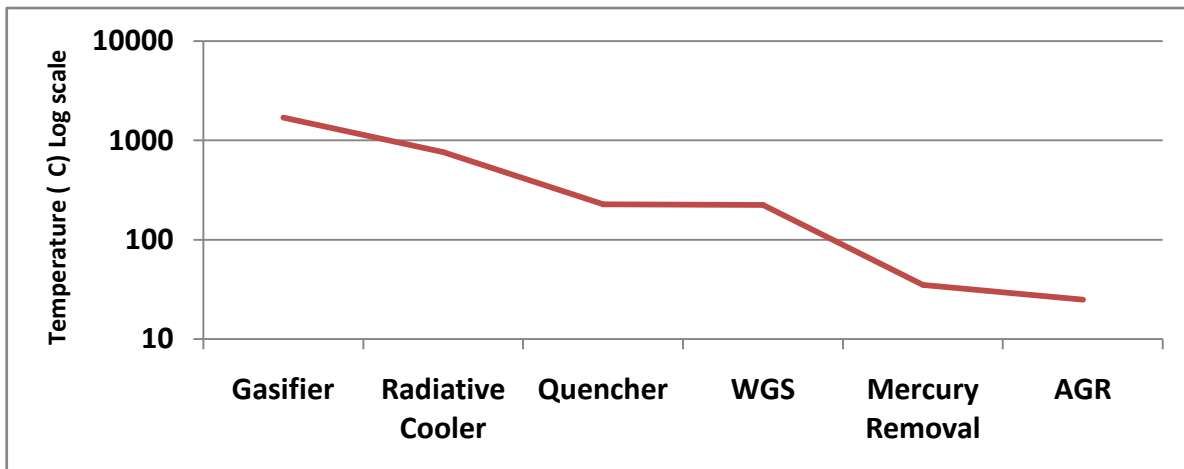


Figure 44: Down Stream AGR Placement Temperature Profile

Figure 44 represents the chosen design path to minimize heat loss and maximize heat recovery through the IGCC process. Since no reheat is required for the WGS, any heat that is

recovered is utilized by the HRSG to produce steam either for electricity production or used for the shift process portion of the WGS.

Since the AGR is placed downstream of the WGS, a sulfur resistant catalyst was required for the shift reactions. The sulfur resistant catalyst serves a dual purpose as it also hydrolyzes COS to H₂S, thus negating the need for a separate COS hydrolysis reactor.

Due to the large capacity of the plant, multiple units are required to perform the given operations. The WGS is a system of two reactors (one high temperature and one low temperature) in series in parallel with another two reactors. There are also two mercury absorber fixed bed reactors.

4.4.7 Results:

The system design of components in the IGCC allows for the consistent decrease in temperature through its operations. The energy (heat) saved by not reheating certain components is utilized as useful energy through the heat recovery steam generation (HRSG) unit. The combination of WGS, mercury removal, AGR, and Claus process permits the high production of hydrogen through the IGCC process. Figure 45 depicts the composition of the synthesis gas stream as it passes through water gas shift (WGS) reactor and the acid gas removal (AGR) reactor.

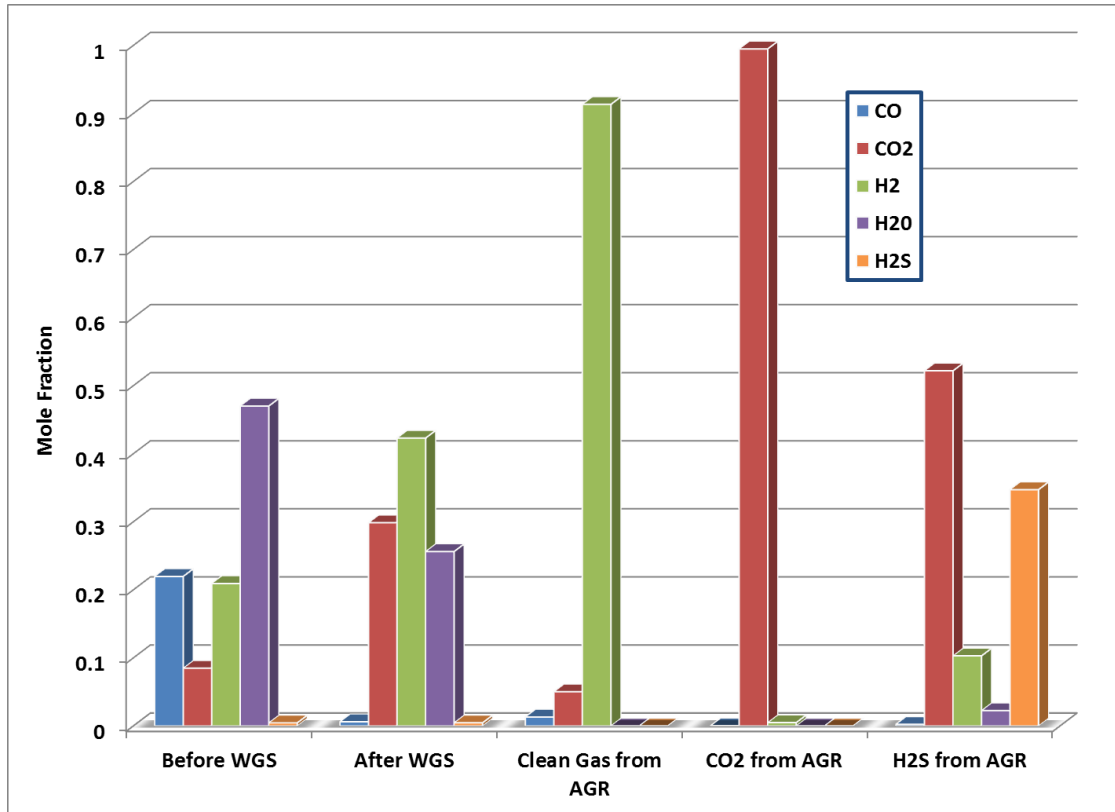


Figure 45: Composition of synthesis gas through WGS and AGR

The clean synthesis gas being sent to the gas turbine is roughly 91.4% H₂ and approximately 5% CO₂. The stream that is to be sent to the EGS is comprised of 99.5% CO₂. Because of the purity of this stream, the effluent requires no further processing or modification before it is pumped underground for heat recovery.

4.4.8 Conclusion

The design of the IGCC plant with the acid gas removal downstream of the water gas shift reactors is essential to minimizing irreversible heat loss through the system. The utilization of the sulfur-resistant Co/Mo catalyst is also vital for the system as it allows the CO in the sour synthesis gas to be shifted to CO₂ thus freeing H₂ from water. This Co/Mo catalyst also serves to hydrolyze COS, thus removing a prior necessary reactor should a sweet synthesis gas shift take place. The large cost of the plant's components is offset by the generation of electricity through the gas turbine and steam turbines. An economic benefit is also associated with the production of elemental sulfur. To maximize efficiency of the plant, any recoverable heat is sent to the heat recovery steam generation unit

4.5 Power Generation

4.5.1 Introduction

In IGCC- Integrated Gasification Combined Cycle where Combined Cycle refers to 2 turbine cycles: Brayton Cycle gas turbines, and Rankine Cycle steam turbines. In a defined IGCC system hydrogen is produced from the gasification of coal, cleaned-up through various processes, and then is sent to a gas turbine for combustion. The combustion of the hydrogen with oxygen will yield water in the form of steam. This gas turbine, model S109H, effluent steam, at a pressure of 2400 psig and 565 °C, is then fed into the first of a series of three steam turbines, termed high pressure steam turbine (HPST) (Matta, Mercer, & Tuthill, 2000) . The effluent from the HPST is then fed into the heat recovery steam generator (HRSG) unit. This HRSG unit has 3 levels of steam admission, one for each of the three steam turbines: High Pressure, Intermediate Pressure, and Low Pressure. The relative HRSG pressures and temperatures of said turbine admissions is 300-400psig, 538-566°C; 300-400psig, 11°C; and 40psig, 11°C (Matta, Mercer, & Tuthill, 2000).

A material limitation of the gas turbine combustion chambers limits firing temperature to 1700 Kelvin. To achieve this in practice, the oxy-combustion of hydrogen is diluted with nitrogen or steam. The research analyzed in this report determines the stoichiometric nitrogen requirement to achieve optimum heat flow, 52,000,000 KJ/min, at the gas turbine's maximum firing temperature, and subsequently the qualitative relation to NO_x emissions from the brayton cycle turbine (GE Energy, 2009).

4.5.2 Methods

Although Figure 46 shows that steam is more effective at diluting flame temperatures, Nitrogen was selected for this project due to the fact that in the arid region of New Mexico, which was selected as the site for this plant; water should be used sparingly as it is a precious commodity. The nitrogen stream in this plant is obtained from the Air Separation Unit (ASU), which separates air into its component oxygen and nitrogen.

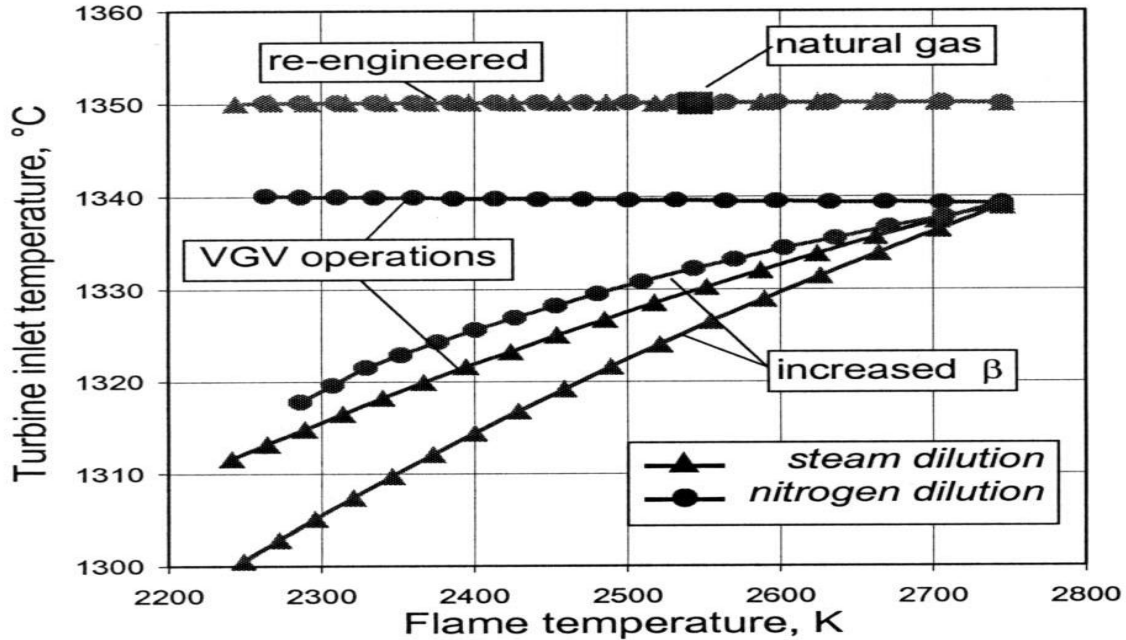


Figure 46: Effects of variable dilution methods and inlet temperatures on flame temperature (Chiesa & Lozza, 2005)

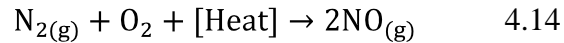
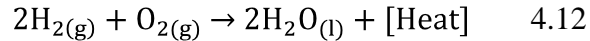
As the combined cycle operations in this plant are part of a larger system, outside data from contributing group members was applied. It was determined that the flow of hydrogen available to the gas turbine from the gas-water shift reactor was 4.42kmol/sec. This stream was assumed to be 100 percent pure hydrogen. For the calculations of reaction heats, it was assumed that only 3 reactions occurred in the combustion process: hydrogen and oxygen to water, nitrogen and oxygen to nitrogen dioxide, and nitrogen and water to nitrogen monoxide.

Gas phase thermochemistry data was obtained from The National Institute of Standards and Technology reference database number 69, in the form of temperature variant coefficients for equation 4.10. Data for variables A-F are shown in appendix table 4.5, and T is the temperature of an environment (National Institute of Standards and Technology, 2008).

$$H^{\circ} = A \times \frac{T}{1000} + B \frac{\left(\frac{T}{1000}\right)^2}{2} + C \frac{\left(\frac{T}{1000}\right)^3}{3} + D \frac{\left(\frac{T}{1000}\right)^4}{4} - \frac{E}{\left(\frac{T}{1000}\right)} + F \quad 4.10$$

The heats of formation were then used to calculate, in accordance with the thermodynamic principle displayed in equation 4.11, total heats for each of the 3 reaction mechanisms considered, displayed in equations 4.12-4.14. Where H is hydrogen, O is oxygen, and N is nitrogen; while ΔH° is the change in enthalpy of the reactions based on moles of each reactant and product present.

$$\Delta H^\circ = H_{\text{products}} - H_{\text{reactants}} \quad 4.11$$



Through the application of equation 4.11, these chemical relationships provided the basis of the heat evolved from each individual reaction. The Hydrogen was considered to be at its adiabatic flame temperature of 3473K, while the temperature of nitrogen formation was assumed to be at the maximum firing temperature of the turbine; 1700K. This method yielded a quantitative maximum Nitrogen dilution amount required, although in practice it would likely be less, which was proven through qualitative analysis. The molar flow rate was then multiplied by the specific heats evolved from specified reactions, which yielded the heat flow rate evolved or stifled from each separate reaction. Through the utilization of Excel's goal seek function; to set the calculated amount of system heat flow equal to the defined maximum allowable heat flow by varying the amount of Nitrogen throughput.

Once the amount of nitrogen flow was obtained, a 'ChemKin' simulation for a defined plug flow reactor at the given gas turbine outlet temperature, 565 °C, in order to determine the amount of Nitrous Oxide that will be in the gas turbine effluent stream. A plug flow reactor was chosen because it most closely simulates real-world continuous flow reaction parameters.

4.5.3 Results

As shown in table 8, the maximum amount of nitrogen that this specific turbine model requires for dilution is 7.16 Kmol/sec, which is approximately 361 metric tons/day; an amount well within the capabilities of our air separation unit to achieve. In practice, this amount will likely be substantially less, for this analysis assumed that the nitrous oxides formed at 1700K(1427 °C), which would vary based on nitrogen inlet and combustion effluent temperatures. The qualitative analysis of this trend is displayed in Figure 47

Table 8: Calculated data based on system inputs, see appendix table 3

Output Data	Value
ΔH_{rxn} [$N_2 + 2O_2 \rightarrow 2NO_2$]	207
ΔH_{rxn} [$N_2 + O_2 \rightarrow 2NO$]	274
ΔG_{rxn} [$H_2 + 1/2O_2 \rightarrow H_2O$] (KJ/mol)	-973
Total System Heat Flow (KJ/min)	(50,961,500)
Required Nitrogen Input (mol/min)	429,870
Required Nitrogen Input (Kmol/sec)	7.16
Required Nitrogen Input (L/min)	2,406,501
Maximum Flow Rate Allowable (Hydrogen) - [Fixed] - L/sec	3,168,057
Maximum Flow Rate Allowable (Hydrogen) - [Fixed] - Kmol/sec	4.71
Actual Net Work Produced (MW)	509.6

It was determined that the best possible temperature range for lowest nitrogen inlet dilution temperature was in a range of 415-510K, which is shown graphically in Figure 47

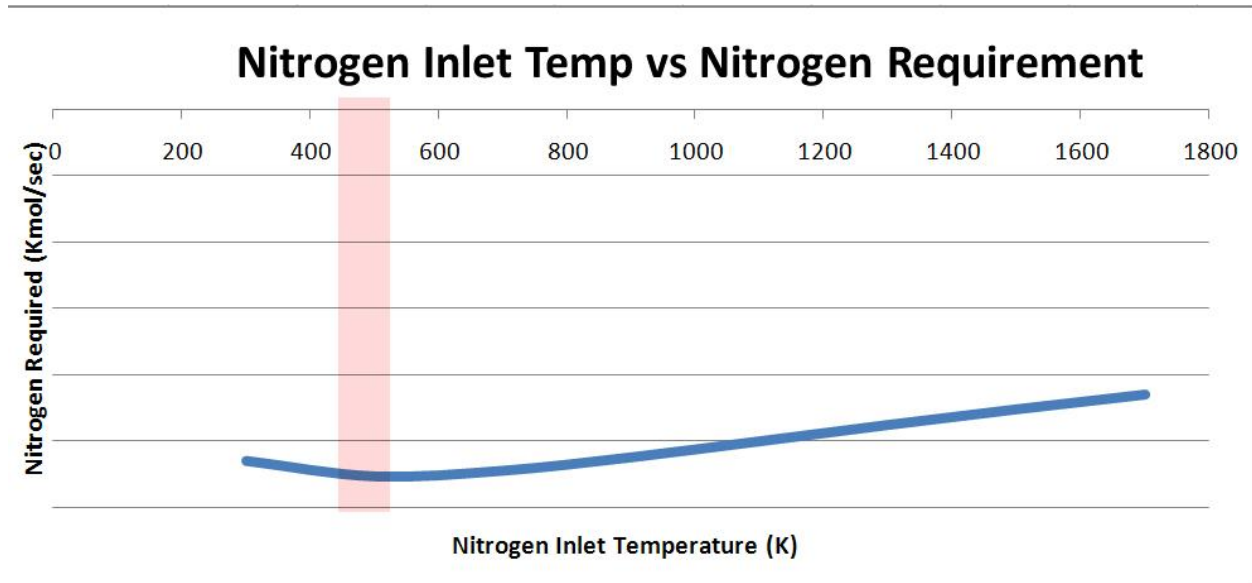


Figure 47: Calculated nitrogen requirement for a given inlet temperature

Subsequent analysis of the effluent stream yielded the results shown in Figure 48. It was therefore concluded that NO_x emissions aren't a large concern to this gas turbine, if the combustion gases are vented at temperatures below 1250 Kelvin (977 °C). Since the turbine

vents combustion effluents at about 838 K (565 °C), it can be concluded that NO_x formation in this system is minimal.

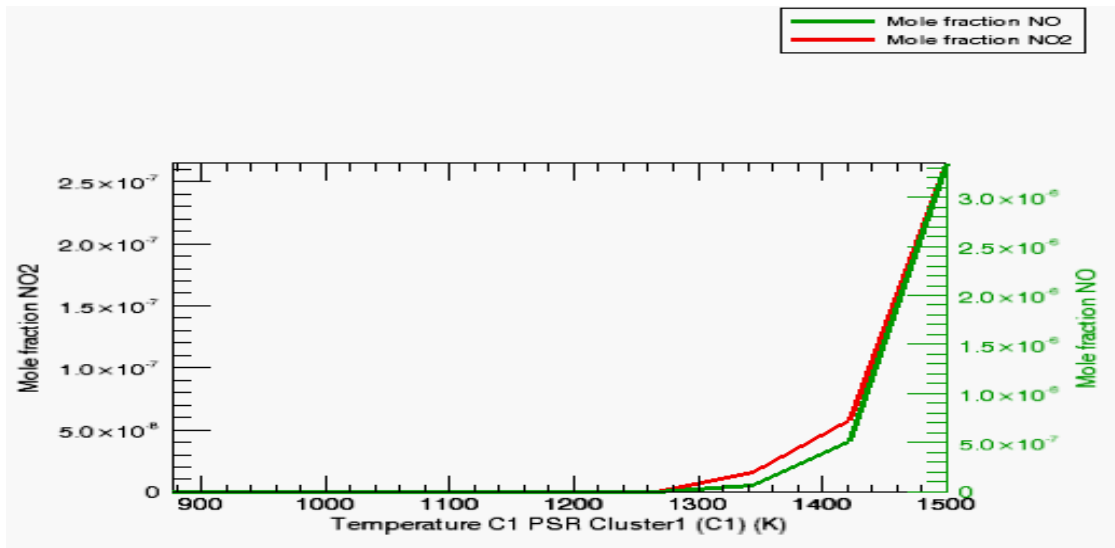


Figure 48: Nitrogen Oxide (NO_x) formation at various effluent temperatures for a defined gas turbine

In the larger context of this system, the combined cycle flow diagram is displayed visually in Figure 49. Although, a little intimidating at first, the diagram simply shows graphically what has been previously stated: fuel flows into the gas turbine, which subsequently sends steam to the high pressure steam turbine, and exhausts the nitrous oxide through the HRSG to extract as much energy as possible. The highest quality steam from the HRSG is sent to the HPST, then recovered again, sent to the intermediate pressure steam turbine, then recovered again and sent finally to the steam turbine; all of which are connected to a generator through rotary shafts.

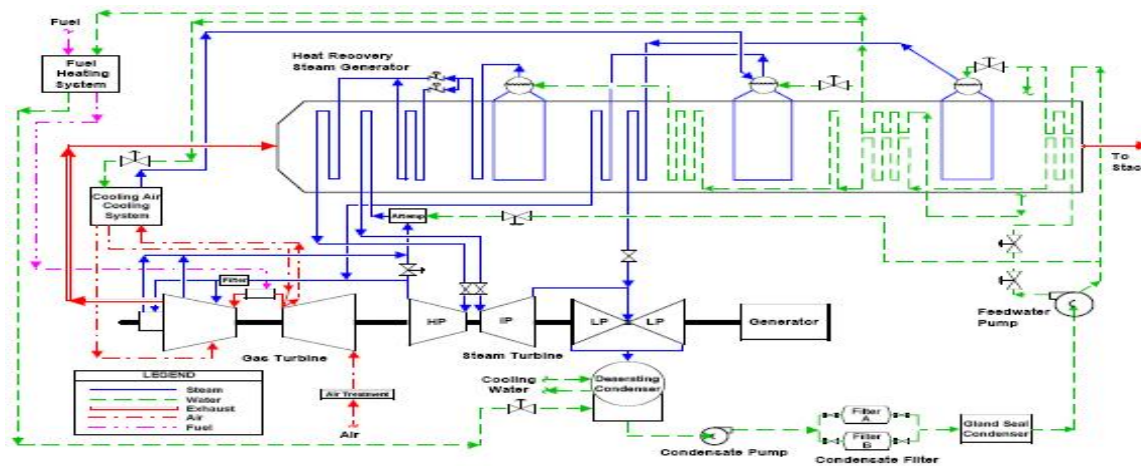


Figure 49: Heat Recovery Operations from Combined Cycle Processes

Since steam coming from the gas turbine is of equal importance to NO_x emission mitigation, another analysis was performed on steam production based on excess, beyond stoichiometric, oxygen provided for combustion in a range of 0-15%, also simulated in 'ChemKin' simulator. As is shown in Figure 50, the optimum point at which the most production of steam with the least production of NO_x occurred at 5% excess oxygen.

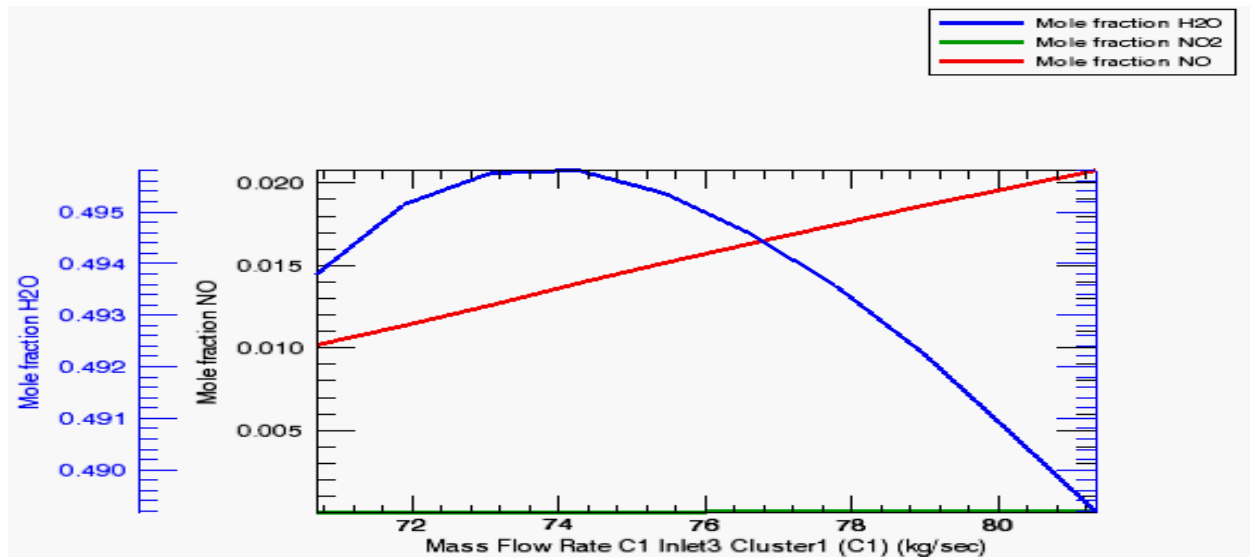


Figure 50: Steam and NO_x produced from the gas turbine, while varying excess oxygen provided

4.5.4 Conclusion

It has been determined through these consecutive analyses, that it is scientifically viable to dilute a GE H-class model S109H turbine within acceptable operating limits of the materials, while not having to expand air separation processing units. Quantitatively the desired system will require a nitrogen throughput of 7.16kmol/sec, for a given hydrogen fuel flow of 4.42Kmol/sec. Additionally, it has been determined through combustion simulation that the specified gas turbine will achieve minimal NO_x emissions, and maximum steam evolution, at its defined exhaust temperature, for combustion with 5% excess air.

4.6 Plant Performance

4.6.1 Assumptions

Table 9: Assumption Table

Key Assumptions for IGCC Plant Configuration	
Gasifier Pressure - 2X GE Energy, Texaco (MPa)	5.6
O ₂ :Coal Ratio (kg O ₂ /kg dry coal)	0.91
Carbon Conversion (%)	98
Syngas HHV at Gasifier Outlet (KJ/Nm ³)	8,644
Steam Cycle Operating Conditions (MPa/°C)	16.5/565
Condenser Pressure (mm Hg)	78
Combustion Turbine	1x H-Class
Gasifier Technology	GEE Radiant Only
Oxidant	95 vol% Oxygen
Coal	Bituminous
Coal Slurry Solids Content, %	63
COS Hydrolysis	Occurs in Sour Gas Shift
H ₂ S Separation	Selexol 1 st Stage
Sulfur Removal, %	99.7
Sulfur Recovery	Claus Plant with Tail Gas Recycle to Selexol/Elemental Sulfur
Particulate Control	Water Quench, Scrubber, and AGR Absorber
Mercury Control	Carbon Bed
NO _x Control	N ₂ Dilution
CO ₂ Separation	Selexol 2 nd Stage
Overall CO ₂ Capture	90.30%

4.6.2 Power Summary

Table 10: Power Summaries

Power Summary (Gross Power at Generator Terminals)	
Gas Turbine Power	471,000
Steam Turbine Power	267,000
Total Power, kWe	738,000
Auxiliary Load Summary, kWe	
Coal Handling	470
Coal Milling	2,270
Sour Water Recycle Slurry Pump	190
Slag Handling	1,160
Air Separation Unit Auxiliaries	1,000
Air Separation Unit Main Air Compressor	67,330
Oxygen Compressor	10,640
Nitrogen Compressors	35,640
CO2 Compressor	31,160
Boiler Feedwater Pumps	4,180
Condensate Pump	280
Quench Water Pump	540
Circulating Water Pump	4,620
Ground Water Pumps	530
Cooling Tower Fans	2,390
Scrubber Pumps	230
Acid Gas Removal	19,230
Gas Turbine Auxiliaries	1,000
Steam Turbine Auxiliaries	100
Claus Plant/TGTU Auxiliaries	250
Claus Plant TG Recycle Compressor	1,780
Miscellaneous Balance of Plant	3,000
Transformer Losses	2,760
Total Auxiliaries, kWe	190,750
Net Power, kWe	547,250
Net Plant Efficiency, %(HHV)	34.6
Net Plant Heat Rate, kj/kWh	11,034
Condenser Cooling Duty 10⁶ KJ/hr (10⁶ Btu/hr)	1,509 (1,430)
Consumables	
As-Received Coal Feed, kg/hr (lb/hr)	220,904 (487,011)
Thermal Input, kWt	1,665,074
Raw Water Withdrawal, m ³ /min (gpm)	22.0 (5,815)
Raw Water Consumption, m ³ /min (gpm)	17.9 (4,739)

Table 10 shows the gross power summary of pre-combustion carbon capture IGCC plant. The power data are based on the DOE Report 2010.

5.0 Policies and Environmental Issues

5.1 Introduction

A power project anywhere in the world will be under close scrutiny of environmentalists, law - makers, regulators and policy planners. It will be regulated under specific laws and regulations to protect the environment from damages due to either potential catastrophes or unforeseen gradual depletion of the environment. Policies and regulations are mandatory to minimize depletion of the environment by stating guidelines and setting standards for health and safety. Some of the policies that will be relevant to the geothermal project are:

- Clean Air Act (IGCC)
- Safe Drinking Water Act (EGS and IGCC)
- Hazardous Waste and Materials Regulations (IGCC)
- Occupational Health and Safety Act
- Toxic Substance Control Act
- Resource Conservation and Recovery Act
- National Pollutant Discharge Elimination System Permitting Program
- National Environmental Policy Act
- Noise Control Act
- Endangered Species Act
- Archaeological Resources Protection Act
- Indian Religious Freedom Act

Other Environmental impacts from geothermal power development are listed below:

- Land use and Land subsidence
- Water pollution and Noise pollution
- Solids and Gaseous Emissions
- Induced seismicity and Landslides
- Water Use and Water Pollution
- Disturbance of natural hydrothermal formations and wildlife habitat and vegetation
- Probability of Catastrophic events

Before the planning and development of any geothermal plant, all these factors need to be considered carefully. The above laws and regulations along with the environmental effects are in no respect secondary to any of the technological decisions and technical machinery that is designed. An optimized futuristic energy-saving system can be designed when the above factors are considered right into the developmental stages of the components of the plant. World over,

about 10,715 MW of geothermal power is online in 24 countries. An additional 28 GW of direct geothermal heating capacity is installed for district heating, space heating, spas, industrial processes, desalination and agricultural applications. Historically, geothermal power has been present near tectonic plate boundaries. Theoretically, geothermal resources can provide sufficient energy to the world, but only a fraction of that may be profitably exploited. The International Geothermal Association projects an installed capacity of 18,500 MW by 2015 based on the projects under consideration. In the United States, 77 power plants produced 3,086 MW of electricity in 2010 ("Geothermal Energy: International Market Update" Geothermal Energy Association). The edge of tectonic plates where high temperature geothermal resource is available is traditionally preferred to build geothermal power plants.

5.2 Gaseous Emissions and the Clean Air Act:

Geothermal energy is one of the least polluting forms of energy, producing virtually zero air emissions. It can work as a base load source of power as well as a fossil fuel power source. "Geothermal activity peaked in the early 1980s as a result of the OPEC oil embargo, the enactment of energy tax incentives for renewable technologies such as geothermal, the implementation of the Public Utility Regulatory Policies Act of 1978, and the funding of a substantial Department of Energy (DOE) research and development program." (Kagel and Gawell) A USGS Circular 790 nationwide geothermal study shows that nine western states may be able to produce and meet 20 percent of national electricity needs.

5.2.1 Air Emissions:

Geothermal Power plants have a very high capacity factor of 89-97%, which is much higher than any other Renewable Resource. An added advantage is, low air emissions. Geothermal facilities comfortably comply with even the more stringent California standards of air quality. "When comparing geothermal energy to existing coal power plants, the current average geothermal generation of 15 billion kWh avoids the release of harmful pollutants and greenhouse gases that would otherwise be generated by coal facilities each year, including 32,000 tons of nitrogen oxides, 78,000 tons of sulfur oxides, 17,000 tons of particulate matter, and 16 million tons of carbon dioxide." (Based on average EIA estimate of yearly geothermal generation, 2000–04) The major gases that are emitted are Nitrogen Oxide, Hydrogen Sulfide, Sulfur Dioxide, Particulate Matter, and Carbon Dioxide emissions.

5.2.2 Nitrogen Oxides:

Geothermal Power Plants do not burn fossil fuel, thereby emitting very low levels of Nitrogen oxides. The amount of NO_x that is emitted is usually from combustion of hydrogen sulfide through hydrogen sulfide abatement systems that is burnt off. So small amounts of nitrogen oxides are sometimes formed, which is miniscule. "When comparing geothermal energy to coal, the current geothermal generation of about 15 billion kWh reduces nitrogen oxide

emissions by around 32,000 tons” (Kagel and Gawell). The projected savings of NOx from this project based on the amount of coal being used is about 8200 tons annually.

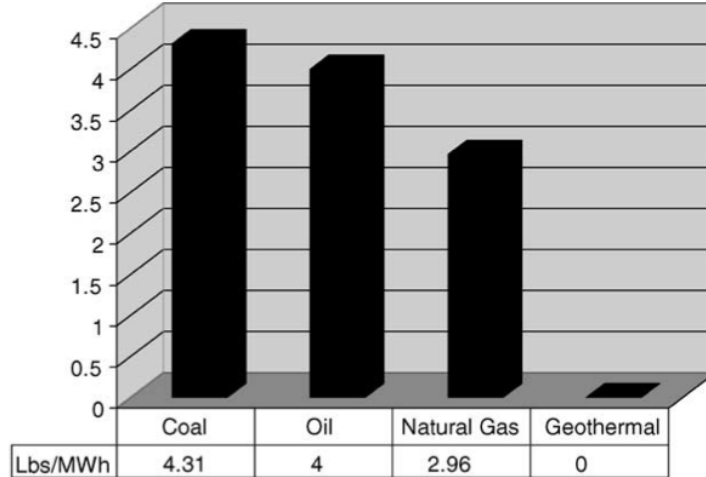


Figure 51: Nitrogen Oxide Comparison.

Coal, oil, and geothermal reported as average existing power plant emissions; natural gas reported as average existing steam cycle, simple gas turbine, and combined cycle power plant emissions. (Kagel and Gawell)

5.2.3 Hydrogen Sulfide (H₂S):

Hydrogen Sulfide abatement systems are able to remove over 99.7% of the H₂S. The conversion to sulfur can be used as fertilizer feedstock and as soil amendment. Flash type power plants produce almost no H₂S emissions and Binary plants release no H₂S at all. (Kagel and Gawell)

5.2.4 Sulfur Dioxide (SO₂):

The hydrogen sulfide released into the atmosphere oxidizes naturally in the air and oxidizes to sulfur dioxide and sulfuric acid. This is the only form of emissions of sulfur dioxide. “When comparing geothermal energy to coal, the current geothermal generation of about 15 billion kWh avoids the potential release of 78,000 tons of sulfur oxides” (Kagel and Gawell). This project will save on approximately 20,000 tons of SO₂ emissions annually.

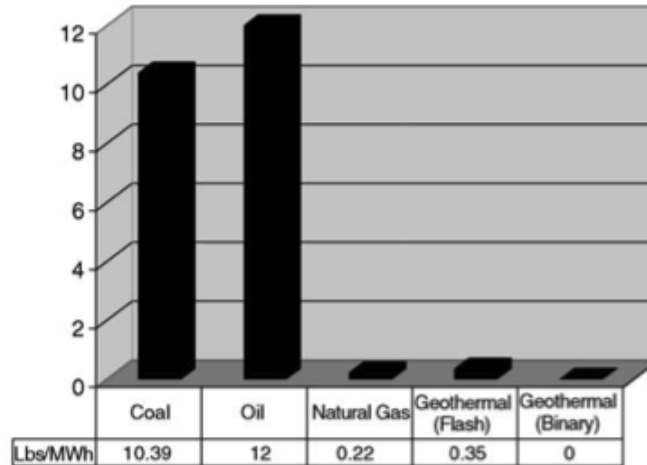


Figure 52: Sulfur Dioxide Comparison.

Coal, oil, and geothermal reported as average existing power plant emissions; natural gas reported as average existing steam cycle, simple gas turbine, and combined cycle power plant emissions. (Kagel and Gawell)

5.2.5 Particulate Matter (PM):

Coal and oil- fired facilities emit hundreds of tons of PM per year whereas geothermal power plants emit zero particulate matter emissions. “In a study of California geothermal plants, PM10 is reported as zero.” (Valentino Tiangco, et al.) “Water- cooled geothermal plants give off small amounts of particulate matter from the cooling tower when steam condensate is evaporated as part of the cooling cycle. Even considering these minimal emissions, it is estimated that geothermal energy produced in the U.S. avoids the emissions of over 17,000 tons of particulate matter each year when compared to coal production.” (Kagel and Gawell) This project saves approximately 4350 tons of PM emissions each year.

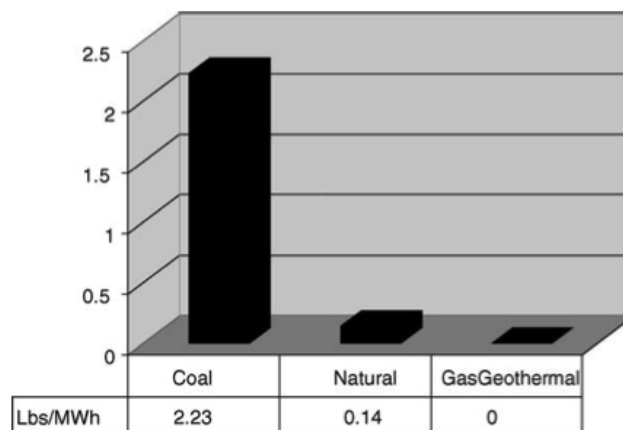


Figure 53: Particulate Matter Comparison.

Comparing pulverized coal boiler, natural gas combined cycle, and geothermal. (Kagel and Gawell)

5.2.6 Carbon Dioxide (CO₂):

Usually, steam is condensed in geothermal facilities after passing through the turbine. Carbon dioxide does not pass through the turbines and is released into the atmosphere through the cooling towers. The plant design determines the amount of carbon dioxide actually released into the atmosphere. It is hard to generalize the quantity of carbon dioxide released into the atmosphere by a geothermal system. But compared to a coal power plant, the most polluting geothermal plant will emit only a fraction of CO₂ compared to a coal power plant. “Geothermal power production currently avoids the emission of 17 million tons of carbon annually when compared to existing coal power plants.” (Kagel and Gawell) The biggest savings of this plant comes from CO₂. It is estimated that this project will save 4.35 Million tons of emissions from coal annually.

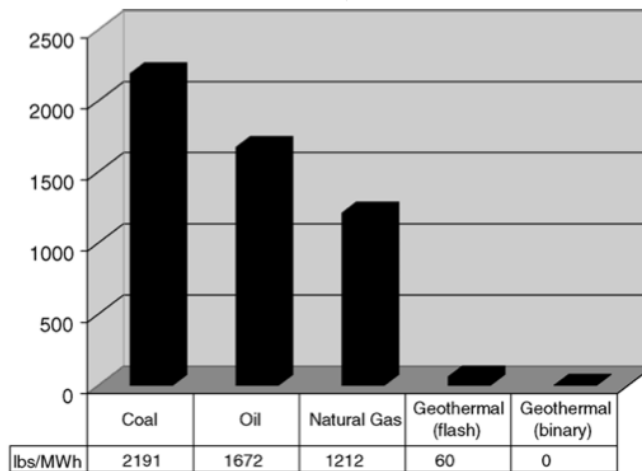


Figure 54: Carbon Dioxide Comparison.

Coal, oil, biomass, and geothermal reported as average existing system emissions; natural gas reported as average existing steam cycle, simple gas turbine, and combined cycle system emissions. (Kagel and Gawell)

5.2.7 Mercury:

In the United States, the Geysers is one of the main geothermal resources that is known to have Mercury. The operation of a binary geothermal power plant will not emit any mercury because of the presence of a closed loop system. The geothermal fluid will be replaced in the reservoir without causing any emissions. If any, the main source of mercury would be in the steam of the geothermal fluid. The installation of mercury abatement technologies in geothermal power plants

can be installed voluntarily. Even the largest mercury emitters (The Geysers) do not emit enough to cause a health risk based on California standards and regulations. "...Mercury levels at geothermal facilities do not trigger federal regulations." (Kagel and Gawell) The mercury filter present in the binary cycle will absorb mercury and removes about 90 percent of the mercury. Only non-hazardous sulfur is left over which may be used as a soil amendment.

The Regional Haze rule is under Section 160-169 of the Clean Air Act and states requirements for the prevention of significant deterioration of air quality (PSD). This rule is applicable to areas where air quality is better than what is required by the National Ambient Air Quality Standards (NAAQS). The NAAQS takes into consideration six air pollutants namely sulfur dioxide, particulate matter, carbon monoxide, ozone, lead and nitrogen dioxide. The Act classifies clean air areas into three categories and states the allowable increments of SO₂. Class I areas are primeval areas like national parks, wilderness areas and the allowable increments of air pollutants is very small. Class II areas are all attainment and areas not classified as Class I. The allowable increments of air pollutants are moderate. Class III areas are those that are designated by states for developments.

The Acid Deposition Control program added Amendments in 1990. Usually, when a target is set to reduce SO₂ or NO_x emissions, a broad set of permits and emissions allowance system is used to allow industrial facilities to adapt to the new regulations. An allowance is an authorization to emit one ton of SO₂. New facilities that are set up will have to obtain allowances from holders of existing allowances. Utilities may obtain allowances from other industries under certain regulations specified by the EPA or may be banked for future use. In some cases, power producers may have access to guaranteed rights of allowances. "The SO₂ emission cap for utilities was set at 8.9 million tons, with some exceptions." (James E. McCarthy) If utilities don't have enough allowances to cover its emissions, a penalty of \$2000 per ton of SO₂ will be charged and will be required to reduce its emissions by another ton the following year.

The SO₂ emission cap-and-trade mechanism is adapted in the acid rain program found in Title IV of the Clean Air Act amendments. There are various other NO_x trading programs along with the Regional Haze Rule.

The EPA keeps an inventory of emissions of SO₂ and takes action under the Clean Air Act if industrial emissions reach levels above a cap of 5.6 million tons per year.

"The Act requires EPA to set specific NO_x emission rate limitations—0.45 lb. per million Btu for tangentially-fired boilers and 0.50 lb. per million Btu for wall-fired boilers—unless those rates cannot be achieved by low-NO_x burner technology." (James E. McCarthy)

5.2.8 Permits and Enforcement:

It is the responsibility of the states to enforce a permit program to monitor emission of air pollutants. New or modified stationary sources need to acquire construction permits. Such permit requirements however include only major emitters that have to potential to emit 100 tons per year of a pollutant. In nonattainment areas permits are required to emit even 10 tons per year of Volatile Organic Compounds. States meet the costs of such a program by charging annual fees from emitters of at least \$25 per ton of regulated pollutants with a voluntary cap on 4000 tons per year above which a fee may not be charged. Compliance monitoring is done by local governments through inspections and is subject to review by the federal government, which may enforce action.

5.3 Emissions Trading:

Emissions trading are also known as a cap-and-trade system. To achieve reductions in emissions of pollutants, financial or economic incentives can be provided by usually a governmental body in a market allowing industries a flexible mechanism to control their emissions. The term Emissions Trading, central to economics has been defined by different authors in the following way:

“A cap-and-trade system constrains the aggregate emissions of regulated sources by creating a limited number of tradable emission allowances, which emission sources must secure and surrender in number equal to their emissions.” (Judson Jaffe, Matthew Ranson and Robert N. Stavins)

5.3.1 CO₂ and cap-and-trade:

In the case of carbon dioxide, it is advantageous to use the cap and trade system because it has a uniform externality and does not have spatial or temporal effects unlike emissions such as sulfur dioxide which have a tendency to create ‘hot spots’ if the emissions of the gas are largely concentrated in one area. Therefore the overall impact of carbon dioxide is the net sum of accumulated stock over a long period of time rather than a short time, say, a year (Butzengeiger, Betz and Bode, 2001). Another important consideration for this system to work is that the participating firms must be largely varied for any potential gains from trading credits. If all firms belonged to just one industry, even if emerging from different timelines would all face more or less the same costs and would not result in any net buyers or net sellers thereby resulting in a sufficiently large liquid market. This would also result in a clear price signal. It is easier for firms to make long term investment decisions since expected profits from returns on investment are much clearer. This way, a restriction on anomalies is also put in place for instance; no single participant will hold extensive market power which would restrict in trading (Quirion, 2002).

5.3.2 Allocation of credits:

Auctioning is the most desirable method of awarding credits to firms. It not only sets a price signal but also promotes a transparent price market. A whole lot of information is made available this way and a trust of certainty in the scheme is created. It enables firms to make long-term investment decisions and allows positioning itself into a net buyer or net seller based on how cheap it is for the firm. It makes clearer for a firm to fund research and development into green technology and allows cutting of distorted taxes on capital and labor due to high unemployment. Auctioning also gives new entrants a fair chance of treatment as the incumbents since the participants themselves are responsible for buying credits and hence allocating allowances.

5.3.3 Economics of cap-and-trade and Emission tax:

In emissions trading, an emission cap is a system which is quantity based since an overall emission volume of a certain greenhouse gas is fixed. All markets are volatile and are subject to risks from natural disasters, availability of raw material, strikes, securities, internal credit issues, product liability, uncertainty in future supply and demand conditions etc. Under these altering and ambiguous conditions, the ability of a governmental agency to alter caps may result in certain firms from benefiting or losing and thus provides an opportunity for corruption.

On the other hand if a price based instrument is introduced such as an ‘Emission Tax’, only a price is fixed but emission levels will be allowed to vary according to economic activities of a country. The only problem with this system is that it may not be significantly successful in achieving emission goals. Introducing an economic tax, just as any other tax is not beneficial for the society as it creates a dead weight loss thus removing capital from the industry but on the other hand the polluter will not have to invest and manage a diverse risk management portfolio (hedging against future uncertainties) as the tax will be charged directly on the profits of the firm. The industry will benefit from less corruption.

As in any case, no single policy can be rewarded as most perfect. It is usually a mixture of flexible properties of beneficial policies that are most desirable. Another option, known as a *safety valve*, is a hybrid of the price and quantity instruments. This is essentially an emission cap and permit trading system but the maximum (or minimum) permit price is capped. Emitters have the choice of either obtaining permits in the marketplace or purchasing them from the government at a specified trigger price (which could be adjusted over time). This, at times may help overcome the difficulties of both systems. It gives governments the flexibility to adjust the system, as new information is available. It can be shown that setting the trigger price high enough, or the number of permits low enough can use the safety valve used to mimic either a pure quantity or pure price mechanism. (Jacoby, D.H.; Ellerman, A.D., 2004-03) A safety valve is able to impose a minimum price per ton of CO₂ emitted.

5.3.4 Acid Rain Program:

The Acid Rain Program is stated in Title IV of the Clean Air Act amendments. It primarily states to achieve reductions in SO₂ and NO_x emissions. The Allowance Trading system is introduced under the Acid Rain Program which takes advantage of the open market to reduce air pollution. Utilities or industries are allotted permits equivalent to the permission to emit 1 ton of SO₂ a year per allowance. Any individual or group can purchase allowances. The Allowance Tracking System is a monitoring system designed by the EPA and tracks allowance accounts and all activities. It is a method of monitoring the compliance of emissions by utilities based on the number of allowances purchased. The Chicago Climate Futures Exchange (CCFE) is an open trading market for exchanging Carbon, SO₂ and NO_x. Some futures and options contracts provide tools for analyzing the emission allowance trade. Price risks remain, but can be managed by using these futures and options programs that the CCFE offers. The SFI Futures Program is one such. Based on the U.S. EPA Acid Rain Program the SO₂ emission allowances.

Table 11: Specifications¹ for Acid Rain Program

	SFI Futures	SFI Options
Description	Physically deliverable futures contract based on EPA Acid Rain Program SO ₂ Emission Allowances	Options on Sulfur Financial Instrument Futures
Contract Size	25 U.S EPA SO ₂ Emission Allowances	1 SFI Futures contract
Ticker Symbol	SFI	SFIC, SFIP
Minimum Tick Increment	\$0.10 per U.S. EPA SO ₂ emission Allowance (\$2.50 per contract)	\$0.05 per Allowance (\$1.25 per contract)
Speculative Position Limits	8,000 contracts (200,000 US EPA SO ₂ emission Allowances per expiring product)	8,000 contracts on a net futures-equivalent basis (200,000 US EPA SO ₂ Emission Allowances)
Block Trade Minimum	20 contracts in any contract/product month	20 contracts in any contract/product month

¹ <http://www.ccf.com/>

Similarly, Based on U.S. EPA Clean Air Interstate Rule (CAIR), the NFI Futures and Options Program is used to trade NO_x Emissions.

Table 12: Specifications² for Clean Air Interstate Rule

	NFI-A Futures	NFI-A Options
Description	Physically deliverable futures contract based on EPA CAIR Annual NO _x Emission Allowances	Nitrogen Financial Instrument Annual Options
Contract Size	1 US EPA CAIR Annual NO _x Allowance	1 NFI-A Futures contract
Ticker Symbol	NFI-A	NFI-AC, NFI-AP
Minimum Tick Increment	\$1.00 per ton (\$1.00 per contract)	\$0.50 per ton (\$0.50 per contract)
Speculative Position Limits	5,000 contracts (5,000 Allowances)	5,000 contracts (5,000 US EPA CAIR Annual NO _x Emission Allowances on net futures-equivalent basis)
Block Trade Minimum	50 contracts in any contract/ product month	50 contracts in any contract/ product month

When Allowance trading started in 1993, the difference between the minimum and maximum price of SO₂ traded was nearly \$400. That is an extremely large difference. The average price of an allowance traded was \$131. The prices continued on an upward trend and reached their peak during the years 2005-2006 after which the trading prices started at an all-time low, with the minimum prices starting around 6 cents. Table 5.3 shows the Trading prices ranging from 1993 to 2011.

² <http://www.ccf.com/>

Table 13: Trading prices of SO₂ allowances

Year	Minimum Price (\$)	Maximum Price (\$)	Average Price (\$)
1993	0.26	450	131
1994	24	400	150
1995	1	350	130
1996	39	300	66.05
1997	0.02	121.02	106.75
1998	56.91	228.92	116.96
1999	41.16	230	207.03
2000	80.05	250	130.69
2001	105	225	173.57
2002	150	215	160.5
2003	2.06	250	171.81
2004	107	300	272.82
2005	300	750	702.51
2006	650	1700	860.07
2007	300	1120	444.39
2008	0.27	651	389.91
2009	0.06	500	69.74
2010	0.06	300	36.2
2011	0.06	66.67	2.81

Figure 55 illustrates the graphical interpretation of the trading prices ranging from 1933 to 2011. It clearly indicates that the Maximum price was around the period 2005-2006, although the maximum volume traded was in the year 2000 and 2002.

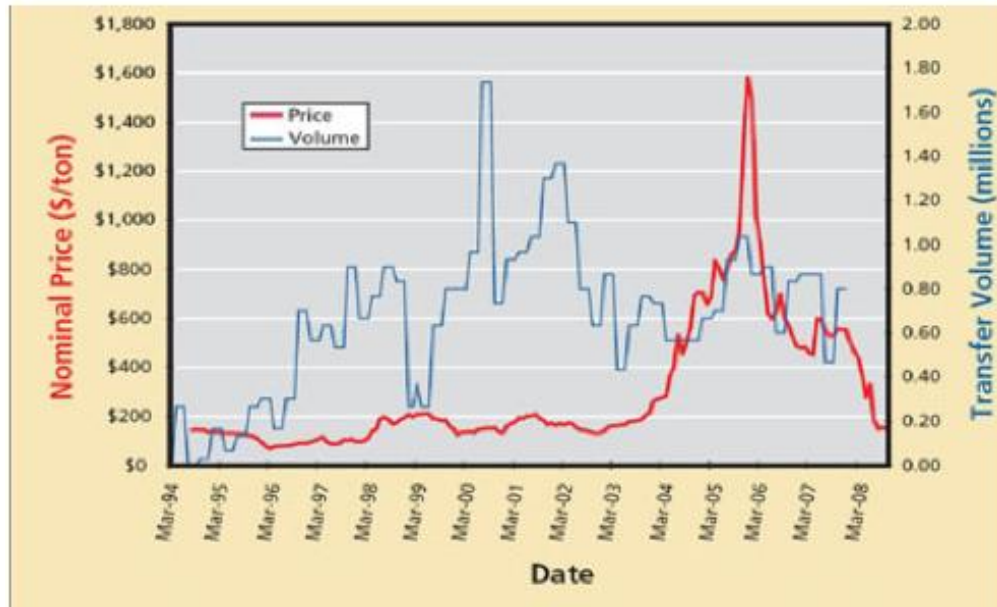


Figure 55: Price & Volume of Sulfur Dioxide Traded³

5.4 Water usage, Water Pollution and the Safe Drinking Water Act:

A geothermal power plant requires water at various stages of its lifecycle. The quantity of water required however is less compared to other types of power development projects. For this project the maximum usage of water is associated with the drilling of the geothermal wells and heat exchangers.

During well drilling, a mixture of water and chemicals, or drilling muds, are used to remove rock chips, cool drill bits and provide structural integrity of the hole until a casing can be set. This mixture is cooled and re-circulated after being strained to remove rock fragments at the surface. The water used for drilling will most likely not be reused as a geothermal working fluid due to the costs of processing. This water will be disposed of using industry best practices which may include mobile onsite treatment prior to transportation off site.

The water for geothermal power generation via heat rejection is required on a continuous basis. Waste heat will need to be removed by cooling towers. Fresh water is required to blow out the buildup of solids in the cold well of the cooling tower in conventional geothermal plants. This water too can be stored in tanks. The steam condensate is sufficient to make up for the evaporation losses of water from the tower.

The Safe Drinking Water Act (SDWA) is a federal law that monitors, sets standards and ensures the quality of drinking water all over the country. Regulations and standards for drinking

³ (<http://www.epa.gov/airmarkets/trading/auction.html>)

water quality are set for localities, states and water suppliers. Many actions are required to protect drinking water sources such as rivers, springs, reservoirs, lakes and ground water wells. The United States Environmental Protection Agency is allowed to set national health standards for drinking water to protect from man-made and naturally occurring contaminants. The SDWA applies to all public water systems in the United States. More than 160,000 public water systems provide drinking water to millions of Americans every day.⁴

Improper disposition of chemicals, pesticides, underground injected wastes, human and animal wastes and naturally occurring substances contaminate drinking water. With respect to wells, the SDWA has an Underground Injection Control (UIC) program that "...is responsible for regulating the construction, operation, permitting, and closure of injection wells that place fluids underground for storage or disposal."⁵

Wells are categorized into different classes based on their use. A Class II well is an injection well that is used to inject fluids. The injected fluid in this case is scCO₂. Usually class II wells are associated with oil and gas extraction. Usually injection wells are surrounded by multiple production wells. The UIC does not regulate production wells. Disposal wells inject brine and other fluids deep into the surface. At times large amounts of brine will be brought to the surface. These produced brines may contain toxic metals and radioactive substances that can be extremely damaging to surface water or the land surface. By injecting this brine deep underground, surface water and soil is protected from contamination.

Similarly, Class VI Wells are used to inject carbon dioxide underground for sequestration or storage. This technology can be used to mitigate emissions from carbon dioxide. Class VI wells ensure that the materials used in the construction of the well are durable with carbon dioxide. The regulations pertaining to the design of the well ensure adequate quality of operation, testing, monitoring and closing of the well in a method that protects underground drinking water. It also addresses the migration effects of carbon dioxide after it has been injected into the ground such as its corrosively with water, relative buoyancy, mobility and the volume injected. Financial Responsibility Requirements for running the wells also have to be met for the life of the well including emergency response and post-injection care of site.⁶

“Section 1422 requires states to meet EPA’s minimum requirements for UIC programs. Programs authorized under section 1422 must include construction, operating, monitoring and testing, reporting, and closure requirements for well owners or operators. Enhanced oil and gas recovery wells may either be issued permits or be authorized by rule. Disposal wells are issued

⁴ <http://water.epa.gov/lawsregs/rulesregs/sdwa/index.cfm>

⁵ <http://water.epa.gov/type/groundwater/>

⁶ <http://water.epa.gov/groundwater/uic/class6/gclass6wells.cfm>

permits. The owners or operators of the wells must meet all applicable requirements, including strict construction and conversion standards and regular testing and inspection.”⁷

“**Section 1425** allows states to demonstrate that their existing standards are effective in preventing endangerment of USDWs. These programs must include permitting, inspection, monitoring, and record-keeping and reporting that demonstrates the effectiveness of their requirements.”⁸

“The UIC Program regulates injection wells that are used to dispose of spent geothermal fluids following power generation. These wells fall under Class V injection wells (40 CFR 144.24). Under Class V, operators may not endanger underground sources of drinking water (USDWs) (40 CFR 144.12), and they must submit basic inventory information (40 CFR 144.26). For EGSs, hydraulic fracturing is needed to stimulate the resource. The UIC Program also applies to hydraulic fracturing for the following activities:

1. Well injection of fluids into a formation to enhance oil and gas production (Class II wells);
2. Hydraulic fracturing used in connection with Class II and Class V injection wells to stimulate a formation; and
3. Hydraulic fracturing activities to produce methane from coal beds in the state of Alabama.” (Clark, 2009)

⁷ <http://water.epa.gov//groundwater/uic/class2/index.cfm>

⁸ (<http://water.epa.gov/groundwater/uic/class2/index.cfm>)



Figure 56: Class VI Wells⁹

Figure 57: Class II Wells¹⁰

Figure 56 and 57 illustrate the Class VI and Class II Injection wells. It clearly shows the secure structure drilled deep inside the surface of the earth well below the underground water table. This deep reach into the surface is able to prevent groundwater from contamination.

5.5 Coal Production and Reserves:

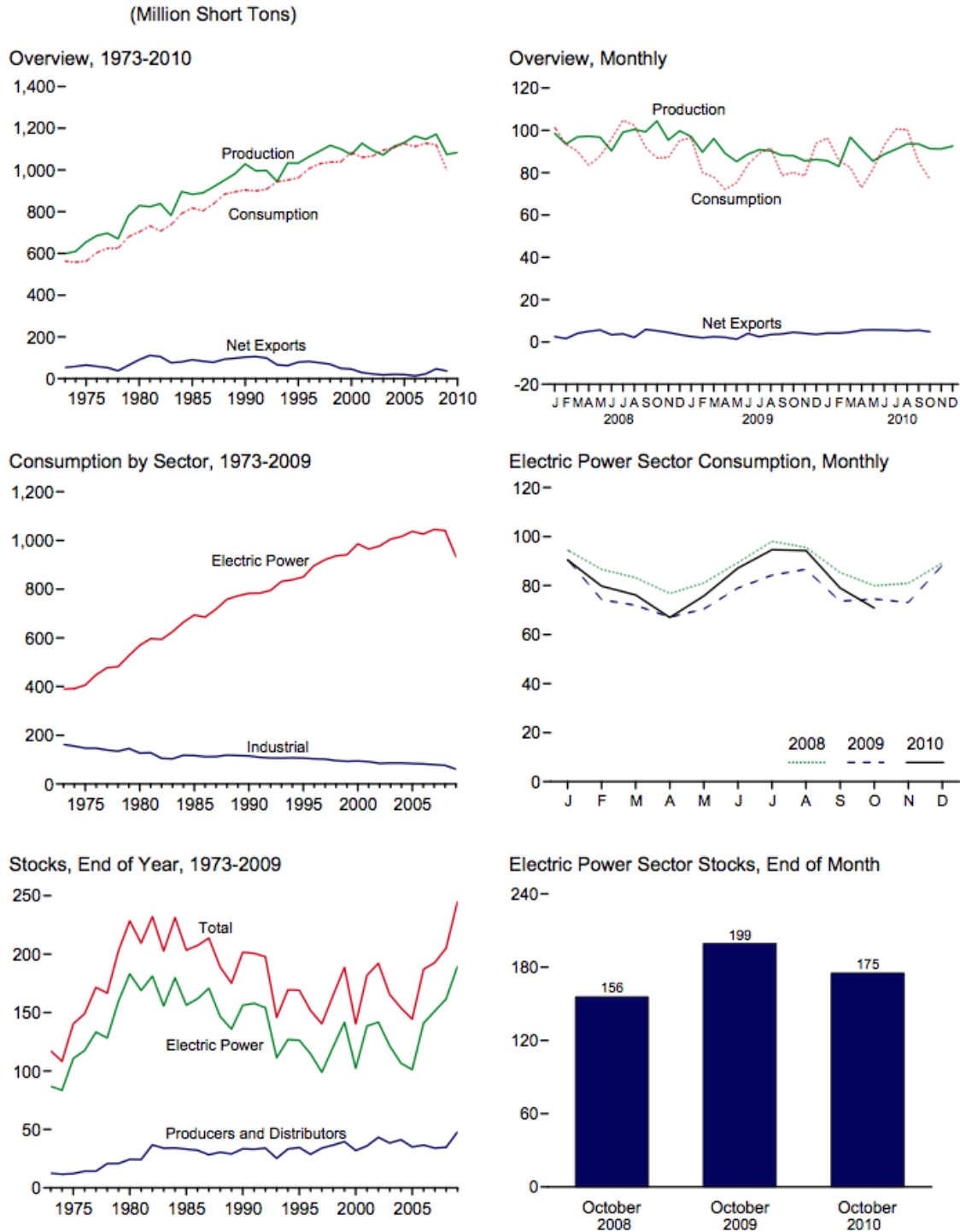
Coal stocks increased to 27.8 million short tons in 2009 from 2008 totaling coal stocks at the end of 2009 to 233.0 million short tons. Coal stocks held totally were higher by 3.5 percent.

⁹ (<http://water.epa.gov/type/groundwater/uic/class6/gclass6wells.cfm>)

¹⁰ (<http://water.epa.gov/type/groundwater/uic/class2/index.cfm>)

Coke plants held a total of 7.1 million short tons at the end of 2009. The electric power sector had total coal stocks of 189.5 Million Short Tons, 17.3 percent over the 2008 level. New Mexico has five coal mines of which four are surface mines and one is an underground mine. There are three surface mines that are located at McKinley, which is located a little over 100 miles from Albuquerque. San Juan is home to one Underground mine and another surface mine. The total production of coal from New Mexico was 25,124 Thousand Short Tons in 2009. The electric power sector consumes 94 percent of all coal in the U.S. The New Mexico coalmines have one of the highest Average Recovery Percentage compared with other states. 92.82 percent of coal can be recovered as of 2009 (This number has increased year after year in the mines in New Mexico). The recoverable coal reserves as of 2009 stands at 380 Million Short Tons. The U.S. Coal supply, disposition and prices are reported by region, namely, Appalachian, Interior and Western. New Mexico occurs in the Western region. In 2009, the Western Region reported the highest production of all regions at 585 Million Short Tons. Out of total production of about 1074.9 Million Short Tons, the Western Region produced about 585 Million Short Tons of which the largest state producing was Wyoming with a total of 431.1 Million Short Tons of coal. New Mexico, an average producer of coal in the Western Region produced about 25.1 Million Short Tons of coal. (Annual Coal Report 2009)

The Average U.S. Open Market Mine Price was \$33.24 in 2009. However, the Average Delivered Price to Electric Utilities stood at \$44.47 in 2009, an increase of \$3.15 per Short Ton from 2008. Other deliveries were made to Coke Plants, other Industrial Plants and Commercial/Institutional setups. The highest delivered price was \$143.01 to Coke Plants, which is typical of the industry. We are interested in the Electric Power sector and by Census, it is found that New Mexico's Electric Power Industry consumed 16,514 Thousand Short Tons of coal in 2009, a 7.1 percentage change from the previous year. The Average Sales Price from the mines in New Mexico was \$30.71 per Short Ton in 2009. However, the Average price of coal delivered to Electric Utility plants has been about \$35.03 per short ton. According to the U.S. Energy Information Administration, "Cost and Quality of Fuels for Electric Plants 2009" published in November 2010, it is shown that New Mexico power plants do not import coal from any other state. Local coal used in 2009 was 16,535 thousand tons. (Quarterly Coal Report July-September 2010)



Web Page: <http://www.eia.gov/mer/coal.html>.
Sources: Tables 6.1-6.3.

Figure 58: Consumption of Coal (Trends over Time)

It is seen that there is more consumption of coal from June to September. Noticing this trend, it is predicted that the geothermal plant will have similar working patterns in terms of production of power and consumption of coal.

Shown in Figure 58, from the EIA's Coal Review of Consumption patterns are a few graphs indicating maximum demand and production, stocks and power sector requirements of coal at different times of the year. Another interesting observation that is noted is that although the power sector's consumption is on an upward trend (more than doubled) in a period of nearly thirty years, the consumption by industrial facilities has actually declined over time, albeit marginally.

Stocks of Coal by Electric utilities and other Producers and Distributors have been on a continuous increase and decrease trend over the period of 30 years. The stocks seem to rise and fall at similar intervals by approximately the same amount. This could be due to similar demands of power output at the same time of the year. It seems like an ideal stock pile number is created since the numbers indicate a close range of stocks at the end of month (October) reviews.

5.6 Conclusion

The environmental impacts associated with the development of EGS are small when compared with other fossil fuel projects. Right from the small land footprint to the savings on carbon dioxide emissions, the future of EGS seems well oriented towards a promising, reliable and clean source of power. If only the cost of this project could be minimized by careful planning, the reality of producing power from a clean source for the next three decades looks promising.

6.0 Social and Cultural Consideration

For the combined $scCO_2$ -EGS IGCC power plant to exist successfully near Albuquerque, NM it must fit into the long term plans of the city and the state while addressing both scientific and public concerns. Land use and cultural issues can halt the project as quickly as technical and policy issues. It is vital that the majority of the concerns be identified addressed before the ground breaking of the plant. By allowing scientific and public concerns to be voiced prior to ground breaking it will allow the community to be a part of the decision making process and may avoid considerable public opposition for the project. Three potential areas that will be important to address for this project are water usage, tourism/ community usage, and induced seismicity.

Sustainable water supply is a major concern for the city of Albuquerque and falls under both land use and cultural issues. Water supply is currently managed through intelligent water use and reuse where lower quality waters are used for industrial purposes (ABC WUA 2007). To achieve sustainable water supply the ABC WUA has pursued the following policies to meet these ends: public education, low water use landscaping new construction, conservation penalties and incentives, mandatory drought management, protect areas of natural infiltration and recharge. The citizens and lawmakers of Albuquerque will react strongly to any large water withdrawals especially during water rationing periods. An initial recommendation for the water usage related to the IGCC is to restrict water usage to the industrial and grey waters that are sourced from the city. Additionally scheduled maintenance downtimes will be selected to correspond to known severe drought periods. At the time of the study it was unclear if the plant area was located within an area of natural infiltration or recharge. However, there is latitude for plant movement near the selected site which should permit key areas of groundwater recharge to be avoided.

The city of Albuquerque is actively planning for its future and the mayor has proposed projects that are to be built over a 25 year period (ABQ the Plan, 2011). The focus of these land use plans is on the interaction of humans, the community, and the environment. The goal is to create a year-long draw for locals and tourists both within the city and in the surrounding scenic areas. Specifically, Rio Grande Enhancements, are planned which will include more scenic overlooks and boardwalks and possible kayaking in the nearby canals (ABQ the Plan, 2011). It is also mentioned briefly that restaurants and other businesses could be developed along these eco-appreciation corridors (ABQ the Plan, 2011). The ABQ Plan (2011) focuses on land use planning that will enhance the interaction of humans with the visual landscape. Large industrial sites will require designs that preserve the natural landscape and minimize their visual footprint to avoid land-use conflicts. To accomplish this feat the power plant will have to blend into its surrounding through the successful application of tactical architectural design.

Induced seismicity, aside from a technical concern, is also justifiably a major cultural concern for any enhanced geothermal system located near a population center. While the

magnitude and frequency of seismic events can be minimized through intelligent injection strategies they cannot be completely avoided. The relatively short distances between the injection sites and the city of Albuquerque make public education vital. To make public education successful it will have to match the demographics of the population center. Though the majority of the Albuquerque population identifies themselves as white/Caucasian, there are a significant percentage of people who are of Hispanic descent (US Census, 2006). At a minimum bilingual educators and mediators will be required for outreach and town hall meetings. It will be best that induced seismicity education be initiated prior to the start of plant operations. By preparing the neighbors of the power plant before any seismic events it may be possible to gain tolerance as the injection strategies are fine tuned. There will be a finite time period that will be strongly related to event magnitude and frequency for which the public and policy makers will allow before opposition rises so injection strategies must develop quickly.

The cultural issues of this project are as important as the technical and policy issues. However unlike the technical and policy issues, cultural issues can if, addressed properly, be overcome. To permit these cultural issues to be overcome more successful dialogue must occur and solutions must be found. It is vital that professional mediators be used during town hall meeting to limit the de-evolution of the meetings while allowing legitimate concerns to be voiced and addressed by the panel of scientists, engineers, policy makers, and social scientists.

In 2005, The Department of Energy stated that 86% of New Mexico's power was coal based. (EIA, 2005) Although a predominant portion of New Mexico's power comes from coal based power plants, the public opinion towards coal plants have been falling dramatically in popularity. A recent event in New Mexico's news headlines illustrates the public perception towards current coal power generation practices.

Desert Rock Energy Company proposed the construction of a 1500 MW coal fired power plant in 2006. This company proposed the construction of a conventional supercritical coal power plant in the four corners region. As a result of the plants predicted environmental repercussions, the proposal was met with harsh social opposition. The tension built so much that in 2009 the Environmental Appeals Board of the EPA passed a remand order for the plant's permit. (New Mexico Business Weekly, 2008)

“The Board concludes, based upon a review of the administrative record, that the Permit should be remanded in its entirety because the Region abused its discretion in declining to consider integrated gasification combined cycle (“IGCC”) as a potential control technology in step 1 of its BACT analysis for the facility.” (EPA, 2009)

The impact of this decision sends a clear message about the region's new standards for power generation. This decision shows that adequate pollution control and CO₂ emissions reduction are prominent ideals in the eye of the public. Failure to properly address the public's concern in this case resulted with serious delays that may end the project.

In light of this recent public event, the combination of EGS and IGCC could not be more timely. This method of power generation provides a unique and powerful solution to reduce

carbon emissions and manage pollution control. It is both a realistic and effective method of harnessing local resources for the highest potential while reducing the environmental repercussions to record lows.

7.0 Infrastructure

7.1 EGS Infrastructure:

The EGS infrastructure is categorized as (i) Temporary Infrastructure and (ii) Permanent Infrastructure. Temporary infrastructure includes camps at well drilling sites, maintenance shop and emergency facility. Permanent infrastructure will be (a) 9 injection wells and 16 production wells of 3 km depth (b) double flash binary system for 125 MW of power generation. (c) Cooling tower for purification and reuse of CO₂. (d) Administrative building for regulating all activities, fire control building, living quarters for employees and maintenance building.

7.2 IGCC Infrastructure:

The IGCC power plant requires an infrastructure of multiple buildings and auxiliary systems to conduct daily operations. Buildings are needed to hold the IGCC reactors and power generators as well as an onsite machine shop, warehouses and waste & water treatment facilities. In addition, an industrial scale water cooling system and pump house will be mandatory for the management of the plant's water supplies. The auxiliary systems required consist of heating, ventilation, air conditioning, lighting and telecommunications systems for areas with personnel.

7.3 Support Facilities:

It is estimated that the IGCC will require 4.2 million gallons of water circulating through the system per day for coal conversion. Although the majority of water is recovered a proportion of the water will be lost. Assuming a 10% loss the plant will require approximately 420,000 gallons per day of make-up water.

If a suitable water source cannot deliver the required water volume at a constant flow rate then onsite water storage will have to be created. For this project it is proposed that the water source will be grey water which will not flow at a constant flow rate therefore holding tanks will be necessary. To ensure continuity of operations in the event of flow interruptions one day worth of water will be stored on site.

The hauling of coal by road or by rail will be decided by the site location and the proximity of railway lines or roads. It will be necessary to build a railway line from the nearest point which lies approximately 8 miles away

8.0 Land Usage and Ownership:

The entire site will be occupied by 13 wells and the total area of land available is 4 Km by 14 Km. The land lie within Indian Reservations nor is it on U.S. Government property. The reservoir presently required is conservatively estimated to occupy a 2 km² surface area. Keeping in mind the geofluid pressure and temperature properties, it is beneficial to place the power plant close to the center of this surface area to minimize transmission distances and heat losses.

The gathering system of the pipeline, mounted on stanchions saves usable land space for agriculture, grazing or other compatible use. The power plant, heat exchangers and other components do not occupy much space. The land occupied by EGS system will be 0.15 km² while by IGCC system will be 1.35 km².

The geothermal fluid balance will need to be accurately monitored. The production rates should not exceed the recharge rates as the reservoir collapse could occur. If of significant amounts surface subsidence could occur. The reservoir will need to be managed and monitored continuously to prevent such dangers from occurring.

9.0 Economics

9.1 Introduction:

There are distinct advantages of coupling a scCO₂ EGS to an IGCC power plant. There are considerable taxes, loans, and CO₂ credits benefits that are associated with both technologies that will lower the cost of electric generation. In addition to these strictly governmental created incentives there is a strong possibility to avoid duplication of different process units which will create cost savings regardless of political climates. It is the goal of this project to create a power plant system that is economically feasible with minimal government mandated support.

9.2 Governmental Derived Incentives:

This form of recovering some of the funds from operation is being explored. The IGCC-EGS project has to qualify to have a stable income from this program.

Form 8933 of the Department of the Treasury Internal Revenue Service is the Carbon Dioxide Sequestration Credit program application. A credit of \$10 per metric ton for qualified carbon dioxide captured and used is awarded to the facility. Similarly, a sum of \$20.24 per ton is awarded to a facility that captures and disposes of CO₂. The form defines Qualified CO₂ as “...Carbon dioxide captured after October 3, 2008, from an industrial source that would otherwise be released into the atmosphere as industrial emission of greenhouse gas, and is measured at the source of capture and verified at the point of disposal or injection. Qualified carbon dioxide also includes the initial deposit of captured carbon dioxide used as a tertiary injectant. However, it does not include carbon dioxide that is re-captured, recycled, or otherwise re-injected as part of the enhanced oil and natural gas recovery process. Qualified carbon dioxide does not include carbon dioxide that is captured and sequestered in a project to the extent required under an agreement executed with the IRS under the qualifying advanced coal project program of section 48A or the qualifying gasification project program of section 48B.”

Similarly, a qualified facility is defined as “...any industrial facility that is owned by the taxpayer where carbon capture equipment is placed in service and that captures at least 500,000 metric tons of carbon dioxide during the tax year.”

If this project qualifies under the applicable rules and assuming there isn't a cap in place for the monetary reward structure, capturing and using approximately 4.35 Million tons of CO₂ at a rate of \$10.12 will project in annual earnings of \$44 Million. Capturing and disposing off about 10% of 4.35 Million tons in the form of underground sequestration will earn \$20.24 per ton generating approximately \$8 Million. Annual earnings from CO₂ can amount to nearly \$50 Million.

9.3 Enhanced Geothermal System Economics:

The success and failure of any geothermal resources is strongly dependent upon the depth and the temperature of the resource. From the 2006 MIT report the costs can be divided into three areas:

- Exploration, drilling, and completion of wells.
- Construction of power conversion facilities
- Discounted future re-drilling and well stimulation.

9.3.1 Exploration, drilling, and completion of wells

The costs for the exploration of geothermal resources is dependent upon the amount of available data that does not have to be self created. A thorough review of the available data is critical. Fortunately within the state of New Mexico, specifically the Albuquerque Basin, there is sufficient subsurface data to successfully guide geothermal exploration. The multiple generations of seismic reflection data across the basin provide an accurate picture of the subsurface. The well-control for these seismic lines is provided by deep oil and gas wells such as Transocean Isleta-1. The drilling records of these deep oil and gas wells provide insights into possible issues that will arise during the drilling of the EGS wells. By anticipating issues it will be possible to minimize rig downtimes and damages to the well during its construction.

The costs of drilling and completion of geothermal wells are incorporated into Wellcost Lite[®] (Mansure et al. 2005). The proposed final total depth for this project is 5km. This corresponds to the Mid-range EGS well category as proposed in the 2006 MIT report. The cost for drilling an EGS well as suggested by the Wellcost Lite[®] model is approximately \$7MM if four casing strings are used. If five casing strings are used then the cost to drill the well rises to approximately \$8.3MM. It is assumed that the values determined by GETEM for the well categories will hold constant for the other aspects of the plant cost estimating. From below these two values typically make up almost 60% of the total project costs for conventional EGS projects. To get the required flow rate the values for a field development category is approximately \$600,000,000. It is very possible that advanced drilling technologies of oil and gas service companies can reduce these costs. An example of significant cost savings was reported by Baker Hughes in early April 2011. Through their efforts they were able to save approximately \$1.3 million.

9.3.2 Construction of power conversion facilities

The construction of the power conversion facilities and geothermal power estimation for the site in this project is accomplished by the spreadsheet model that was developed by Entingh et al. (2006). The Geothermal Electricity Technology Evaluation Model (GETEM) is capable of taking user defined inputs and allows the user to select different estimating criteria within the model. Furthermore, the version of GETEM used in this project was able to estimate binary but

not flash geothermal power plants. While this model is “...sufficient to calculate electric power costs, [it is] not necessarily sufficient for other purposes” (Entingh et al., 2006). These other purposes are associated with the other costs that are associated with exploration, well drilling, well completion, and stimulation and are addressed in other sections of this report. The system that was modeled here was based on the following assumptions:

- Geofluid inlet temperature: 200°C
- Geofluid pressure: 3000 PSIA
- Depth: 5 km
- Circulation Rate: 100kg/s per injector
- Power Production Desired: 100MW
- Thickness: 1.5km
- Area: 4km²

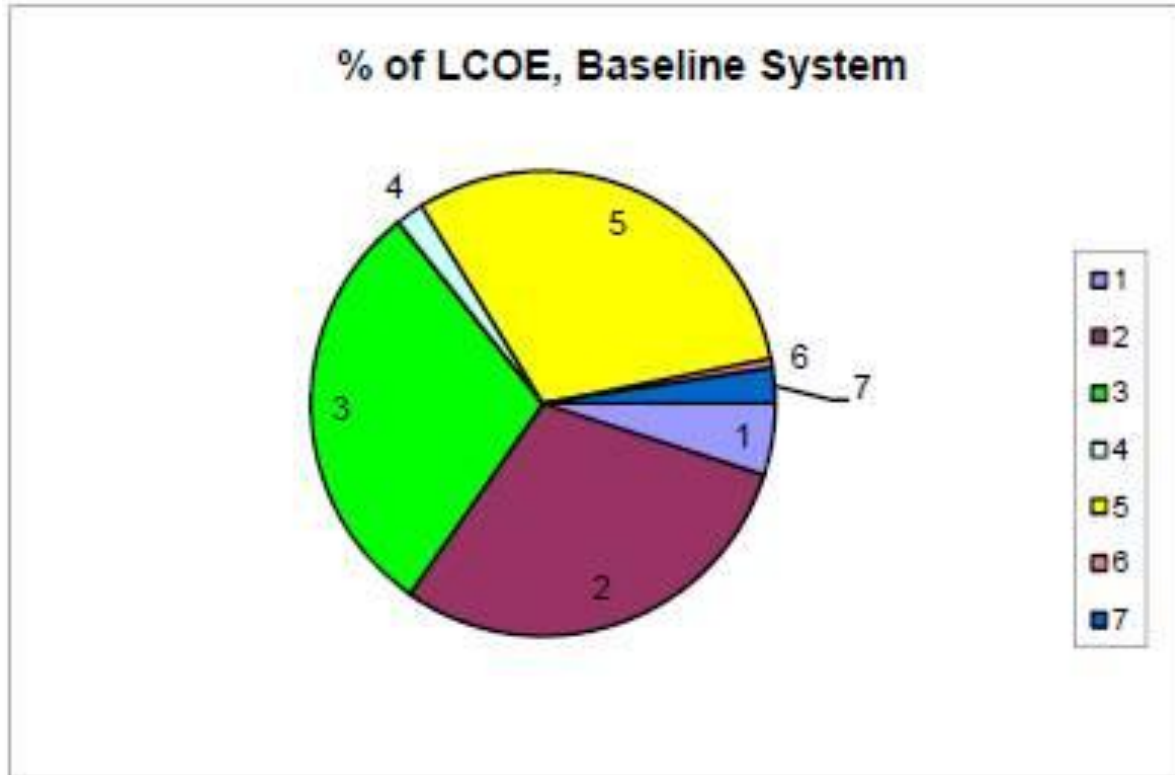
The results of the analysis for the EGS system proposed for this project are summarized in Figure 58. This analysis serves as a reference point for comparison to a water-based EGS system which follows similar approaches by other authors (Tester et al., 2006, Preiss 2006). The relative plant costs for each component within the EGS system are shown in Table 6.1

Table 14: Determining binary power-plant size and cost (GETEM results).

Plant Type	Power-Plant Size	Circulation Rate	I:P ratio	Number Wells		Plant Capital Cost	Total Cost	LCOE	Kwh per year(\$K)
	(MW)	(kg/s)	#	Injector	Producer	(\$K)	(\$K)	cents/Kwh	
EGS	10	100	1:1	1	1	19,000	80,000	27.1	70,080
EGS	50	100	1:2	3	6	90,300	262,000	18.5	350,400
EGS	100	100	1:2	6	11	177,500	554,500	17.4	700,800
EGS	250	100	1:2	14	27	433,800	115,900	16.7	1,752,000
EGS	500	100	1:2	27	54	854,350	2,270,300	16.4	3,504,000
EGS	1000	100	1:2	54	108	1,684,000	4,481,400	16.3	7,008,000
IGCC	550	-	-	-	-	1,490,000	1,659,500	12.6	3,854,400

Relative power production and costs developed using the GETEM spreadsheet model for binary power plants. This analysis was used as a basis for comparisons for double-flash geothermal power plant costs.

Figure 58: Fraction costs of the EGS field development and binary power plant (GETEM results).



		A. Baseline Case	Capital	O&M	Total	% of all Costs
Legend for Pie Chart Sectors:						
1. Exploration and Confirmation		0.86		0.00	0.86	5%
2. Wells in Field, after Confirmation phase		4.17		1.00	5.17	30%
3. Field, Make up costs		5.13		0.00	5.13	30%
4. Field, Other (Pipes, Pumps, Well Stimulation, Make Up Costs)		0.34		0.00	0.34	2%
5. Energy Conversion System		3.32		2.00	5.32	31%
6. Royalty		0.00		0.11	0.11	1%
7. Contingency		0.44		0.00	0.44	3%
Total		14.26		3.11	17.38	100%
% of all Costs:		82%		18%	100%	

This Figure 58 presents a generic cost breakdown for a binary power plant. Of the factors that contribute significantly to the overall cost of the plant it can be observed that the well field, well field make up, and power plant dominate.

9.3.3 Discounted future re-drilling and well stimulation

Discounted future re-drilling and stimulation savings are realized through operator experience at the site. It is assumed that as more wells are drilled and stimulated the operator will become more efficient in their activities. In areas of complex geology these savings will be less than areas that are less complex. For this project the first wells are to be drilled in the deeper basin fill areas. For all future wells the depth to sound bedrock will be shallower because the geothermal field movement will be towards the edge of the rift basin.

Well stimulation costs will also follow a similar trend. For the initial wells more of the reservoir will be within the un-fractured crystalline basement rocks which will require more effort to stimulate and create an effective zone of connected fractures. As the future wells are drilled where the crystalline basement rocks are shallower, more of the basement faulting of the rift basin will be included within the reservoir. These faults and associated fractures will require less stimulation to create the same effective zone of connective fractures.

9.4 Gravity Separation- scCO₂-Double Flash Conversion System

As discussed in the Geothermal Energy Conversion chapter, the proposed power plant to convert the produced fluids heat into electric power is two different processes. There will be a scCO₂ stream and a water stream if there is economically sufficient produced water. For estimating the economics of this project it is first necessary to determine the level of water production required for an economically feasible double flash power plant. This can be accomplished without simulation data. Later this analysis can be applied to modeled produced water to further prove or disprove the viability of producing electricity from water produced from a scCO₂ injection scheme.

To determine the economic feasibility of creating a dedicated double flash geothermal for the produced water a series of calculations was completed because the current version of GETEM contains no functional flash power plant calculations within the spreadsheet model. To determine the capital costs and the operation costs equations from Sanyal (2004), MIT (2006), and Dagdan (2007) were used. The results of this analysis are presented in Table 15. A further sensitivity analysis to determine if the potential flows would be economical were conducted at flow rates of 100kg/s, 200kg/s, and 300kg/s. Additionally power prices at \$0.05, \$0.10, and \$0.15/kwh were determined. Included within these calculations are the O&M costs presented by Sanyal (2004) which are tied to the size of the plant. A flat geothermal credit of \$0.02/kwh was also included in the calculation. It can be seen that all of three options warrant their own double flash system with the system paid for within the first five years. This is particularly attractive because if water is used within the heat exchanger of the scCO₂ turbine then this additional water can be processed through the double flash system within the low pressure turbine which would lower the costs of the project.

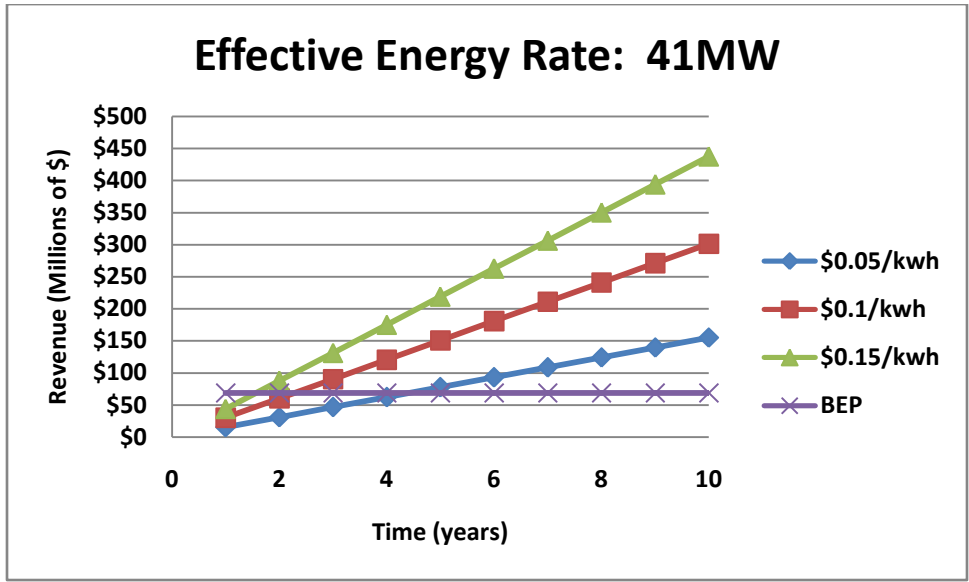
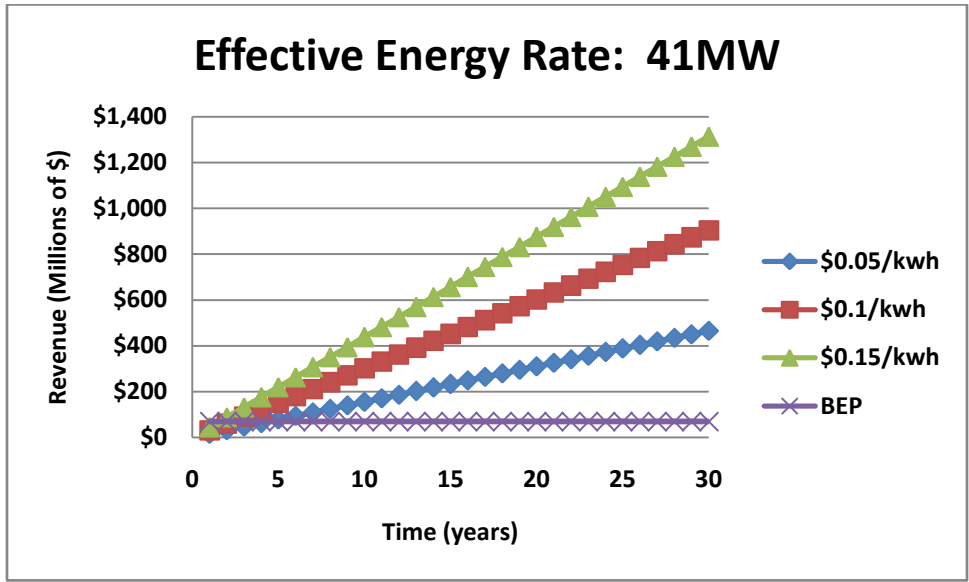
At this time a complete cost analysis for the brayton cycle turbine and associated heat exchanger proposed for this project cannot be completed because the turbine is not yet commercially available. Through up scaling of the documented turbine at SNL it is possible to arrive at a projected 15MW of power production for 1000kg/s of scCO₂. This will result in approximately 5.26x10⁷ KWh of production. In addition to this value there will be an additional 153MW from the heat exchanger associated with the brayton cycle turbine which will result in approximately 5.4x10⁸ KWh of production. These are rough numbers that will need to be further constrained via further reservoir simulation and efficiency data for the turbine at the proposed conditions. However, these values are promising.

Table 15: Double Flash Cost and Production Estimations

Working Fluid	T _{in} [C]	T _{out} [C]	Flow rate [kg/s]	Energy Rate [MW]	Effective Energy Rate Eff(0.50) [MW]	Plant Cost \$/kw	Plant Cost \$	Operational Cost cents/kwh	KWH [292 days]
Water	210	15	10	8	4	1881	7,847,250	2	29,240
Water	210	15	25	20	10	1838	19,175,700	1.925	73,103
Water	210	15	50	41	21	1771	36,948,300	1.85	146,207
Water	210	15	75	63	31	1707	53,448,000	1.775	219,311
Water	210	15	100	83	41	1649	68,794,000	1.7	292,415
Water	210	15	150	125	63	1541	96,453,800	1.625	438,623
Water	210	15	200	166	83	1446	120,698,000	1.55	584,831
Water	210	15	250	208	104	1363	142,172,500	1.475	731,039
Water	210	15	300	250	125	1289	161,417,500	1.4	877,247

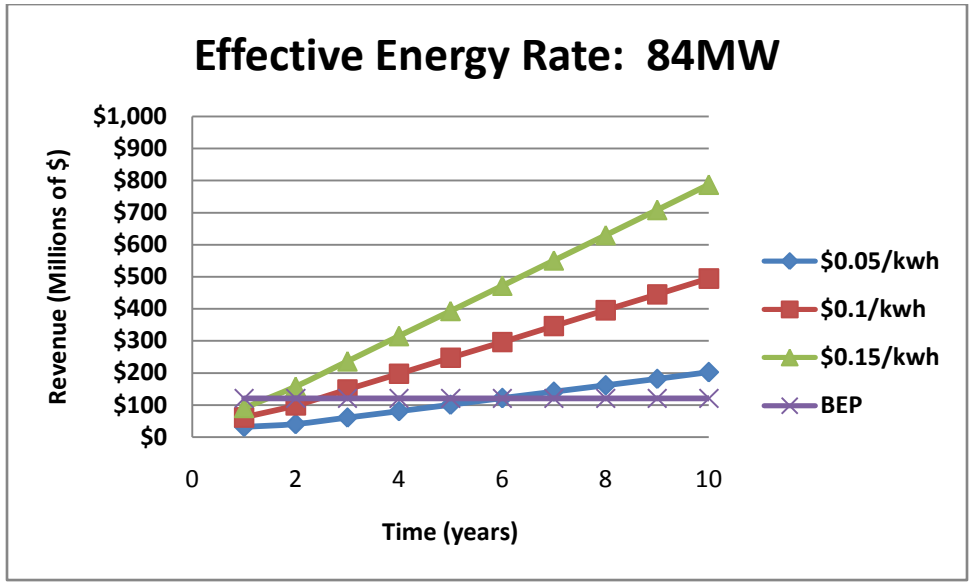
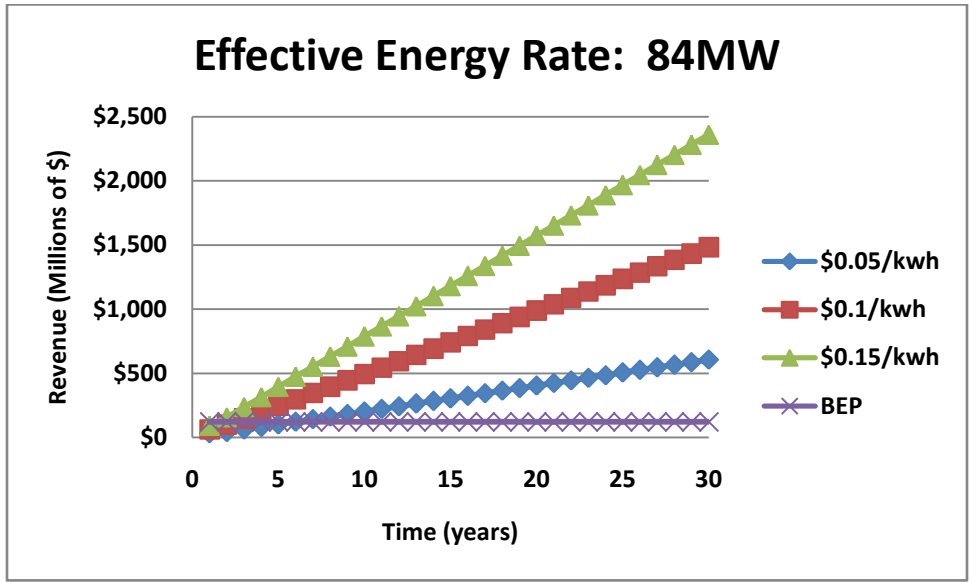
This analysis is based upon calculations from MIT (2006) [Plant Cost] and Sanyal (2004) [O&M Cost]. By varying the flow rates of produced water and the resulting KWH calculations the economic feasibility of the double flash geothermal power plant can be determined independent of simulated production rates.

Figure 59: Determining Break Even Point for Double Flash Plants 41MW



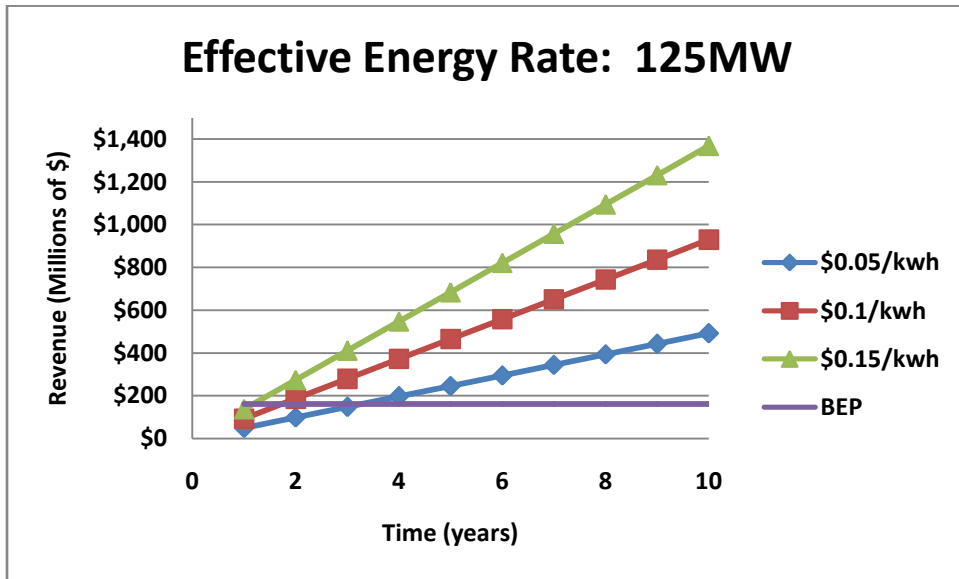
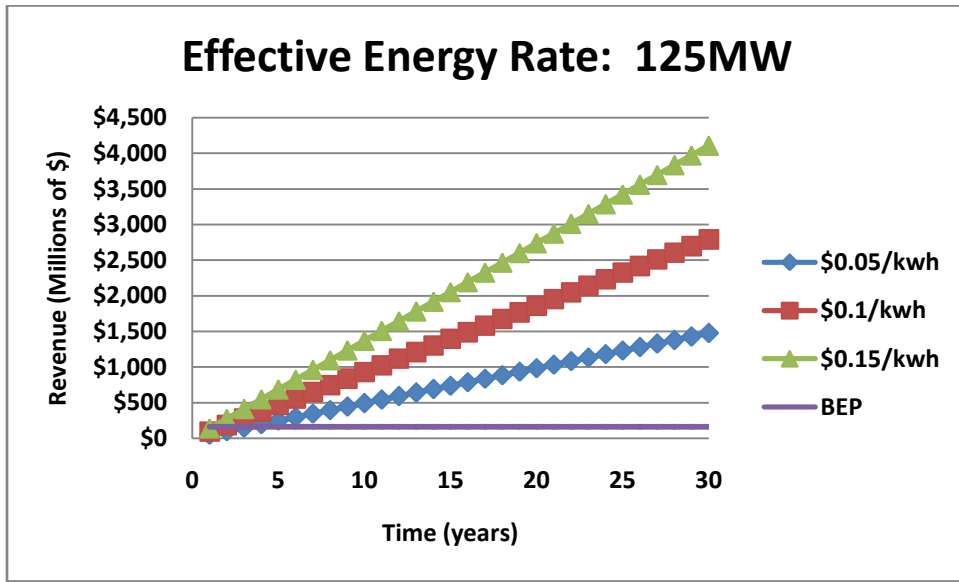
These plots show the time until the break-even point for a 41 MW plant at \$0.05, \$0.1, and \$0.15/kwh. Production is assumed to be constant at the flow rate noted in Table 16 over the 30 year design life of the plant.

Figure 60: Determining Break Even Point for Double Flash Plants 84MW



These plots show the time until the break-even point for a 84 MW plant at \$0.05, \$0.1, and \$0.15/kwh. Production is assumed to be constant at the flow rate noted in Table 16 over the 30 year design life of the plant.

Figure 61: Determining Break Even Point for Double Flash Plants 125MW



These plots show the time until the break-even point for a 125 MW plant at \$0.05, \$0.1, and \$0.15/kwh. Production is assumed to be constant at the flow rate noted in Table 16 over the 30 year design life of the plant.

9.5 IGCC- Economics:

The cost estimating methodology is described below. Costs of the plant were based on the actual cost data obtained from the DOE report.

Capital Cost:

Capital Cost comprises of Bare Erected Cost (BEC), Total plant cost (TPC), total overnight cost (TOC) and Total As Spent Cost (TASC). BEC comprises of process equipment, on-site facilities and infrastructure that support the plant and the direct and indirect labor required for its construction. TPC comprises of the cost of services provided by the engineering, procurement and construction contractor and project and process contingencies in addition BEC. TOC comprises of owner's cost plus TPC. TASC consist of total expenditure incurred during capital expenditure period including their escalation.(DOE Report, 2010)

Operation and Maintenance Cost:

The operation and maintenance cost includes

- 1) Operating labor
- 2) Maintenance – material and labor
- 3) Administrative and support labor
- 4) Consumables
- 5) Fuel
- 6) Waste Disposal

There are two principal components of Operation and Maintenance Cost. They are

- (1) Fixed Operating Cost – This is independent of power generation.
- (2) Variable Operating Cost – This is proportional of power generation.

Contingency

Process and project contingencies are taken into consideration in order to estimates to account for unknown costs that are not counted or unforeseen due to a lack of complete project definition and engineering. Contingencies are added because experience has shown that such costs are likely, and expected, to be incurred even though they cannot be explicitly determined at the time the estimate is prepared. (DOE Report, 2010)

Capital cost contingencies do not cover uncertainties or risks associated with

- (1) Scope changes
- (2) Changes in labor availability or productivity
- (3) Delays in equipment deliveries
- (4) Changes in regulatory requirements
- (5) Unexpected cost escalation
- (6) Performance of the plant after startup

Process Contingency

Process contingency is intended to compensate for uncertainty in cost estimates caused by performance uncertainties associated with the development status of a technology. Process contingencies are applied to each plant section based on its current technology status. (DOE Report 2010)

Table 16: Key Assumptions for IGCC plant

Capital Depreciation Period	20 years
Capital Expenditure Period	5 years
Operational Period	30 years
Inflation	3%
MW net	548
Charge Capital Factor	0.124

Table 17: Fixed Operation Cost for IGCC plant

Fixed Operational Cost	
Item	Operational Cost/Yr
Labor	\$ 24,288,722
Administration	\$ 6,072,181
Taxes/Insurance	\$ 33,153,996
Sub Total	\$ 63,500,000

The fixed operational costs in Table 17 are annual costs incurred that are independent of electricity production or coal usage. The variable operational costs in Table 18 display the annual costs incurred by the project that are dependent on the amount of electricity produced by the system

Table 18: Variable Operational Costs for IGCC plant

Variable Operating Cost			
	kg/day	\$/kg	Annual Cost
Fuel	5,300,680.0	\$ 0.04	\$ 65,152,185
Slag	581,405.9	\$ 5.22	\$ 3,419,072
Mercury Waste	49.4	\$ 270.42	\$ 15,046
Material repair			\$ 32,391,969
Sub Total			\$ 100,978,272

Variable Operating Cost for Gas Cleaning Unit					
	Consumption		Unit Cost	Initial Fill Cost (Capital Cost)	Annual Cost
	Initial	/day			
Water (/1000 gallons)	\$ -	\$ 4,187	\$ 1.08	\$ -	\$ 1,486,136
MU & WT Chem (kg)	\$ -	\$ 11,338	\$ 0.37	\$ -	\$ 1,240,783
Carbon (Mercury Removal) (kg)	\$ 16,450	\$ 49.40	\$ 2.31	\$ 38,079	\$ 37,614
Water Gas Shift Catalyst (m ³)	\$ 177	\$ 0.12	\$ 17,626.50	\$ 3,115,692	\$ 1,780,544
Selexol Solution (m ³)	\$ 1,130	\$ 0.36	\$ 3,539.90	\$ 3,999,927	\$ 413,672
Claus Catalyst (m ³)	\$ -	\$ 0.06	\$ 4,638.52	\$ -	\$ 86,715
Sub Total				\$ 7,153,698	\$ 5,045,464
Total Variable Operating Cost					\$ 106,023,736

Table 19: Capital Costs for IGCC

Equipment and Materials	
Item	Capital cost
ASU	\$ 262,169,112
Gasifier & accessories	\$ 480,618,111
Turbines & accessories	\$ 118,259,011
Gas Cleanup & accessories	\$ 351,061,002
Misc.	\$ 269,660,003
Sub Total	\$ 1,481,767,239

The capital costs displayed in Table 19 are the initial costs incurred for installing the IGCC system. These costs include all of the major components and the smaller ones that are not listed but are contained in the miscellaneous (Misc.) section of the table. Misc. also includes any housing facilities and other necessary infrastructure. The total capital cost of the plant is approximately \$1.5 billion and the total operating cost for the IGCC plant (fixed and variable) is approximately \$170 million.

LCOE

The levelized cost of electricity is the revenue received by the generator per net megawatt-hour during the power plant's first year of operation, assuming that the COE escalates thereafter at a nominal annual rate of 0 percent, i.e., that it remains constant in nominal terms over the operational period of the power plant. To calculate LCOE, PSFM model was used.

$$LCOE = \frac{Capital\ Cost * C F + Fixed\ O\&M}{C F * 8760} + Var\ O\&M + Fuel\ cost + CO_2\ cost \quad 6.1$$

The levelized cost of electricity will be 12.6 cents/kWh.

9.6 Economics of Water

It is estimated that the IGCC will require 4.2 million gallons of water circulating through the system per day for coal conversion. Although the majority of water is recovered a proportion of the water will be lost. Assuming a 10% loss the plant will require approximately 420,000 gallons per day of make-up water.

Even if a suitable water source can deliver the required water volume at a constant flow rate onsite water storage should be created to maintain water levels in the event of supply disruptions. For this project it is proposed that the water source will be grey water which will not flow at a constant flow rate therefore holding tanks will be necessary. To ensure continuity of operations in the event of flow interruptions one day worth of water will be stored on site at a minimum. This volume of water will be stored in 11 tanks, each with a holding capacity of 37,700 gallons at a cost of \$530,000 per tankⁱ for a total cost of \$5,830,000.

To deliver the water from the municipal water supply and sewer plant will required approximately a pipeline of 5 miles. The cost of building a pipeline according to the Canadian Energy Pipeline Association is approximately \$28,000 (USD) per mile. “A gathering system includes pumps, headers, separators, emulsion treaters, tanks, regulators, compressors, dehydrators, valves and associated equipment.”ⁱⁱⁱ

The cost of building a pipeline is the product of the distance to source, pipeline diameter and the unit cost (per mile). The estimated cost for the pipeline is \$530,000. The estimated cost of the gathering facility is \$320,000. The total cost to deliver water to the plant without water fees is approximately \$850,000

9.7 Transportation and Costs

Coal can be bought at the live price specified by the manufacturer. The hauling of coal by road or by rail will be decided by the site location and the proximity of railway lines or roads. It will be necessary to build a railway line from the nearest point which lies approximately 8 miles away. The cost of building a single track freight railway line across a flat belt, geologically stable landscape with simple signaling can be built for approximately \$3.2 million per mile which will result in cost of \$25.6 million for this project.

The Burlington Northern Santa Fe Railway Company is the predominant coal haulage service prevalent in the Western territory. After studying the contract patterns of haulage rates in New Mexico, it is determined that a distance of about 150 miles from the

San Juan Basin to the plant can be covered at a cost of \$14.37 per ton. The costs per car are about \$2050 because each car has a capacity of 143 tons. The minimum number of cars ranges from 104-115 per train. The entire contract would cost \$1,695,000 per trip. The total cost to purchase and deliver the required coal for the IGCC power plant will be \$79 million.

9.8 Overall Economic Analysis

An economic analysis was performed for the combination of the EGS and IGCC systems to determine the Net Present Value (NPV) of the overall system and establish probable payback periods based on the cost of electricity, possible electricity inflation rates, and the possibility of governmental funding for carbon capture and storage (CCS).

9.8.1 Assumptions for Economic Analysis

The assumptions for the economic analysis are contained in the table below:

Table 20: Assumptions for Economic Analysis

Assumptions		
Initial Electricity Price (\$/kWh)	\$	0.09
Lifetime of Plant (yr)		30
Interest Rate		3%
Capacity Factor (%)		80%
Capacity Factor (days)		292
EGS		
Geothermal Credit (\$/kWh)	\$	0.02
Capital Cost	\$	177,400,000
Operating Cost (\$/yr)	\$	20,507,000
Plant Size (MW)		125
Electricity Production (kWh/yr)		876,000,000
IGCC		
Capital Cost	\$	1,490,000,000
Operating Cost (\$/yr)	\$	169,500,000
Sulfur Value (\$/yr)	\$	1,277,500
Plant Size (MW)		548
Electricity Production (kWh/yr)		3,840,384,000

The assumptions presented in Table 20 depict the main overall assumptions for the entire project such as electricity cost, plant lifetime, interest rate, and capacity factor. The capital cost and operating costs for the EGS and IGCC systems are shown separately as well as any other associated benefits with each of the systems. No operational costs are incurred and no revenue is generated during year 0, only the capital cost is incurred.

9.8.2 NPV Analysis of Project

A Net Present Value analysis of the combined systems determines the payback period in present worth (today's dollars) by discounting the future cash flows over the

lifetime of the system through the use of the assumed interest rate. By taking into account the total initial capital costs and calculating the net/cumulative value of the project, payback periods are determined when the value of the project becomes positive. This method estimates the time in which the project will pay off all initial and operational debt thus establishing a Payback Time (PBT) which is graphically represented in the figure below.

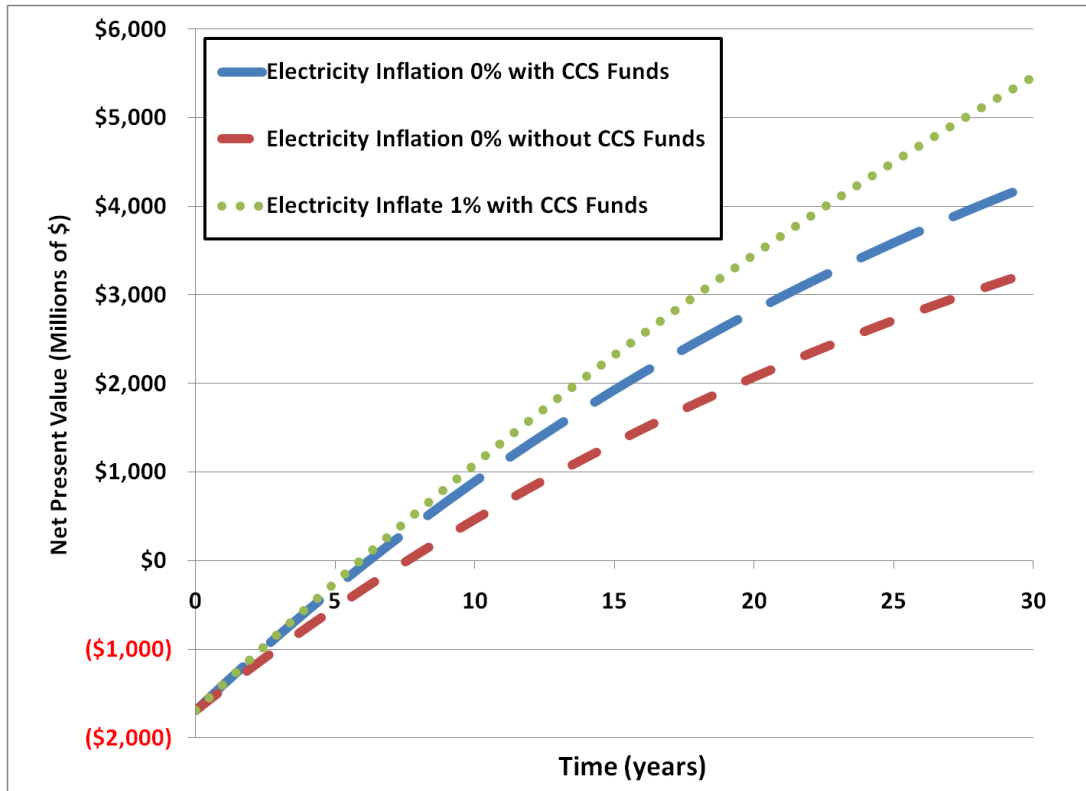


Figure 62: NPV of EGS and IGCC Combined Systems

The three cash flows in Figure 62 display different possible economic outcomes based on electricity inflation rates (0 or 1%) and whether or not the annual \$50 million possibility of government funding for CCS is available. These cash flows are depicted across the 30 year estimated life span of the project. All of the PBTs fall in a range from 6-8 years. The least favorable economic estimation with no increase in electricity and no CCS funding from the government still has quick PBT in terms of the overall lifetime of the project.

Other favorable fiscal possibilities could become more likely as electricity rates increase further, as additional environmental restrictions are placed on utilities and emission trading is opened on the free market, and as other government subsidies are provided for either CCS or lack of emissions per power generated. Synthesis gas could

also be used to produce liquid fuels which may pose to be a more economically viable option over producing electricity if the price of oil continues to rise.

The final present worth of the project over the 30 year lifetime is between \$3 billion and over \$5.5 billion as determined by the NPV method of analysis. This results in a return on investment (ROI) of 91% to 223% calculated by the following equation:

$$ROI = \frac{\textit{Gain from investment} - \textit{Cost of investment}}{\textit{Cost of investment}} \quad 6.3$$

10.0 Conclusions:

The synergy between scCO₂ EGS and IGCC provides an approach to develop geothermal resources in arid regions throughout New Mexico. While the IGCC process does require water to produce electricity, a very scarce commodity in the desert southwest, it maximizes the energy that is created from it. The 38,000 gpd or 180 kg/s of water that is required for the EGS/IGCC plant provides an estimated 700MW of power delivered to the grid instead of approximately 90MW to the grid if only water was used within the EGS system.

The specific location of the site is also equally attractive for delivering electricity to market. Short transmission distances to Albuquerque, NM and Andrews AFB provide strategic, secure, and reliable electricity with minimal transmission losses. This is in line with current DOE and DOD directives and could very well spur economic growth in and around Albuquerque, NM.

To realize the full potential of the next-generation coal-based power plants substantial governmental incentives, low cost loans, and continued governmental interest are necessities if carbon dioxide emissions are to be reduced by significant levels. Equally important is the necessity of created informed communities around the proposed power plants. By educating the surrounding communities of the benefits and risks that are associated with the plants, will allow for informed discussions and conclusive solutions to issues that will arise during this energy project. It is critical to provide facts before facts are fabricated and unrealistic fears spread to the community which will stop any project.

The economic assessment of the project estimates that in the worst case scenario (no increase in electricity and CCS government funds are unavailable) the system will pay for itself in 8th year of operation. In this case the final present worth of the project over the 30 year lifetime is would be \$3 billion and have an ROI of 91%. The best

estimated scenario results in a PBT of 6 years, a \$5.5 billion total present worth over 30 years, and an ROI of 223%.

According to the results of the economic assessment, the project is a worthwhile investment. Further investigation of costs and benefits associated with both portions of the project would serve to reinforce the findings and provide a more accurate estimation of the outcome of the project.

11.0 References

1. Dagdan, A., 2007, "Performance Analysis and Optimization of Double-Flash Geothermal Power Plants." *Journal of Energy Resources Technology*, v. 129, p. 125-133.
2. [MIT Report] *The Future of Geothermal Energy*, 2006
3. Pruess, K., 2006, "Enhanced geothermal systems (EGS) using CO₂ as working fluid – A novel approach for generating renewable energy with simultaneous sequestration of carbon." *Geothermics*, v.35, p. 351-367.
4. Sanyal, S.K., 2004, "Cost of Geothermal Power and Factors That Affect It," *Proceedings, Twenty-Ninth Workshop on Geothermal Reservoir Engineering*, Stanford University, Stanford, California, January 26-28, 2004
5. Mansure, A. J., S.J. Bauer, and B.J.Livesay. 2005, "Geothermal Well cost Analyses 2005." *Geothermal Resources Council Transactions*, v29, p515-519
6. Entingh, D.J. 2006, "DOE Geothermal Electricity Technology Evaluation Mode (GETEM): Volume 1-Technical Reference Manual. "
7. U.S. Energy Information Administration, Office of Oil, Gas and Coal Supply Statistics, *Annual Coal Report 2009*.
8. U.S. Energy Information Administration, *Electric Power Industry 2009, Year in Review*
9. U.S. Energy Information Administration "Coal Production and Preparation Report"
10. U.S. Department of Labor, Mine Safety and Health Administration, "Quarterly Mine Employment and Coal Production Report"
11. U.S. Energy Information Administration, "Power Plant Operations Report"
12. Federal Energy Regulatory Commission FERC "Monthly Report of Cost and Quality of Fuels for Electric Plants"
13. U.S. Energy Information Administration, "Cost and Quality of Fuels for Electric Plants 2009" published in November 2010.
14. Geothermal Energy Association, Washington D.C. by Dan Jennejohn, April 2010 in "US Geothermal Power Production and Development Update"

15. U.S. Energy Information Administration, "Electric Power Monthly" February 2011
16. "Perspectives on the Economics of Geothermal Power" by Adil Caner Sener, Johan Rene van Dorp, and Jesse Dylan Keith.
17. "The Future of Geothermal Energy" Impact of Enhanced Geothermal Systems (EGS) on the United States in the 21st Century. (Jefferson W. Tester, 2006)
18. "Geothermal Energy : Electricity Production and Environmental Impact" by DiPippo, *Energy Policy*.
19. . Promoting Geothermal Energy: Air Emissions Comparison and Externality Analysis, Alyssa Kagel and Karl Gawell
20. (Valentino Tiangco, et al., Emission Factors of Geothermal Power Plants in California, in GRC TRANSACTIONS, 19, Oct. 1995, at 147–151)
21. Average EIA estimate of yearly geothermal generation, 2000– 2004, available at <http://www.eia.doe.gov/emeu/aer/txt/ptb0802c.html>, and using percentages of each type of generation based on gross capacity listed at GEA Web site
22. . U.S. EPA, Average Power Plant emissions from EPA 2000 emissions data, available at <http://www.epa.gov/cleanenergy/egrid/highlights>.
23. Clean Air Act: A summary of the Act and its major requirements by (James E. McCarthy)
24. Judson Jaffe, Matthew Ranson and Robert N. Stavins (2009). *Linking Tradable Permit Systems: A Key Element of Emerging International Climate Policy Architecture*
25. Butzengeiger, Betz and Bode (2001)
26. (Quirion, 2002)
27. (Ellerman, 2005)
28. Jacoby, D.H.; Ellerman, A.D. (2004-03). "The safety valve and climate policy". *Energy Policy* (Sciencedirect.com)
29. Estimates approximated by referring to current rates of proportional tank sizes. (Hanson Tanks, <http://www.hansontank.com/water-storage-tanks.html>)
30. Schlumberger Oilfield Glossary (<http://www.glossary.oilfield.slb.com/Display.cfm?Term=gathering%20system>)
31. (U.S. Energy Information Administration Annual Coal Report 2009)
32. Quarterly Coal Report July-September 2010
33. Estimated Contract from a similar Quote from the Lee Ranch Mine, El Segundo Mine, McKinley Mine to Arizona Electric Power Cooperative, Inc. Apache

- Generating Plant near Cochise, AZ on the BNSF - Deming, NM – Union Pacific Railroad Company Route. January 27, 2011
34. Haselbeck et al. (2010) *Cost and Performance Baseline for Fossil Energy Plants. Volume One: Bituminous Coal and Natural Gas to Electricity*. Retrieved from www.netl.doe.gov
 35. Liu et al. (2009) *Hydrogen and Syngas Production and Purification Technologies*. 2010. Hoboken, NJ. John Wiley and Sons inc.
 36. Phillips, Jeffrey. *Different Types of Gasifiers and Their Integration with Gas Turbine*. Retrieved from Netl reference shelf. Figures 1-2 <http://www.netl.doe.gov/technologies/coalpower/turbines/refshelf/handbook/1.2.1.pdf>
 37. McDaniel et al. (2002) *Tampa Electric Polk Power Station Integrated Gasification Combined Cycle Project*. Retrieved from www.tecoenergy.com
 38. Chiesa, P., & Lozza, G. (2005). Using Hydrogen as Gas Turbine Fuel. *Journal of Engineering for Gas Turbines and Power*, 127, 73-80.
 39. GE Energy. (2009). *Heavy Duty Gas Turbine Products (GEA - 12985H)*. General Electric Company.
 40. Matta, R., Mercer, G., & Tuthill, R. (2000). *Power Systems for the 21st Century – “H” Gas Turbine (GER - 3935 B)*. Schenectady: GE Power Systems.
 41. National Institute of Standards and Technology. (2008). *NIST Chemistry WebBook*. Retrieved April 27, 2011, from National Institute of Standards and Technology: <http://webbook.nist.gov>
 42. U.S. Energy Information Administration. (2010, December 16). *Consumption and Efficiency*. Retrieved April 28, 2011, from U.S. Energy Information Administration: <http://www.eia.gov/consumption/>
 43. Bauer, P.W. 1983, Geology of the Precambrian rocks of the Southern Manzano
 44. Mountains, New Mexico. New Mexico Bureau of Mines and Mineral Resources Open File Report 339
 45. Blackwell, D.D. and M. Richards, 2004, Geothermal Map of North America, AAPG
 46. Duffield, W.A. and J.H. Sass, 2003, Geothermal Energy-Clean Power from the Earth’s Heat: US Geological Survey C1249

47. Granuch, V.J.S. and M.R. Hudson, 2007, Guides to understanding the aeromagnetic expression of faults in sedimentary basins: Lessons learned from the central Rio Grande Rift, New Mexico: *Geosphere*. v.3; no.6; p. 596-623.
48. Johnson, R.C. T.M. Finn, and V.F. Nuccio, 2001, Potential for a Basin-Centered Gas Accumulation in the Albuquerque Basin, New Mexico: US Geological Survey Bulletin 2184-C
49. Jiracek, G.R., C.A. Swanberg, P. Morgan, and M.D. Parker, 1983, Evaluation of the Geothermal Resource in the Area of Albuquerque, New Mexico, New Mexico Energy Research and Development Institute Report No. 2-67-2135
50. Kelley, V.C., 1977, Geology of Albuquerque Basin, New Mexico: New Mexico Bureau of Mines and Mineral Resources Memoir 33
51. Loughlin, G.F. and Koschmann, A.H., 1942, Geology and ore deposits of the Magdalena mining district, New Mexico: US Geological Survey, Professional Paper 200, 168p.
52. Mankin, C.J. 1952, Stratigraphy and Sedimentary Petrology of Jurassic and Pre-Graneros Cretaceous Rocks, Northeastern, New Mexico: New Mexico Bureau of Mines and Mineral Resources Open File Report 49
53. Molenaar, C.M., 1988, Petroleum and hydrocarbon plays of the Albuquerque-San Luis rift basin, New Mexico and Colorado: US Geological Survey Open-File Report 87-450-S
54. Morgan, P., W.P. Seager, and M. P. Golmbeck, 1986, Cenozoic thermal, mechanical, and tectonic evolution of the Rio Grande Rift: *Journal of Geophysical Research*, v. 91, no. 86, p. 6263-6272.
55. Myers, D.A. and E.J. McKay, 1974, Geologic map of the southwestern quarter of the Torreon 15-minute quadrangle, Tarrant and Valencia counties, New Mexico: U.S. Geological Survey Miscellaneous Geological Investigations map, I-820
56. Raster Technologies© 2011, <http://www.rasertech.com/geothermal>.
57. Reiter, M., C.L. Edwards, H. Hartman and C. Weidman, 1975, Terrestrial heat flow along the Rio Grande rift, New Mexico and southern Colorado: *Geological Society of American Bulletin*, V. 86
58. Russel, L.R. and S. Snelson, 1994. Structural Style and Tectonic Evolution of the Albuquerque Basin Segment of the Rio Grande Rift, New Mexico, U.S.A.: AAPG Memoir. Vol.59. pg. 205-258

59. Siemers, W.T., 1973, Stratigraphy and Petrology of Mississippian, Pennsylvanian, and Permian Rocks in the Magdalena area, Socorro County, New Mexico: New Mexico Bureau of Mines and Mineral Resources Open File Report 54
60. Stark, J.T., 1956, Geology of the South Manzano Mountains, New Mexico: New Mexico Bureau of Mines and Mineral Resources Bulletin 34
61. Stone, W.J. and N.H. Mizzell, 1977, Geothermal Resources of New Mexico-A Survey of Work to Date: New Mexico Bureau of Mines and Mineral Resources Open File Report 73
62. USGS Mineral Resources On-line Spatial Data for New Mexico, <http://mrdata.usgs.gov/>
63. [MIT Report] The Future of Geothermal Energy, 2006
64. D. Brown, 2000, A hot dry rock geothermal energy concept utilization supercritical CO₂ instead of water, Proceedings, Twenty-Fifth workshop on Geothermal Reservoir Engineering, Stanford University, 233-238
65. C. Fouillac, B. Sanjuan, S. Gentier, I. C-Lauriol, 2004, — Could sequestration of CO₂ be combined with the development of enhanced geothermal systems, paper presented at 3rd Annual conference on carbon capture and sequestration, Alexandria, VA
66. Sanyal, S.K. *et al.*, 2007. — Geothermal Well Productivity: Why hotter is not always better, Geothermal Resource Council Transactions, Vol 31, p 573 – 579
67. K. Pruess, 2006, — Enhanced Geothermal Systems (EGS) using CO₂ as working fluid- A novel approach for generating renewable energy with simultaneous sequestration of carbon, Geothermics, 35, 351
68. K. Pruess, M. Azaroual, 2006, — On the Feasibility of Using Supercritical CO₂ as heat transmission fluid in an engineered hot dry rock geothermal system, 31st workshop of geothermal reservoir engineering, Stanford University
69. S.L. Milora, J.W. Tester, 1976, — Geothermal energy as a source of electric power: Thermodynamic and economic criteria, MIT press
70. Western Geothermal Association, Geothermal Task Force Report, January 2006, p 60 - 66
71. Sanyal, S.K. *et al.*, 2007. — Is EGS commercially feasible?, Geothermal Resource Council Transactions, Vol 31, p 313 – 322

72. Tester, J.W. *et al*, 2006 — The Future of Geothermal Energy: Impact of Enhanced Geothermal Systems on the United States in the 21st Century, MIT Report
73. T. Xu, K. Pruess, 2004 — Numerical Simulation of Injectivity Effects of Mineral Scaling and Clay Swelling in a Fractured Reservoir, Transactions, Geothermal Resources Council, 28
74. Pruess, K., 1983. — Heat Transfer in Fractured Geothermal Reservoirs with Boiling, Water Resources Research, Vol 19, 1, p 201 – 208
75. Pruess, K. *et al.*, 1982. — Model studies of the depletion of two-phase geothermal reservoirs, Soc. Pet .Eng.J., 22(2), P 280-290
76. Pruess, K., T. N. Narasimhan, 1982b. — A practical method for modeling fluid and heat flow in fractured porous media, SPE-10509, paper presented at the Sixth Symposium on Reservoir Simulation, Soc. Pet .Eng.J., New Orleans, LA
77. Pruess, K., Karasaki, K., 1982. — Proximity functions for Modeling Fluid and Heat Flow in Reservoirs with stochastic Fracture distributions, Proceedings Eighth Workshop Geothermal Reservoir Engineering, Stanford University, Stanford, CA
78. Bennion D., “Permeability and relative permeability measurements at reservoir conditions for CO₂-water systems”, SPE paper # 106995
79. Elsworth D., “Theory of thermal recovery from a spherically stimulated HDR reservoir”, Journal of Geophysical Research, 1989a, 94(B2): 1927-1934
80. Elsworth D., “A comparative evaluation of the parallel flow and spherical reservoir models of HDR geothermal systems”, Journal of Volcanology and Geothermal Research, 1990, 44: 283-293
81. CMG STARS™ manual.
82. O’Sullivan M. J., 1985. Geothermal Reservoir Simulation. *Energy Research*, **9**: 319-332
83. Parlaktuna M., 1995. Geothermal Reservoir Engineering, Middle East Technical University
84. Duchane D., Brown D., 1995. Hot dry rock (HDR) geothermal energy research and development at Fenton hill, New Mexico. Twentieth workshop on Geothermal Reservoir Engineering, Stanford University, Stanford, California.

85. Atrens A., Gurgenci H., Rudolph V., 2009. Exergy analysis of a CO₂ thermosiphon. Thirty-Fourth workshop on Geothermal Reservoir Engineering, Stanford University, Stanford, California.
86. Bombarda, P., and Macchi, E., 2000, "Optimum Cycles for Geothermal Power Plants," Proceedings World Geothermal Congress 2000, Kyushu, Japan, May 28-June 10, P. 3133-3138
87. Cengel, Y.A. and M.A. Boles. Thermodynamics and Engineering Approach. McGraw-Hill. 2010
88. Dagdan, A., 2007, "Performance Analysis and Optimization of Double-Flash Geothermal Power Plants." Journal of Energy Resources Technology, v. 129, p. 125-133.
89. Mendrinos, D., E. Kontoleonos and C. Karytsas, "Geothermal Binary Plants: Water or Air Cooled?" Accessed March 2011. Centre for Renewable Energy Resources, 19th km Marathonos Ave., 109009 Pikermi Attikis, Greece
90. Raster Technologies© 2011, <http://www.rasertech.com/geothermal> Last accessed: 04-30-2011
91. Sanyal, S.K., 2004, "Cost of Geothermal Power and Factors That Affect It," Proceedings, Twenty-Ninth Workshop on Geothermal Reservoir Engineering, Stanford University, Stanford, California, January 26-28, 2004
92. Environmental Appeals Board, 2009, "Remand Order, In Re: Desert Rock Energy Company LLC, PSD Appeal Nos. 08-03, 08-04, 08-05 & 08-06," United States Environmental Protection Agency. Washington, D.C.
93. New Mexico Business Weekly, 2008, "State Appeals EPA Permit for Desert Rock Coal Plant,"
<http://www.bizjournals.com/albuquerque/stories/2008/09/29/daily44.html>
94. U.S. Energy Information Administration, 2005, "New Mexico Electricity Consumption by Sector 2005,"
<http://apps1.eere.energy.gov/states/electricity.cfm/state=NM#fuel>

Appendix

2.1 Appendix 2.A Igneous and metamorphic formation descriptions (After Bauer, 1983)

Sais Formation:

Divided stratigraphically from oldest to youngest (This formation only)

- Blue-gray to pinkish blue-gray, vitreous, well-recrystallized, massive to thinly bedded, medium-grained orthoquartzite.
- Orange weathering quartz muscovite schist which grades to a distinctive red schist
- Red, maroon to purple, generally thin-bedded orthoquartzite containing abundant crossbeds and interbeds of spotted quartzites, pink micaceous quartzite with very thin schistose interlayers, and dark gray quartzites.
- A group of generally light-colored, resistant, massive to thin-bedded, medium-grained orthoquartzites consisting of a sequence of pink-white to red, resistant, vitreous quartzite; dark, chlorite-muscovite schist; a thin bedded, mixed sequence of quartzite and schist; and a pink-white, resistant quartzite which is locally intensely fractured.

Blue Springs Formation:

A complex unit composed of various thin-bedded, fine-grained metasedimentary rocks. The bulk of this formation consists of dark chlorite-muscovite schist and finely laminated, extremely fine-grained quartzite, although other interlayered lithologies are present.

White Ridge Formation:

From the work Bauer (1983) there is some discussion if this formation is one unit or two units. To avoid confusion his original terminology is maintained for this report.

- Eastern Limb Unit: A sequence of generally thin-bedded resistant quartzites with interbedded schists and schistose quartzites. Approximately five times the thickness of the Western Limb Unit.
- Western Limb Unit: Red, well-recrystallized, very resistant quartzite; a schistose quartzite with thin interbeds of light-colored schist and quartzite; a pink to white, resistant, massive, hematitic

quartzite; a gray micaceous quartzite to quartzose schist; a massive, gray, extremely resistant quartzite with thin interbeds of pink, vitreous, hematitic quartzite with local crossbeds; a thick sequence of orange weathering, pinkish, micaceous quartzite.

Sevilleta Formation:

This formation is a stratigraphically and structurally complex association of metaigneous and metasedimentary rocks. As presented in Bauer (1983), the formation is divided into two separate units.

- Western Felsic Metaigneous Terrain: Consists mainly of felsic metaigneous rock with relatively minor amounts of amphibolites, quartzite, and schist. The felsic metaigneous rocks are generally pink or gray, blocky-fracturing, commonly somewhat schistose, with light-colored quartz and feldspar megacrysts which may be relict phenocrysts.
- Eastern Amphibolitic Terrain: Contains approximately equal volumes of mafic metaigneous and metasedimentary rocks.
 - Mafic Metaigneous Facies:
 - Feldspar-hornblende schist with small lenticular feldspar megacrysts
 - Coarse-grained metadiorite
 - Chlorite-hornblende amphibolites with large coarse-grained metadioritic pods and stringers
 - Fine to coarse grained amphibolites.
 - Metasedimentary Facies:
 - Quartzites are generally thin-bedded, micaceous, and white to gray, although some more massive, vitreous facies are present.
 - Quartz-muscovite schist and quartzose schists
 - Coarse-grained garnet-staurolite-muscovite-biotite schist
 - Garnet-staurolite units are also present and grade into garnet-chloritoid schist.

Priest Quartz Monzonite:

Fresh surfaces are pink and weathered surfaces are gray and crumbly. Dikes of pegmatite, aplite, quartz, and epidote intrude into the nearby country rock.

Appendix

Table 4. 1: thermochemical coefficients obtained from NIST for various chemicals and temperature

Temp (K)	500 - 1700	1700 - 6000	Temp (K)	298 - 1200	1200 - 6000	Temp (K)	298 - 1200	1200 - 6000	Temp (K)	298 - 6000	Temp (K)	298 - 1000	1000 - 2500	2500 - 6000
A	30.09200	41.96426	A	23.83491	35.99169	A	16.10857	56.82541	A	21.13571	A	33.06618	18.563083	43.41356
B	6.83251	8.62205	B	12.58878	0.95717	B	75.89525	0.73805	B	-0.38842	B	-11.36342	12.25736	-4.29308
C	6.79344	-1.49978	C	-1.13901	-0.14803	C	-54.38740	-0.14472	C	0.04355	C	11.43282	-2.85979	1.27243
D	-2.53448	0.09812	D	-1.49746	0.00997	D	14.30777	0.00978	D	0.02469	D	-2.77287	0.26824	-0.09688
E	0.08214	-11.15764	E	0.21419	-3.00409	E	0.23942	-5.45991	E	-0.02568	E	-0.15856	1.97799	-20.53386
F	-250.88100	-272.17970	F	83.35783	73.10787	F	26.17464	2.84646	F	466.31100	F	-9.98080	-1.14744	-38.51516
G	223.39670	219.78090	G	237.12190	246.16190	G	240.53860	290.50560	G	178.82630	G	172.70797	156.28813	162.08135
H	-241.82640	-241.82640	H	90.29114	90.29114	H	33.09502	33.09502	H	472.68320	H	0.00000	0.00000	0.00000

H₂O NO NO₂ N

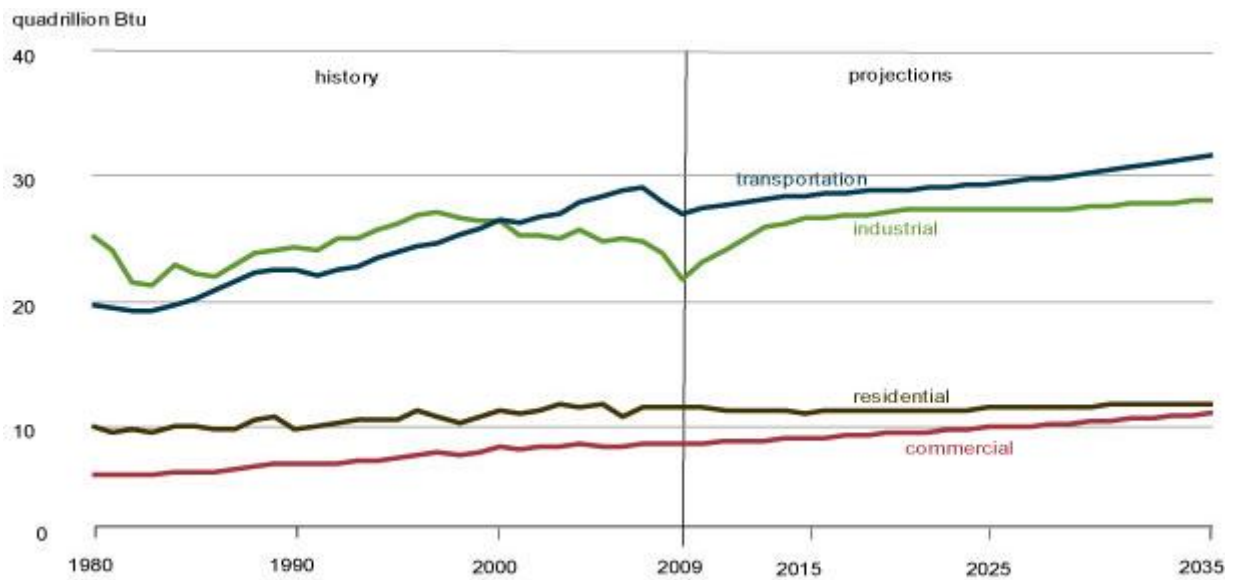


Figure 1 – projected energy usage by sector in quadrillion BTUs

Table 3 – combined cycle system input parameters

Input Parameters	Value
Hydrogen Volumetric Flow Rate (kmol/sec) (given from shift reactor)	4.42
Hydrogen Volumetric Flow Rate (L/min) (given from gasification)	2,974,029
Oxygen Input (excess)	15%
Maximum Firing Temperature (K) [fixed]	1,700
Maximum Heat Flow (KJ/sec) [fixed]	(866,667)
Maximum Heat Flow (KJ/min) [fixed]	(52,000,000)
Molar Percent of Hydrogen Separation	91%
Rated Net Power (Our Plant) (MW)	510
Maximum Heat Flow (Our Plant) (KJ/min)	(50,961,500)
Air Cooling Flow Rate (kg/sec)	685
steam from gasifier (Kg/sec)	4.50

ⁱ An estimate approximated by referring to current rates of proportional tank sizes. (Hanson Tanks, <http://www.hansontank.com/water-storage-tanks.html>)

ⁱⁱ Schlumberger Oilfield Glossary (<http://www.glossary.oilfield.slb.com/Display.cfm?Term=gathering%20system>)